



UNIVERSIDAD DE CHILE  
FACULTAD DE CIENCIAS FÍSICAS Y MATEMÁTICAS  
DEPARTAMENTO DE GEOLOGÍA

**GLACIAL GEOMORPHOLOGY AND PALEOGLACIAL BEHAVIOR ESTIMATION IN  
SIERRA BAGUALES (50° S): PALEOCLIMATIC FACTORS THAT CONTROLLED  
GLACIER VARIATIONS WITHIN THE PLEISTOCENE – HOLOCENE  
REGIONAL CONTEXT.**

TESIS PARA OPTAR AL GRADO DE DOCTOR EN  
CIENCIAS MENCIÓN GEOLOGÍA

**JOSE MIGUEL ARAOS ESPINOZA**

PROFESOR GUÍA:  
JACOBUS PHILIPPUS LE ROUX

MIEMBROS DE LA COMISIÓN:  
MARCELO SOLARI CORVALAN  
MAISA ROJAS CORRADI  
GABRIEL VARGAS EASTON

SANTIAGO DE CHILE  
2016

RESUMEN DE LA TESIS  
PARA OPTAR AL GRADO DE  
DOCTOR EN CIENCIAS MENCION GEOLOGIA  
POR: José Miguel Araos Espinoza  
PROF. GUIA: Jacobus Philippus Le Roux

El cordón montañoso de Sierra Baguales (CMSB) corresponde a una estribación oriental de los Andes Patagónicos localizado entre los 50° y 51° S, topográficamente aislado del Campo de Hielo Patagónico Sur (CHPS) y bajo la zona de influencia de los Vientos del Oeste. Su relieve presenta depósitos y morfologías glaciares potencialmente útiles para la reconstrucción de las glaciaciones pleistocenas–holocenas, que ocurrieron en las inmediaciones de la Capa de Hielo Patagónica, y que posiblemente presentaron respuestas individuales frente a los cambios ambientales posteriores al Último Máximo Glacial (UMG).

Utilizando métodos estadísticos sencillos y multivariados, se analizó la morfometría de 143 circos glaciales, distribuidos entre el actual límite este del CHPS y el sector oriental del CMSB, aproximadamente a 200 km de la costa pacífica. Para este último sector, mediante fotointerpretación, uso de Sistemas de Información Geográfica (SIG) y trabajo de campo, se confeccionó el primer mapa de la geomorfología glacial y periglacial del área de estudio, se estableció además la relación entre el índice de resistencia geológica (Geological Strength Index, GSI), el gradiente de precipitación y el área de los circos que fueron ocupados y erosionados por antiguos glaciares alpinos. Para circos ocupados por estos glaciares se elaboraron perfiles teóricos de la topografía del hielo, basados en un modelo de plasticidad perfecta. Las edades de los cambios ambientales locales fueron estimadas mediante dataciones  $^{14}\text{C}$ , y la interpretación de la variación de la Línea de Equilibrio Altitudinal (Equilibrium Line Altitude, ELA), se basó en evidencias geomorfológicas e índices de la proporción del área de acumulación de tales glaciares (Accumulation Area Ratio, AAR). El descenso de la ELA fue convertido a temperatura utilizando un gradiente atmosférico promedio.

Para el CMSB es posible reconocer dos niveles de glaciación que presentan un ascenso altitudinal hacia el interior del continente. Su distribución espacial y elevación están controladas por factores tectónicos (alzamiento andino), el gradiente de precipitaciones y el contraste climático este (marítimo templado) - oeste (seco frío), presente en Patagonia austral desde el UMG.

El límite inferior está conformado por amplios circos glaciales, distribuidos en las zonas más bajas de los valles principales. Estos no presentan evidencia actual de procesos nivales o glaciales y han sido sujetos a erosión fluvial y procesos gravitacionales. Este nivel puede asociarse al avance de los glaciares efluentes de la Capa de Hielo Patagónica durante el Holoceno y probablemente estuvieron parcial o totalmente cubiertos de hielo durante el UMG o glaciaciones anteriores.

Por otra parte, el límite superior está conformado por circos glaciales localizados al este del CHPS y fundamentalmente en la sección oriental del CMSB, y su tamaño se reduce progresivamente hacia el este, debido a la mayor resistencia de la roca y al gradiente de precipitaciones regional. Estos circos presentan evidencia de morrenas laterales y frontales asociadas a glaciares alpinos, algunos de los cuales se encuentran actualmente activos. Este nivel correspondería a aquellos glaciares que perduraron durante una etapa posterior al Holoceno medio, y que se vieron favorecidos por la exposición y pendiente de los circos, además de las bajas temperaturas imperantes en las secciones más elevadas marginales al CHPS y particularmente al oriente del CMSB.

Las edades radiocarbónicas obtenidas pueden considerarse como evidencia del cambio ambiental asociado a una reducción de las temperaturas y aumento de las precipitaciones debido a la migración latitudinal e incremento de la fuerza de los Vientos del Oeste durante el Holoceno medio. Para el CMSB, donde la temperatura atmosférica local desde el Tardiglacial era aproximadamente  $3,8 \pm 0,8^\circ \text{C}$  más fría que en la actualidad, las temperaturas se mantuvieron posiblemente más bajas en relación al contexto regional, fundamentalmente por el clima frío y seco prevaleciente al interior del continente y la elevación de las cuencas en las que se emplazaron los antiguos glaciares alpinos. Estos glaciares eventualmente avanzaron y confluyeron para formar un pequeño Campo de Hielo. Tales avances podrían relacionarse a las variaciones glaciares reportadas para el Lóbulo Frías, ubicado a similar latitud, en el margen este del CHPS.

The Sierra Baguales Mountain Range (SBMR) forms the eastern foothills of the Patagonian Andes located between 50° and 51° S, topographically isolated from the Southern Patagonian Icefield (SPIF) and under the influence of the Westerly Winds. Its landscape shows glacial deposits and morphologies, potentially useful for the reconstruction of the Pleistocene–Holocene glaciations, which occurred in the vicinity of the Patagonian Ice Cap, and possibly showed individual responses to environmental change after the Last Glacial Maximum (LGM).

Using simple and multivariate statistical methods, the morphometry of 143 glacial cirques, distributed between the current eastern limit of the SPIF and the easternmost SBMR, approximately 200 km from the Pacific coast, was analyzed. For the latter sector, using photo-interpretation, Geographic Information Systems (GIS) and field work, the first glacial and periglacial geomorphological map of the area was constructed. The relationship between the Geological Strength Index (GSI), rainfall gradient, and cirque areas, which were occupied and eroded by former alpine glaciers, was also established. To this end, theoretical profiles of the ice topography, based on a perfect plasticity model, were developed. Ages of local environmental changes were estimated using <sup>14</sup>C dating. Equilibrium Line Altitude (ELA) variations were interpreted based on geomorphological evidence and the accumulation area ratio (AAR). The lowering of the ELA was converted to the change in temperature by multiplying it with an average atmospheric lapse rate.

For the SBMR, it is possible to recognize two glaciation levels which rise towards the interior of continent. Their spatial distribution and elevation were controlled by tectonic factors (Andean uplift), the rainfall gradient and the climate contrast from east (temperate maritime) to west (dry cold), present in southern Patagonia since the LGM.

The lower group of glacial cirques is distributed in the lower areas of the main valleys. These have no current evidence of snow or glacial processes and have been subject to fluvial erosion and gravitational processes. These cirques can be associated with outlet glacier advance of the Patagonian Ice Cap during the Holocene, and were probably partially or completely covered with ice during the LGM or prior glaciations.

On the other hand, the upper group of glacial cirques is located east of the SPIF and mainly in the eastern section of the SBMR. Their size is reduced progressively to the east due to the increased resistance of the rocks on which they developed and the regional rainfall gradient. These cirques show evidence of lateral and frontal moraines of alpine glaciers, some of which are currently active. This cirque group corresponds to those glaciers that remained after the middle Holocene, favored by a gentle slope and aspect, in addition to low temperatures prevailing in the highest marginal sections of the SPIF and particularly the SBMR.

Radiocarbon ages can be considered as evidence of environmental change linked to the temperature decrease and rainfall increment resulting from the latitudinal shift and the increase in strength of the Westerly Winds during the middle Holocene. For the SBMR, where the local atmospheric temperature from the Tardiglacial was approximately  $3.8 \pm 0.8^\circ\text{C}$  colder than today, temperatures possibly remained lower in relation to the regional context, mainly due to the cold and dry climate prevailing towards the interior of the continent, and the elevation of the basins where the former alpine glaciers were located, which eventually advanced and coalesced to form a small Icefield. Such advances could be related to variations in the Frias Lobe, at the same latitude of the SBMR but closer to the SPIF eastern margin.

## DEDICATORIA

*A mi Padre, en el infinito, y a mi Madre*

*A Emilyn, Martina y la pequeña Amandita*

## AGRADECIMIENTOS

Agradezco a CONICYT por el financiamiento para el desarrollo de esta investigación mediante la Beca de Doctorado Nacional y el fondo de Gastos Operacionales para Proyecto de Tesis Doctoral.

A mi profesor, Jacobus Le Roux, por su guía y consejo, además por darme la libertad de seguir adelante con mis preguntas científicas (uno de los desafíos más espeluznantes de estos años).

A los profesores del Departamento de Geología: Cesar Arriagada, Katja Deckart, Sebastien Carretier, Reynaldo Charrier, Francisco Hervé, Luisa Pinto y Gabriel Vargas, también a Juan Luis García, Lasafam Iturrizaga, Maisa Rojas, Esteban Sagredo y Marcelo Solari por sus recomendaciones y consejos, muchos de los cuales trascienden a esta investigación. A la Señora Maritza Acuña por su apoyo en el sinnúmero de labores administrativas necesarias para el desarrollo del Doctorado.

A los coautores del primer capítulo, Mike Kaplan (*For your interest in the study site, your advice, and the alternative method for estimating the quartz amount on boulders*) y Matteo Spagnolo (*For your assistance in morphometric attribute definition and data processes*), y a Néstor Gutiérrez por su colaboración en el índice GSI desarrollado en el segundo capítulo.

A los dueños de las estancias “Las Cumbres” y “Baguales”, Juan McLane, y “Verdadera Argentina”, Juan Pablo Riquez, y sus respectivas familias, por recibirnos en sus casas y por toda la ayuda facilitada en terreno.

A mis amigos, Ricardo Arce, Raúl Martínez y Jorge Marín, por los grandes momentos vividos y recordarme que no solo lo que tiene hielo, o que tuvo hielo en el pasado, es de interés para el resto de las personas.

A los “carretas” de terreno, Ricardo Arce, Mauricio Gonzales, Nestor Gutiérrez y Ana Vásquez. A Juan Carlos Aravena y Rodrigo Villa-Martinez de la Universidad de Magallanes, a la Fundación CEQUA (Centro de Estudios del Cuaternario), a Juan San Martín y al hostal “Coloane”, además de José Luis Oyarzun por ayudarnos con la vital logística de terreno.

Especialmente quiero agradecer a mis padres por enseñarme todo, y mucho más, de lo necesario para embarcarme en esta aventura.

Particularmente quiero agradecer a Emilyn Soto, por su amor incondicional, voluntad, alegría, resiliencia, paciencia para aguantar el ritmo de vida doctoral y los terrenos, además por los litros y litros de café y los pastelillos...sin ti y nuestras hijas esto no habría sido posible.

Muy agradecido, muy agradecido, muy agradecido...

## TABLE OF CONTENTS

INTRODUCTORY REMARKS.....	15
CHAPTER I:	
FACTORS CONTROLLING ALPINE GLACIATIONS IN THE SIERRA BAGUALES MOUNTAIN RANGE OF SOUTHERN PATAGONIA (50° S), INFERRED FROM THE MORPHOMETRIC ANALYSIS OF GLACIAL CIRQUES.....	28
Abstract.....	28
Resumen.....	29
Introduction.....	30
Study area	
Geologic and climatical setting.....	31
Geomorphology.....	32
Methodology.....	33
Results	
Cirque classification according to their activity.....	41
Cirque shape.....	42
Elevation, slope and aspect.....	44
L/H W/H and L/W ratios.....	45
Morphological cirque types.....	46
Composite map.....	48
Discussion.....	49
Cirque distribution, elevation and dimensions.....	51
Paleoglacial significance.....	51
Conclusions.....	52
Acknowledgements.....	53
Bibliography.....	54

CHAPTER II:	
RELICT GLACIAL LANDSCAPE IN THE SIERRA BAGUALES MOUNTAIN RANGE (50°-51° S): EVIDENCE OF GLACIATION DYNAMICS AND STYLES IN THE EASTERN FOOTHILLS OF THE SOUTHERN PATAGONIAN ANDES.....	61
Abstract.....	61
Introduction.....	62
Study area.....	63
Methods	
Geomorphological mapping.....	66
Radiocarbon dates.....	67
ELA estimation and reconstruction of surface profile of former glaciers.....	67
SBMR temperature variation based on former ELA position.....	68
Results	
Glacial geomorphology.....	69
Radiocarbon dates.....	75
ELA behavior and temperature variation.....	76
Surface profiles of former glaciers.....	76
Discussion.....	77
Conclusions.....	79
Acknowledgements.....	80
Bibliography.....	80
FINAL REMARKS.....	88
APPEND 1.....	94
APPEND 2.....	98

## INDEX OF FIGURES

<p>Figure 1.1. Sketch of southern Patagonian glaciations during LGM of the major paleo-glacier lobes from 46° to 54° S. Modified from Rabassa <i>et al.</i> (2011), and references therein. Last 5 Kyr B.P. shows neoglacial chronologies proposed from the fluctuation of Patagonian glaciers in the Holocene by Mercer and by Aniya, modified from Glasser <i>et al.</i> (2004).....</p>	17
<p>Figure 1.2. SRTM Digital Elevation Model of Southern Patagonia showing major lakes and structural regions (FTB: Magallanic Fold-and-Thrust Belt, FB: Magellanes Foreland Basin; DM: Deseado Masiff). Contour lines show equal precipitation (DGA, 1987) and the orographic effect of the Andean Main Range and Sierra Baguales Mountain Range. PA: Punta Arenas, PNat: Puerto Natales, White dotted box shows study area.....</p>	20
<p>Figure 2.1a. Right box shows the location of the study area. Elevations were obtained from the SRTM model. The brown dotted line shows the major moraine systems east of Lago Argentino, Brazo Rico and Brazo Sur (Mercer, 1976; Strelin and Malagnino, 2000; and references therein), and south and east of Lago Toro and Lago Sarmiento respectively (Sagredo <i>et al.</i>, 2011; Garcia <i>et al.</i>, 2013). Cirque activity corresponds to 1). current glacier activity, 2). perennial snow activity, 3). no glacier or snow activity, 4). not categorized. Figure 2.1b. Mapped cirque floor elevations, which show the increase in elevation towards the east. A – A' shows a topographic profile from the SPIF to the easternmost SBMR.....</p>	34
<p>Figure 2.2. Google Earth © image showing the study area from the SW. Photographs a) and b) (see location on Google image) show a hanging valley and glacial cirque, and photo c) shows a glacial valley. Current snow and glacier processes are particularly active along the high elevations on the eastern side of the SBMR (i.e., see Figure. 2.1).....</p>	35



Figure 2.3. Lateral moraine (dark lines) below the cirques shown in figure 2a (F3 in Fig. 2.1b).....	35
Figure 2.4. Striated erratic (F4 in Fig. 2.1b).....	36
Figure 2.5. Definition of key morphometric attributes. Left box shows the length (L) and azimuth (for aspect) in a grey line and width (W) in a white dashed line. i - ii correspond to a topographic profile on ASTERGDEM. The right box shows the characteristics of range (H) and the topographic profile.....	37
Figure 2.6. Cirque showing evidence of glacier activity, at the easternmost section of the SBMR (F6 in Fig. 2.1b).....	42
Figure 2.7. Cirque showing perennial snow activity (F7 in Fig. 2.1 b).....	42
Figure 2.8. Frequency distribution of L, W and H. Cirque mean surface (km <sup>2</sup> ) decreases with an increasing in depth (H). Otherwise, when the average slope becomes gentle (i.e. decrease of H), cirques are most likely to grow longitudinally and laterally. As shown in figure 2.1, large cirques are concentrated along the eastern margin of the SPIF and gradually get smaller towards the interior of the continent around the SBMR.....	43
Figure 2.9. Rose diagram showing frequency distribution of aspect. Cirques with a SW aspect tend to be located in the intermediate zone and altitudinal range E (1,472 – 1,741 m a.s.l), while cirques with S aspects are preferably located at the SPIF. Otherwise cirques with a S to SE aspect show a homogeneous distribution within the study area and an altitudinal range between C to D (1,126 –1,292 and 1,293 – 1,471 m a.s.l.). Moreover, cirques with W to SW aspects tend to show larger surface areas.....	45

Figure 2.10. Tree cluster of cirques (Euclidean distance measurements and amalgamation conducted by Ward`s method). The analysis shows two major morphological types where the differences are based on the cirque activity (i.e. glacial, perennial snow, or absence of both), surface, shape and spatial distribution. Morphological type 2 tends to show largest cirques compared with the morphological type 1..... 47

Figure 2.11. Composite map of study area. Cirques were categorized using 10 parameters extracted from the morphometric analysis (Table 1.2). Black dotted lines show outlines of LGM lobes. Cirque areas closest to the SPIF, such as in the far SW, were partly covered or adjacent to the large ice sheet during the LGM (Garcia *et al.*, 2012; Strelin *et al.*, 2011). This contributed to their higher areal development in relation to those located in the eastern SBMR, which were isolated from the ice sheet outlet lobes. Note that high values show the spatial distribution of currently active snow/ice processes, which particularly for the eastern SBMR, are conditioned by cirque floor elevations (Fig. 2.1) and the rainshadow effect. The lowest values spatially match with evidence of areas covered or adjacent to former outlet glaciers of the SPIF, and cirques with no evidence of current glacier or snow activity..... 50

Figure 3.1. The right box shows the general location of the study area, and the blackstippled box shows the SBMR. Major lakes appear in dark blue, SPIF is shown in light blue. The black stippled line shows an outline of the mapped moraine systems around Lago Argentino (Strelin and Malagnino, 2009, and references therein, Kaplan *et al.*, 2005; 2008; 2011; Strelin *et al.*, 2014), and Lagos Toro and Sarmiento (Marden, 1997, Sagredo *et al.*, 2011; Garcia *et al.*, 2012). CG: Cerro Guido; RC: Rio Las Chinas; TdP: Torres del Paine, which correspond to meteorological stations of the Direccion General de Aguas (DGA). Elevations were obtained from an SRTM model..... 65

Figure 3.2. SBMR glacial geomorphology. White boxes show the location of

samples for radiocarbon dating. RB-RB` shows the location of the topographic profile (Figure 3.8). AA`, BB`, CC` show the former surface topography of alpine glaciers (Figure 3.10)..... 71

Figure 3.3. U-shaped valley in the area where the former Alpine glaciers coalesced to form a small Icefield (F3 in Fig. 3.2)..... 72

Figure 3.4. Remnant of lateral moraine and boulders deposited and aligned with the moraine (F4 in Fig. 3.2)..... 72

Figure 3.5. Lateral moraine and boulders below the U-shaped valley shown in Figure 3 (F5 in Fig. 3.2)..... 73

Figure 3.6. Figure 3.6. Hummocky terrain and remnants of lateral moraine. These deposits, located in the middle section of the Baguales River basin, constitute evidence of a former Icefield (F6 in Fig. 3.2)..... 73

Figure 3.7. Eroded kame terraces along the Baguales River (see also Figure 3.8) (F7 in Fig. 3.2)..... 74

Figure 3.8. RB-RB' topographic profile..... 74

Figure 3.9. Spatial distribution of rock mass strength in SBMR, the box on the left shows that at greater rock resistance cirque areas tend to decrease..... 75

Figure 3.10. Former surface topography profiles of alpine glaciers. Topography and ice thickness vary depending on changes in the bedrock slope..... 77

## INDEX OF TABLES

Table 1.1. Data source for cirque mapping .....	36
Table 1.2. Summary of cirque morphometric characteristics.....	38
Table 1.3. Correlation between analyzed morphometric characteristics. S, P, L, and W parameters have a high positive correlation followed by the altitude range (H). These variables are dependent and determine mainly the shape and cirque development. On the other hand, the $E_{med}$ , $E_{min}$ and $S_{mean}$ parameters have a weak negative correlation with the shape parameters. Particularly M has a strong negative correlation with the planimetric development and cirque incision. See Table 1.2 for definition of attributes....	44
Table 1.4. Distribution of cirque attributes with aspect. See Table 2 for definition of attributes.....	46
Table 1.5. Summary statistics of morphometric characteristics for cirque types obtained from cluster analysis. See Table 2 for definition of attributes.....	48
Table 2.1. Meteorological stations and data obtained from the DGA of the Chilean Ministerio de Obras Publicas website ( <a href="http://snia.dga.cl/BNAConsultas/reportes">http://snia.dga.cl/BNAConsultas/reportes</a> ).....	69

## INTRODUCTORY REMARKS

Patagonian glaciations developed since the end of the Miocene (ca. 6 Myr) in multiple events of varying duration and intensity (Rabassa *et al.*, 2011), forming a region that displays the longest and most complete records of glacial geomorphology of different ages and extensions in the world (Mercer, 1983; Clapperton, 1993; Coronato *et al.*, 2004; Rabassa *et al.*, 2005; Rabassa and Coronato, 2009; Rabassa *et al.*, 2011).

The oldest known glaciations took place between approximately 7 and 5 Myr during latest Miocene-earliest Pliocene, while during the middle-late Pliocene, a minimum of 8 glaciations occurred. After the Great Patagonian Glaciations (GPG) that developed between 1.168 and 1.016 Myr during the early Pleistocene, the Patagonian Andes were covered by a mantle of ice that continued from 37° south to Cape Horn (56° S) and were affected by 14 – 16 cold (glacial/stadial) events with their corresponding warm (interglacial/interstadial) equivalents (Lagabrielle *et al.*, 2010; Rabassa *et al.*, 2011; Solari *et al.*, 2012).

Thirteen post-GPG glacial variations can be identified by moraine systems throughout Patagonia. Some of these moraines indicate that a major glacial advance occurred during 150 – 140 Kyr (Kaplan *et al.*, 2004; Singer *et al.*, 2004; Douglass and Bockheim, 2006). Kaplan *et al.* (2005), identify major glacier advances between 71 and 57 Kyr at Lake Buenos Aires, which was in part obliterated by the more extensive 29 to 14 Kyr glacial advance.

The Last Glacial Maximum (LGM) occurred between about 30 and 16 Kyr, being broadly synchronous across Patagonia, and in-phase with other areas around the globe (Sagredo *et al.*, 2011). Southern Patagonian ice was most extensive from 25 to 18 Kyr, with a peak around 25–24 Kyr. This was a period of rising and maximum summer insolation intensity in the Southern Hemisphere, largely due to the precession of the equinoxes. A stronger influence of the Antarctic Frontal Zone and equator ward movement of cold air from the south relative to the present is one way to explain negated local summer insolation intensity, and glaciations broadly in phase with global changes (Kaplan *et al.*, 2008).

Recent studies (Kaplan *et al.*, 2010; Putnam *et al.*, 2010; Strelin *et al.*, 2011) show evidence for a late glacial ice expansion in southern middle latitudes near the end of the Antarctic Cold Reversal (ACR) at ca. 13.0 Kyr, followed by substantial glacier

recession in the subsequent millennium. McCulloch *et al.* (2000) argue that deglaciation of the LGM occurred synchronously at 14,600 – 14,300  $^{14}\text{C}$  yr BP (17,500-17,150 Cal yr BP). However, marine and ice-core evidence indicates environmental changes associated with the onset of the ACR much earlier than 13.0 Kyr (EPICA Community Members, 2004 [EPICA—European Project for Ice Coring in Antarctica]); Blunier and Brook, 2001). Thus, according to Garcia *et al.* (2012); Sugden *et al.* (2005) and Kaplan *et al.* (2008) the nature of climate dynamics throughout the ACR around Patagonia remains unclear.

Glacial geological studies in the Southern Hemisphere mid-latitudes (40–54°S) indicate renewed glacial activity in Patagonia and New Zealand's South Island during the most recent half of the Holocene epoch. The so-called neoglaciation (e.g. Porter, 2000) started at 7– 6 Kyr, and could be related to cooling and increased precipitation during the ablation (DJF) season, along with slightly higher precipitation and temperature seasonality suggested by simulations carried out in the context of the PMIP2 initiative [Modelling Inter-comparison Project] (Rojas and Moreno, 2011), which is consistent with a cooler temperature and an increase in precipitation trend that peaked at ca. 5000 cal yr. BP, after an extremely warm and dry phase in the early Holocene. Such climatic variations would be linked to a latitudinal shift that controlled the strength of the southern Westerlies (Moreno, 2004; Villa-Martinez and Moreno, 2007), featuring multiple advances at sub-millennial timescales, and culminated with the advance of alpine glaciers in both regions at a similar time as the European Little Ice Age (Rojas and Moreno, 2011).

Glasser *et al.* (2004) undertook a major revision of the Holocene glacier advances, that began around 5,000  $^{14}\text{C}$  years BP, coincident with a strong climatic cooling around this time (the Neoglacial interval). Glacier advances can be assigned to one of three time periods following a 'Mercer-type' chronology, or one of four time periods following an 'Aniya-type' chronology. The 'Mercer-type' chronology has glacier advances 4700–4200  $^{14}\text{C}$  years BP; 2700–2000  $^{14}\text{C}$  years BP, and during the Little Ice Age. The 'Aniya-type' chronology has glacier advances at 3600  $^{14}\text{C}$  years BP, 2300  $^{14}\text{C}$  years BP, 1600–1400  $^{14}\text{C}$  years BP and during the Little Ice Age (Fig. 1.1).

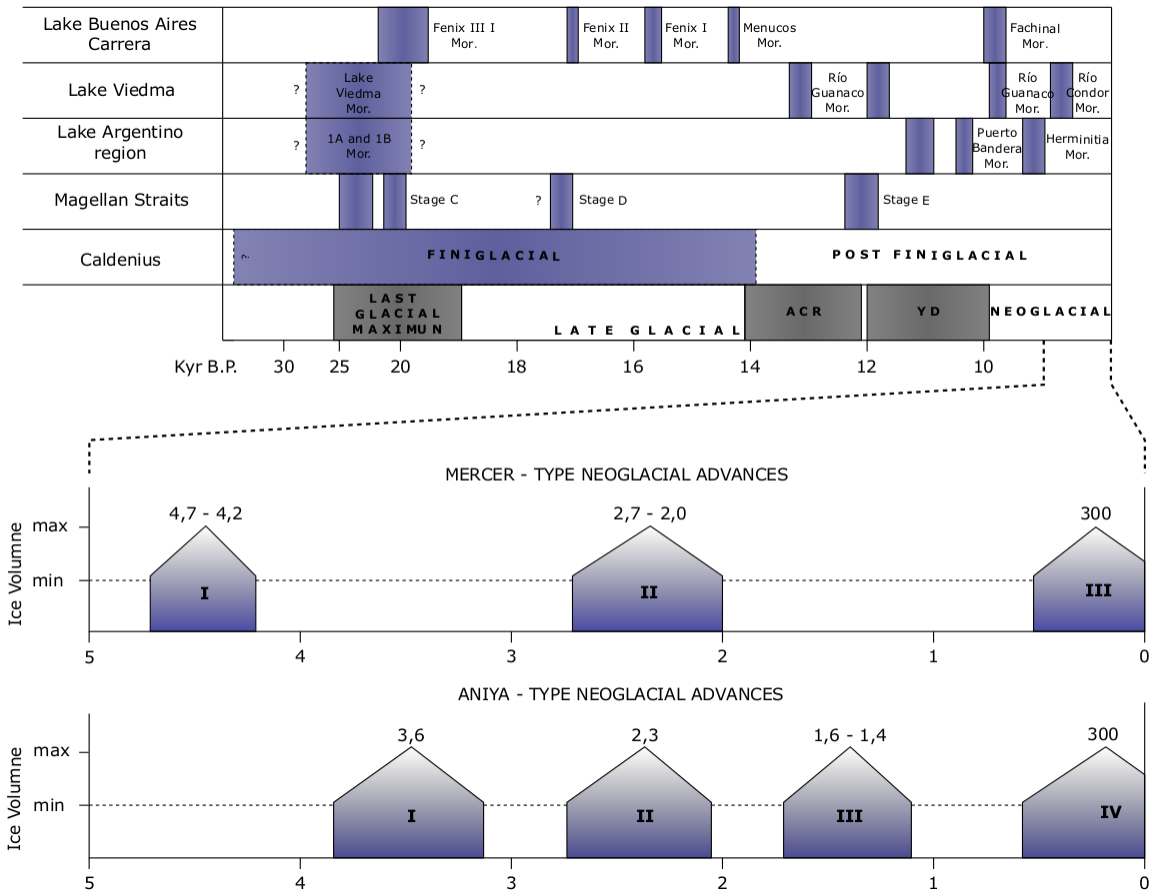


**Figure 1.1. Sketch of southern Patagonian glaciations during LGM of the major paleo-glacier lobes from 46° to 54° S. Modified from Rabassa *et al.* (2011), and references therein. Last 5 Kyr B.P. shows neoglacial chronologies proposed from the fluctuation of Patagonian glaciers in the Holocene by Mercer and by Aniya, modified from Glasser *et al.* (2004)**

The discussion of Holocene glacial history in Patagonia is dominated by the nature of climatic conditions and the sequence of events subsequent to the last glaciation at 13 Kyr. The chronology of the events of glacial advance and retreat vary depending on the sites and the evidence analyzed. However, there is consensus on the existence of a contrast in the nature of the deglaciation between the northern and southern sections of the former Patagonian ice cap (Marden, 1997). In addition, those glaciers located to the west were more sensitive to precipitation, whereas those located towards the east were more sensitive to changes in temperature (Warren and Sugden, 1993).

During the Pleistocene-Holocene, a succession of continental and alpine glaciations formed the distinctive glacial relief of the Patagonian Andes due to the relationship between tectonic uplift and the regional climate pattern (Montgomery *et al.*, 2001; Ramos and Ghiglione, 2008; Kaplan *et al.*, 2009). According to Rabassa (2008) these factors still actively model processes in the remnants of the Patagonian Ice Cap: the Northern and Southern Patagonian Icefields (NPIF, SPIF), and the Cordillera Darwin Icefield (CDIF).

Particularly, continental glaciations have been widely studied since late last century, after the work of Nordenskjöld (1899) and Caldenius (1932) in the moraine belts located east of Patagonia and Tierra del Fuego. Subsequently, in the Magallanes region, McCulloch *et al.* (2000), Heusser (2003), Coronato *et al.* (2004), Sugden *et al.* (2005), Sagredo *et al.* (2011), and Solari *et al.* (2012), among others, highlighted the regional and global paleo-ecological implications of glacier variations. Specifically for the Torres del Paine area, Marden (1997), Fogwill and Kubik (2005) and Garcia *et al.* (2012), among others, developed the first chronology of the glacial variations that occurred since the transition between the Pleistocene and Holocene. Much of the research indicates that the dynamics of these glaciations is related to the latitudinal displacement of the Westerly Winds (Hulton *et al.*, 1994; McCulloch *et al.*, 2000; Hulton *et al.*, 2002; Rabassa *et al.*, 2005; Sugden *et al.*, 2005; Rodbell *et al.*, 2009).

However, there is still a lack of information about the characteristics and variations of alpine glaciations, specifically those that developed, evolved and in many cases disappeared in mountainous areas surrounding the remnants of the Pleistocene Ice Cap. Here the morphological and stratigraphic evidence of alpine glaciations is more difficult to identify, due to ice advances associated with colder conditions, or because of the effect of fluvial erosion and gravitational processes (Ehlers and Gibbard, 2007; Hughes *et al.*, 2007).

Nevertheless, according to Mercer (1983), a large part of Patagonia still retains glacial deposits, which can be found in valleys that do not currently have active glaciers and can be considered as relict surfaces. In many cases, they present evidence of the relationship between orogenic uplift and glaciations (Lagabrielle *et al.*, 2010).

The Sierra Baguales Mountain Range (SBMR), located between 50°44' S and 72°24' W, shows evidence of continental and alpine glaciations, which can be



considered as a recent relict relief. This area is therefore ideal to estimate the variations of former glaciers that were located there, and to use this information as a *proxy* to estimate Pleistocene-Holocene environmental changes in these eastern foothills of the Patagonian Andes.

In this region, the southern hemisphere annular mode, and other hemispheric modes, have a significant influence on precipitation and temperature behavior (Silvestri and Vera 2003; Gillett *et al.*, 2006; Quintana and Aceituno 2012; Garreaud *et al.*, 2013). The north-to-south-oriented Andean Mountain Chain, with peaks reaching over 3,000 m, depicts the only high mountain barrier in the high latitudes of the Southern Hemisphere (Aravena and Luckman. 2009; Garreaud *et al.*, 2013), that contain the NPIF and SPIF besides the CDIF. According to Garreaud *et al.* (2008). The dominant mean westerly air flow leads to almost constant advection of moist air masses across the perpendicular orographic obstacle of the Andes, producing one of the most extreme climate divides in the world, with very wet conditions to the west and very dry conditions to the east of the Andes Cordillera (Fig. 1.2).

East or southeast-moving cyclonic depressions, driven by the Westerlies, rise abruptly over the Andes, producing high precipitation on the Pacific-facing slopes between 48° and 52° S (Aravena and Luckman, 2009). According to Garreaud *et al.* (2013) Western Patagonia features a modest seasonal cycle and annual mean precipitation in the 5000–10000 mm range (Miller, 1976). Such high accumulations arise from the orographic enhancement of synoptic-scale precipitation upstream of the mountains (Roe, 2005) and support extensive rainforests, major rivers, and numerous glaciers. The mean precipitation decreases to less than 300 mm/year. Just a few tens of kilometers downstream of the continental divide, leading to a rapid disappearance of vegetation and a rain shadow that extends all the way to the Atlantic coast, where the mean precipitation only reaches 500–700 mm/year (Prohaska, 1976; Paruelo *et al.*, 1998; Carrasco *et al.*, 2002).

According to Strelin *et al.* (2014) at 50° S, pervasive cloudiness (more than 70% daily cover) and orographically controlled annual precipitation, which ranges from 2,000 to 7,000 mm, characterize the western Pacific mountain facade (Carrasco *et al.*, 2002). On the high part of the Cordillera, annual snowfall peaks at ~10,000 mm water equivalent, nourishing the SPIF (DGA, 1987). Markedly drier air masses reach the

eastern foothills of the Cordillera, resulting in an annual precipitation of only 200 mm at El Calafate. The Westerlies become stronger during the summer due to the southward shift of the Subtropical Anticyclone and the consequent steepening of the latitudinal pressure gradient. On both sides of the Cordillera the mean annual air temperature is ~ 6°C, with a higher seasonal and daily amplitude on the eastern more-continental (oceanic) side and a lower seasonal and daily amplitude on the western side (Carrasco *et al.*, 2002), under the prevailing oceanic, cold climate conditions.

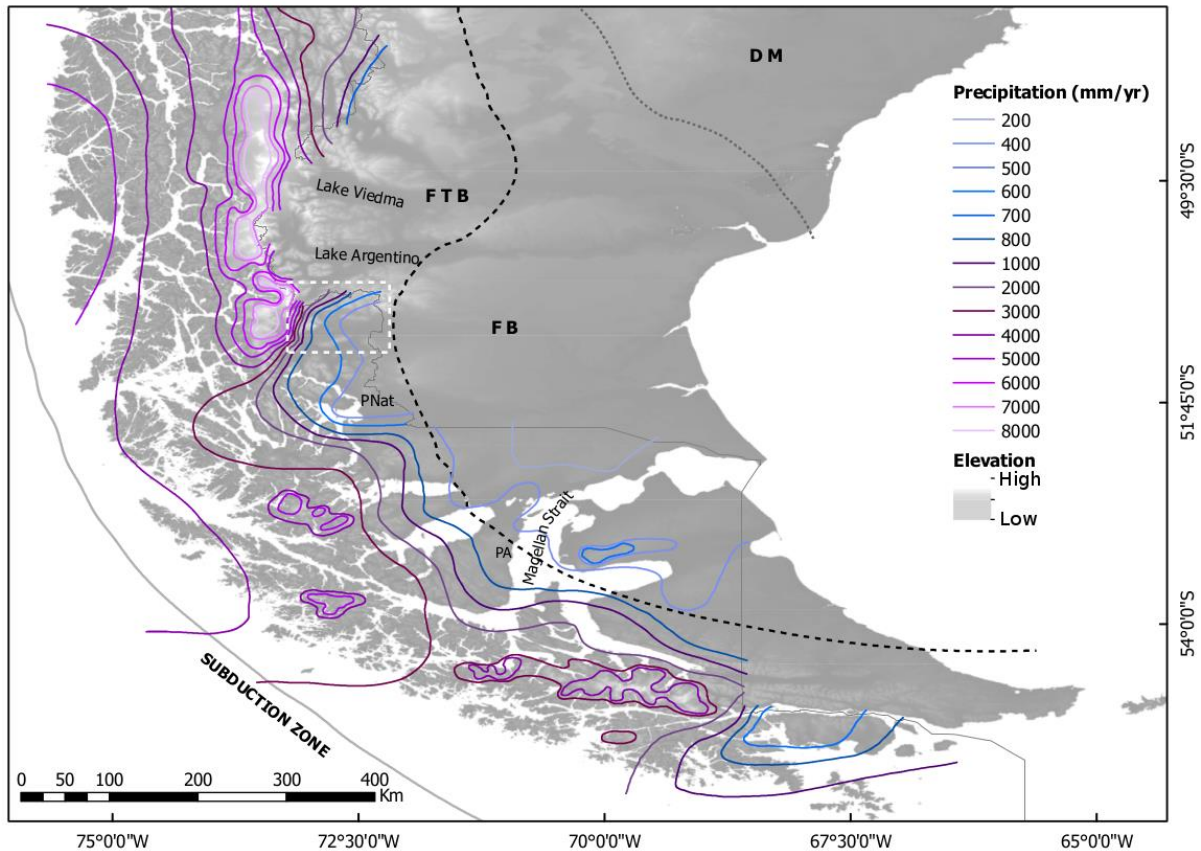


**Figure 1.2. SRTM Digital Elevation Model of Southern Patagonia showing major lakes and structural regions (FTB: Magallanic Fold-and-Thrust Belt, FB: Magellanes Foreland Basin; DM: Deseado Masiff). Contour lines show equal precipitation (DGA, 1987) and the orographic effect of the Andean Main Range and Sierra Baguales Mountain Range. PA: Punta Arenas, PNat: Puerto Natales, White dotted box shows study area.**

Given this geographical and climatic context, the SBMR represents a useful study site for the reconstruction of the paleogeographic and paleoglacial evolution of the eastern Andean foothills. Here, geomorphological and stratigraphic evidence indicate

the action of continental glaciation in the lower parts of the main valleys and alpine glaciation in the upper reaches of the main river basins.

Such evidence provides a reasonable framework for understanding the environmental and non-environmental factors that control the development of different styles of glaciation. In the case of continental glaciation, its response to environmental changes is very slow, whereas alpine glaciation reacts much faster. The latter can therefore be used as a useful indicator of climate change on a regional scale (Sugden and John, 1976; Vieira, 2008).

In the light of the above, the working hypothesis of this research is that: The particular geographic and climatic setting of the SBMR forming the eastern foothills of the Patagonian Andes, under to a cold and dry climate, could have favored the development of alpine glaciations in its highest sections. Under a scenario of persistent low atmospheric temperatures, in comparison to the Pleistocene-Holocene regional climate context, these alpine glaciers could have advanced, converged and formed a small Icefield, which eventually would correspond to a separate glaciation from the Pleistocene ice cap that covered the Main Andean Range since the Pleistocene.

The main objective is to describe and interpret the glacial and periglacial geomorphology of an area not previously studied, in order to identify the controlling factors involved in the glaciations that occurred in these eastern foothills of the Patagonian Andes and compare the behavior of former alpine glaciers of the SBMR with outlet glaciers of the Patagonian Ice Cap, within the context of Southern Patagonia climate setting and regional environmental changes since the LGM.

Secondary objectives are to

Map and describe the glacial and periglacial geomorphology of SBMR,

Estimate the spatial extent of the former glaciated area of SBMR,

Estimate the altitudinal variation of the equilibrium line altitude in the former glaciers of the SBMR, and finally, to

Estimate the range of atmospheric temperature decrease in the SBMR during the early Holocene.

This dissertation is a compilation of two manuscripts (chapters) that correspond to the following studies:

Chapter I: “Factors controlling alpine glaciations in Southern Patagonia around 50° S, inferred from the morphometric analysis of glacial cirques”. This chapter identifies the controlling factors of regional alpine glaciations in a strip located at 50° S, between the eastern edge of the SPIF and the eastern part of the SBMR. Here, 143 glacial cirques were identified and mapped, while their morphometric parameters were analyzed using statistics and GIS methodologies. This allowed us to identify two levels of glaciation associated with tectonic, climatic, and former regional glacial activity, besides factors such as the aspect, elevation and spatial distribution of the glacial cirques.

Chapter II: “Relict glacial landscape in the Sierra Baguales Mountain Range (50°-51° S): Evidence of glaciation dynamics and styles in the eastern foothills of the southern Patagonian Andes”. This chapter offers a detailed description of the glacial and periglacial geomorphology, integrating the lithology, regional precipitation gradient, and ice floor topography as controlling factors in the development of glacial styles. Furthermore, the first radiocarbon dates for this site indicate a middle Holocene environmental change and probably glacial advance during the middle Holocene (6 Kyr). The chapter also includes data analysis aimed to estimate variations of the Equilibrium Line Altitude (ELA) of former glaciers of the SBMR, and can serve as a proxy for the SBMR paleo-temperature behavior, and to establish a comparison of continental and alpine glaciations after the LGM.

Finally, it is expected that the integration of these studies will cast new light on individual and isolated glaciations that developed in the vicinity of the Pleistocene ice cap and help to estimate climatic and non-climatic factors that influenced those glaciations. It can also contribute to the understanding of environmental evolution in the southern section of South America during the Pleistocene-Holocene.

## **Bibliography**

Aravena, J. C., and B. H. Luckman. 2009. Spatio-temporal rainfall patterns in southern South America. *International Journal of Climatology*, 29, 2106– 2120.

Blisniuk, P., Stern, C., Chamberlain, B., Idleman, B. and Zeitler, P. 2005. Climatic and ecologic changes during Miocene surface uplift in the Southern Patagonian Andes. *Earth and Planetary Science Letters*, 230, 125–142.

Blunier, T., Brook, E. 2001. Timing of millennial scale climate change in Antarctica and Greenland during the last glacial period. *Science*, 291, 109-112.

Caldenius, C. 1932. Las glaciaciones cuaternarias en la Patagonia and Tierra del Fuego. *Geografiska Annaler*, 14, 1–164.

Clapperton, C. 1993. Nature of environmental changes in South America at the Last Glacial Maximum. *Palaeogeography, Palaeoclimatology, Palaeoecology*, 101 (3-4), 189–208.

Carrasco, J., G. Casassa, and Rivera, A. 2002. Meteorological and climatological aspects of the Southern Patagonia Ice Cap. *The Patagonian Icefields: A Unique Natural Laboratory for Environmental and Climate Change Studies*, G. Casassa, F. V. Sepu´lveda, and R. M. Sinclair, Eds., Kluwer Academic, 29–41.

Coronato, A., Meglioli, M. and Rabassa, J. 2004. Glaciations in the Magellan Strait and Tierra del Fuego, Southernmost South America. In: Ehlers, J. and Gibbard, P. (Eds.) *Quaternary Glaciations: Extent and Chronology. Part III: South America, Asia, Africa, Australia and Antarctica*. Quaternary Book Series, Elsevier, Amsterdam, pp. 45–48.

DGA, 1987. National water balance. *Direccion General de Aguas Tech. Rep.*, 60 pp.

Douglass, D. and Bockheim, J. 2006. Soil-forming rates and processes on Quaternary moraines near Lago Buenos Aires, Argentina. *Quaternary Research*, 65, 293–307.

Ehlers, J. and Gibbard, P. 2007. The extent and chronology of Cenozoic global glaciations. *Quaternary International*, 164, 6-20.

Escobar, F., Vidal, F. and C. Garin. 1992. Water balance in the Patagonia Icefield. *Glaciological Researches in Patagonia, 1990*, R. Naruse, Ed., Japanese Society of Snow and Ice, 109– 119.

Fogwill, C. and Kubik, P. 2005. A glacial stage spanning the Antarctic Cold Reversal in Torres del Paine (51 ° S), Chile, based on preliminary cosmogenic exposure ages. *Geografiska Annaler, Series A: Physical Geography*, 87 (2), 403–408.

Fuenzalida, H., P. Aceituno, M. Falvey, R. Garreaud, M. Rojas, and Sánchez, R. 2007. Estudio de variabilidad climática en Chile para el siglo XXI (Study on climate variability for Chile during the 21st century). National Environmental Committee Tech. Rep. [Available online at <http://www.dgf.uchile.cl/> PRECIS.]

Glasser, N., Harrison, S., Winchester, V. and Aniya, M. 2004. Late Pleistocene and Holocene palaeoclimate and glacier fluctuations in Patagonia. *Global and Planetary Change*, 43, 79-101

García, J., Kaplan, M., Hall, B., Schaefer, J., Vega, R., Schwartz, R. and Finkel, R. 2012. Glacier expansion in southern Patagonia throughout the Antarctic Cold Reversal. *Geology*, 40 (9), 859–862.

Garreaud, R. M. Vuille, R. Compagnucci, and Marengo, J. 2009. Present day South American climate. *Palaeogeography Palaeoclimatology Palaeoecology*, 281, 180–195.

Heusser, C. 2003. Ice age southern Andes: a chronicle of palaeoecological events. New York University, 260 pages.

Hughes, P., Gibbard, P. and Woodward, J. 2007. Geological controls on Pleistocene glaciation and cirque form in Greece. *Geomorphology*, 88 (3–4), 242–253.

Hulton, N., Purves, R., McCulloch, R., Sugden, M. and Bentley, M. 2002. The Last Glacial Maximum and deglaciation in southern South America. *Quaternary Science Reviews*, 21, 233–241.

Hulton, N., Sugden, D., Payne, A. and Clapperton, C. 1994. Glacier modeling and the climate of Patagonia during the Last Glacial Maximum. *Quaternary Research*, 42 (1), 1–19.

Kaplan, M., Sagredo, E., Moreno, P., Rojas, M., Villa-Martínez, R. and Garcia, J. 2010. Glacial and Climate History of Central and Southern Patagonia: Recent Insights. American Geophysical Union, Fall Meeting 2010, abstract #GC23H-05

Kaplan, M., Hein, A., Hubbard, A. and Lax, S. 2009. Can glacial erosion limit the extent of glaciation? *Geomorphology*, 103, 172–179.

Kaplan, M., Moreno, P. and Rojas, M. 2008. Glacial dynamics in southernmost South America during Marine Isotope Stage 5e to the Younger Dryas chron: A brief review with a focus on cosmogenic nuclide measurements. *Journal of Quaternary Science*, 23, 649-658.

Kaplan, M., Douglass, D., Singer, B., Ackert, R. and Caffee, M. 2005. Cosmogenic nuclide chronology of pre-last glaciation maximum moraines at Lago Buenos Aires, 46°S, Argentina. *Quaternary Research*, 63, 301-315.

Kaplan, M., Ackert, R., Singer, B., Douglass, D. and Kurz, M. 2004. Cosmogenic nuclide chronology of millennial-scale glacial advances during O-isotope Stage 2 in Patagonia. *Geological Society of America Bulletin*, 116, 308-321.

Lagabrielle, Y., Labaume, P. and Blanquat, M. 2010. Mantle exhumation, crustal denudation, and gravity tectonics during Cretaceous rifting in the Pyrenean realm (SW Europe): insights from the geological setting of the Iherzolite bodies. *Tectonics*, 29, 4.

Marden, C. 1997. Late-glacial fluctuations of South Patagonian Icefield, Torres del Paine National Park, southern Chile. *Quaternary International*, 38–39, 61–68.

McCulloch, R., Bentley, M., Purves R., Hulton, N., Sudgen, D. and Clapperton, C. 2000. Climatic inferences from glacial and palaeoecological evidence at the last glacial termination, southern South America. *Journal of Quaternary Science*, 15 (4), 409–417.

Mercer, J. 1983. Cenozoic glaciation in the Southern Hemisphere. *Annual Review of Earth and Planetary Sciences*, 11, 99–132.

Montgomery, D., Balco, G. and Willett, S. 2001. Climate, tectonics, and the morphology of the Andes. *Geology*, 29 (7), 579–582.

Moreno, P. 2004. Millennial-scale climate variability in northwest Patagonia over the last 15 000 yr. *Journal of Quaternary Science*, 19 (1), 35–47.

Nordenskjöld, O. 1899. Geological map of the Magellan territories with explanatory notes. Kungl. Boktryckeriet. PA Norstedt & Söner, 1(3), 81-85.

Rabassa, J., Coronato, A. and Martínez, O. 2011. Late Cenozoic glaciations in Patagonia and Tierra del Fuego: an updated review. *Biological Journal of the Linnean Society*, 103 (25), 316–335.

Rabassa, J. and Coronato, A. 2009. Glaciations in Patagonia and Tierra del Fuego during the Ensenadan Stage/Age (Early Pleistocene–earliest Middle Pleistocene). *Quaternary International*, 210 (1–2), 18–36.

Rabassa, J. 2008. Late cenozoic glaciations in Patagonia and Tierra del Fuego. In: *The Late Cenozoic of Patagonia and Tierra del Fuego*. Elsevier, Amsterdam. pp 151-204.

Rabassa, J., Coronato, A. and Salemme, M. 2005. Chronology of the Late Cenozoic Patagonian glaciations and their correlation with biostratigraphic units of the Pampean region (Argentina). *Journal of South American Earth Sciences*, 20 (1–2), 81–103.

Ramos, V. and Ghiglione, M. 2008. Tectonic evolution of the Patagonian Andes. In: *The Late Cenozoic of Patagonia and Tierra del Fuego*. Elsevier, Amsterdam. pp 57–71.

Rodbell, D., Smith, J. and Mark, B. 2009. Glaciation in the Andes during the Late Glacial and Holocene. *Quaternary Science Reviews*, 28 (21–22), 2165–2212.

Rojas, M., Moreno, P. 2011. Atmospheric circulation changes and neoglacial conditions in the Southern Hemisphere mid-latitudes: insights from PMIP2 simulations at 6 kyr. *Climate Dynamics*, 37, 357-375.

Rosenblüth, B., H. Fuenzalida, and Aceituno, P. 1997: Recent temperature variations in southern South America. *Int. J. Climatol.*, 17, 67–85.

Sagredo, E., Moreno, P., Villa-Martínez, R., Kaplan, M., Kubik, P. and Stern, C. 2011. Fluctuations of the Última Esperanza ice lobe (52°S), Chilean Patagonia, during the last glacial maximum and termination 1. *Geomorphology*, 125, 92–108.



Singer, B., Ackert, R. and Guillou, H. 2004.  $^{40}\text{Ar}/^{39}\text{Ar}$  and K-Ar chronology of Pleistocene glaciations in Patagonia. *Geological Society of America Bulletin*, 116, 434-450.

Solari, M., Le Roux, J., Hervé, F., Airo, A. and Calderón, M. 2012. Evolution of the Great Tehuelche Paleolake in the Torres del Paine National Park of Chilean Patagonia during the Last Glacial Maximum and Holocene. *Andean Geology*, 39, 1, 1–21.

Strelin, J., Denton, G., Vandergoes, M., Ninnemann, U. and Putman, A. 2011. Radiocarbon chronology of the late-glacial Puerto Bandera moraines, Southern Patagonian Icefield, Argentina. *Quaternary Science Reviews*, 30, 2551–2569.

Sudgen, D., Bentley, M., Fogwill, C., Hulton, N., McCulloch, R. and Purves, R. 2005. Late-glacial glacier events in southernmost south America: A blend of “northern” and “southern” hemispheric climatic signals?. *Geografiska Annaler, Series A: Physical Geography*, A 87 (2), 273–288.

Sugden, D and John, B (1976) *Glaciers and Landscape*. E. Arnold. London. 376 pages.

Vieira, G. 2008. Combined numerical and geomorphological reconstruction of the Serra da Estrela plateau icefield, Portugal. *Geomorphology*, 97 (1-2), 190–207.

Villa-Martinez, R. and Moreno, P. 2007. Pollen evidence for variations in the southern margin of the westerly winds in SW Patagonia over the last 12,600 years. *Quaternary Research*, 68, 400–409.

Warren, C. and Sugden, D. 1993. The Patagonian Icefields: a glaciological review. *Arctic and Alpine Research*, 25, 4, 316–331.

## CHAPTER I:

### FACTORS CONTROLLING ALPINE GLACIATIONS IN THE SIERRA BAGUALES MOUNTAIN RANGE OF SOUTHERN PATAGONIA (50° S), INFERRED FROM THE MORPHOMETRIC ANALYSIS OF GLACIAL CIRQUES

**Factores de control sobre las glaciaciones alpinas del cordón montañoso de Sierra Baguales (50° S), inferidos del análisis morfométrico de circos glaciales.**

*Paper submitted to Andean Geology*

José M. Araos<sup>1,2\*</sup>, Jacobus P. Le Roux<sup>1,3</sup>, Michael R. Kaplan<sup>4</sup>, Matteo Spagnolo<sup>5</sup>.

<sup>1</sup> Programa de Doctorado en Ciencias, mención Geología. Departamento de Geología, Facultad de Ciencias Físicas y Matemáticas, Universidad de Chile, Plaza Ercilla # 803, Santiago, Chile.

<sup>2</sup> Departamento de Geografía. Facultad de Ciencias Sociales. Universidad Alberto Hurtado, Cienfuegos # 41, Santiago, Chile.

<sup>3</sup> Andean Geothermal Centre of Excellence, Universidad de Chile, Plaza Ercilla # 803, Santiago, Chile.

<sup>4</sup> LDEO of Columbia University, Palisades, NY, USA.

<sup>5</sup> School of Geosciences, University of Aberdeen, Aberdeen, UK AB243UF

#### **Abstract**

Alpine cirques are characteristic features of a mountainous relief and their morphology can be controlled by climatic and non-climatic variables. The alpine-glaciated Sierra Baguales Mountain Range, forming the eastern foothills of the Southern Patagonian Andes, has well-developed cirques that present an ideal opportunity to study the factors that control cirque morphology. A hundred and forty-three cirques were described with

reference to 14 morphometric attributes and analyzed using statistical analysis and GIS methodologies. The cirques were classified into two types using cluster analysis complimented with a composite map technique for the first time applied to cirque analysis. Type 1 cirques represent glacial processes isolated from the Southern Patagonian Icefield, developed under local cold and dry climatic conditions. Type 2 cirques are associated with older, more extensive glacial processes controlled by regional-scale climate variables and the presence of the Pleistocene ice sheet. The results show that the development of most of the cirques is related to erosion by cirque-type glaciers that were controlled mainly by their aspect, exposure to moisture from the Westerly Winds, and cirque floor slope. Finally, it is concluded that the evolution of cirque-type glaciations in the Sierra Baguales Mountain Range was not uniform. Cirque glaciers that developed to the west, near the Southern Patagonian Icefield, were more dynamic, and therefore their cirques experienced more erosion and were enlarged more, than those to the east.

### **Keywords**

Alpine cirque; Sierra Baguales Mountain Range; glacial geomorphology.

### **Resumen**

El cordón montañoso de Sierra Baguales, estribación oriental de Los Andes Patagónicos, muestra evidencia del desarrollo de circos glaciales de tipo alpino, morfologías características del relieve de montaña, cuyo desarrollo puede ser controlado por variables climáticas y no climáticas. El área de estudio representa por tanto, un sitio ideal para estimar aquellos factores que controlaron el desarrollo de glacitaciones confinadas a circos glaciales. Ciento cuarenta y tres de estos circos fueron estudiados considerando 14 atributos morfométricos, estos fueron analizados mediante el uso de Sistemas de Información Geográfica (SIG) y metodologías estadísticas. Un análisis de conglomerados, complementado con el desarrollo de un mapa compuesto, técnica aplicada por primera vez en el análisis de circos glaciales, permitió diferenciar dos tipos de circos glaciales: El tipo 1 representa circos aislados del Campo de Hielo Sur, cuyos glaciares se desarrollaron bajo condiciones climáticas frías y secas, de carácter local. El tipo 2 representa circos asociados a glacitaciones más extensas y

antiguas, donde los glaciares se desarrollaron bajo condiciones climáticas de escala regional y la influencia del Campo de Hielo Sur. Los resultados muestran que las glaciaciones alpinas fueron controladas por factores tales como la exposición de los glaciares a la radiación solar y a los vientos del oeste (Westerlies), además de la pendiente del piso de los circos glaciales. El desarrollo de estas glaciaciones no fue uniforme, puesto que los glaciares alpinos más cercanos al Campo de Hielo Sur fueron más masivos y dinámicos en comparación a aquellos ubicados hacia el oriente de la estribación andina.

### **Palabras clave**

Circos alpinos, cordón montañoso de Sierra Baguales, geomorfología glacial.

### **Introduction**

The Cenozoic history of the southern Andes has been largely influenced by the relationship between tectonic uplift, climate, and glaciations (Montgomery *et al.*, 2001; Ramos and Ghiglione, 2008; Kaplan *et al.*, 2009). The region contains ample geomorphological evidence of continental glaciations of different ages and extents (Rabassa and Coronato, 2009; Rabassa *et al.*, 2011). This is especially true for the outlet glaciers of the Southern Patagonian Icefield (SPIF), the dynamics of which were related to climate, in particular the latitudinal displacement and changes in the intensity of the Westerly Winds (Hulton *et al.*, 1994; McCulloch *et al.*, 2000; Hulton *et al.*, 2002; Rabassa *et al.*, 2005; Sugden *et al.*, 2005; Rodbell *et al.*, 2009). However, far less attention has been paid to the characteristics and behavior of former alpine glaciations in southern South America, specifically individual and small, independent cirque glaciers that have developed, evolved, and in many cases disappeared in the proximity of the SPIF.

The study of alpine-glaciated landscapes in Patagonia is important, because they provide a sensitive proxy for paleoclimate settings. Geomorphological evidence is useful to highlight the factors that controlled the development of cirque-type glaciation, such as the regional snow-line dominant wind direction, rain shadow, and insolation effects (e.g. Evans, 1977; Olyphant, 1981; Federici and Spagnolo, 2004; Evans, 2006; Hughes *et al.*, 2007; Křížek *et al.*, 2012; Delmas *et al.*, 2013; Barr and Spagnolo, 2015).

In this study, we examine glacial cirque features in the Sierra Baguales Mountain Range (SBMR), a large glaciated range beyond the main cordillera spine, topographically isolated from the SPIF, and influenced by the core of the Westerlies (Villa-Martinez and Moreno, 2007). Some of the most typical and frequent SBMR glacial landforms are cirques, many of which are still occupied by small glaciers or permanent snow patches.

The aims of this study are to describe and analyze glacial cirques located around 50° S, in an area which had not been investigated before, and to evaluate the possible controlling factors in their development. Our description of the morphometric characteristics of glacial cirques is based on the interpretation of aerial photos, satellite images and field mapping. Data analysis was conducted using GIS and statistical software.

## **Study area**

### **Geologic and climatical setting**

The Andean Patagonian Massif was formed during the second and third stages of the Andean Tectonic Cycle (late Early Jurassic-Present), and is a product of subduction accompanied by a succession of extensional and contractional episodes related to changes in the dynamics, geometry and convergence speed of the Farallon and South American Plates (Charrier *et al.*, 2007). The Andean Massif forms an arc that corresponds to the western boundary of the Magallanes Basin (Ramos, 1989; Diraison *et al.*, 2000).

Uplift of the Patagonian Andes was produced mainly by a strong increase in the convergence rate and a decrease in the obliquity between the plates (Charrier *et al.*, 2007; Ramos and Ghiglione, 2008). At about 14 Myr, the Andean massif reached its maximum elevation and the rain shadow effect intensified, continuing throughout the Quaternary. According to Ramos and Ghiglione (2008), the orographic effect of the Andes generated a climatic contrast in southern Patagonia and influenced the styles of development of continental and alpine glaciations during the Last Glacial Maximum (LGM), as well as during prior cold periods.

The study area is presently characterized by a cold temperate climate, with a significant west-east rainfall and temperature gradient associated with the presence of the Andes. Cyclones involving the Westerly Winds originate in the polar front, generating high amounts of rainfall and low temperatures that directly affect the local climate (Garreaud, 2007). West of the study area, the annual precipitation reaches up to 10,000 mm in the accumulation zone of the SPIF (Cassasa *et al.*, 2014), but further east (including the sector focused on here), the climate becomes drier and the annual precipitation only reaches 200 mm at Lago Argentino (Strelin *et al.*, 2011). To the south of the SBMR, a weather station (< 100 m altitude) at Torres del Paine records an annual precipitation of about 700 mm (Peña and Gutiérrez, 1992).

The SBMR, largely drained by the Baguales River, is located between 50° 44' S and 72° 24' W, and comprises part of the foothills of the Southern Patagonian Andes. In some parts of the SBMR the cirques are developed over sedimentary rocks of the Eocene Man Aike Formation, a sequence of shales, sandstones and conglomerates with numerous mollusk fossils that overlies the Cretaceous Dorothea Formation and is, in turn, overlain by continental shales and sandstones rich in plant fossils belonging to the Río Leona Formation. The latter is followed by sandstones, conglomerates and mudstones of the Estancia 25 de Mayo and Santa Cruz Formations (Le Roux *et al.*, 2010; Bostelmann *et al.*, 2013). Gutiérrez *et al.* (2013) mentioned that the Estancia 25 de Mayo Formation is intruded by laccolith-type plutons and olivine-gabbro sills. In other parts of the SBMR, the cirques are developed on these volcanic units.

## **Geomorphology**

Previous studies discussed various aspects of the glacial geomorphology of the region (Marden, 1997; Fogwill and Kubik, 2005; Glasser *et al.*, 2008; Strelin *et al.*, 2011; Garcia *et al.*, 2012; Solari *et al.*, 2012). These studies showed that between 50° and 51° S, the valleys distributed along the eastern margin of the SPIF contain moraine systems that indicate the action of effluent glaciers from the SPIF. In contrast, we focused on the SBMR where glacial cirques provide evidence of mainly an alpine (non-ice sheet) style of glaciation (Fig. 2.1). According to aerial photographs and satellite imagery, plus field observations, it is clear that some of the cirques in the SBMR and its surroundings are still occupied by glaciers. Cirques have been subject to different erosion processes (Fig.

2.2) as testified, for example, by the presence of mass wasting deposits on the cirque flanks and floors. Some cirques host remnants of ancient moraine-dammed lakes, and there is also evidence of eroded remnants of lateral moraines (Fig. 2.3), besides faceted and striated blocks of different sizes (Fig. 2.4).

No direct age control for the age of last occupancy is available for the glacier cirques or the SBMR. However, we can establish a tentative framework for the chronology of glacial variations based on nearby studies. For cirques located near the current SPIF in areas covered by the Pleistocene ice sheet (Fig. 2.1), we infer that deglaciation started between ~17 and 15 Kyr (McCulloch *et al.*, 2000; Sagredo *et al.*, 2011; Strelin *et al.*, 2011). West of the SBMR, the Southern Andes underwent substantial ice regrowth during the Late Glacial Interval or Antarctic Cold Reversal (ACR), from ~14 to 13 Kyr (Fogwill and Kubik, 2005; Moreno *et al.*, 2010; Strelin *et al.*, 2011). By implication, we infer that cirques in the study area were re-occupied during the ACR. Subsequently, glaciers in the nearby Andes experienced repeated fluctuations throughout the Holocene (e.g., Strelin *et al.*, 2014). We consider that the SBMR cirques, at least those currently occupied by ice, experienced similar variability. However, it remains unclear whether cirques without glaciers were reoccupied during the Holocene. Future studies will help to define the timing of cirque glacier activity throughout the study area and test the assumptions above.

## **Methodology**

A total of 143 glacial cirques were identified and mapped. Mapping was carried out using (i) topographic maps at a scale of 1:50,000 (Portezuelo Baguales, Cerro La Mesa, Sierra Contreras) of the Chilean Instituto Geográfico Militar (IGM), (ii) aerial photographs at a scale of 1:70,000 obtained from the Servicio Aerofotogramétrico of the Chilean Air Force (SAF). And (iii) Landsat imagery and digital elevation models (ASTERGDEM, with a resolution of 1 arc-second, and GMTDE2010, with a resolution of 7.5 arc-second) obtained from the USGS Earth Explorer website (<http://earthexplorer.usgs.gov/>) (Table 1.1). Three field campaigns were carried out during 2013 and 2014 to map cirques and observe, describe and interpret the general geomorphology of the SBMR.

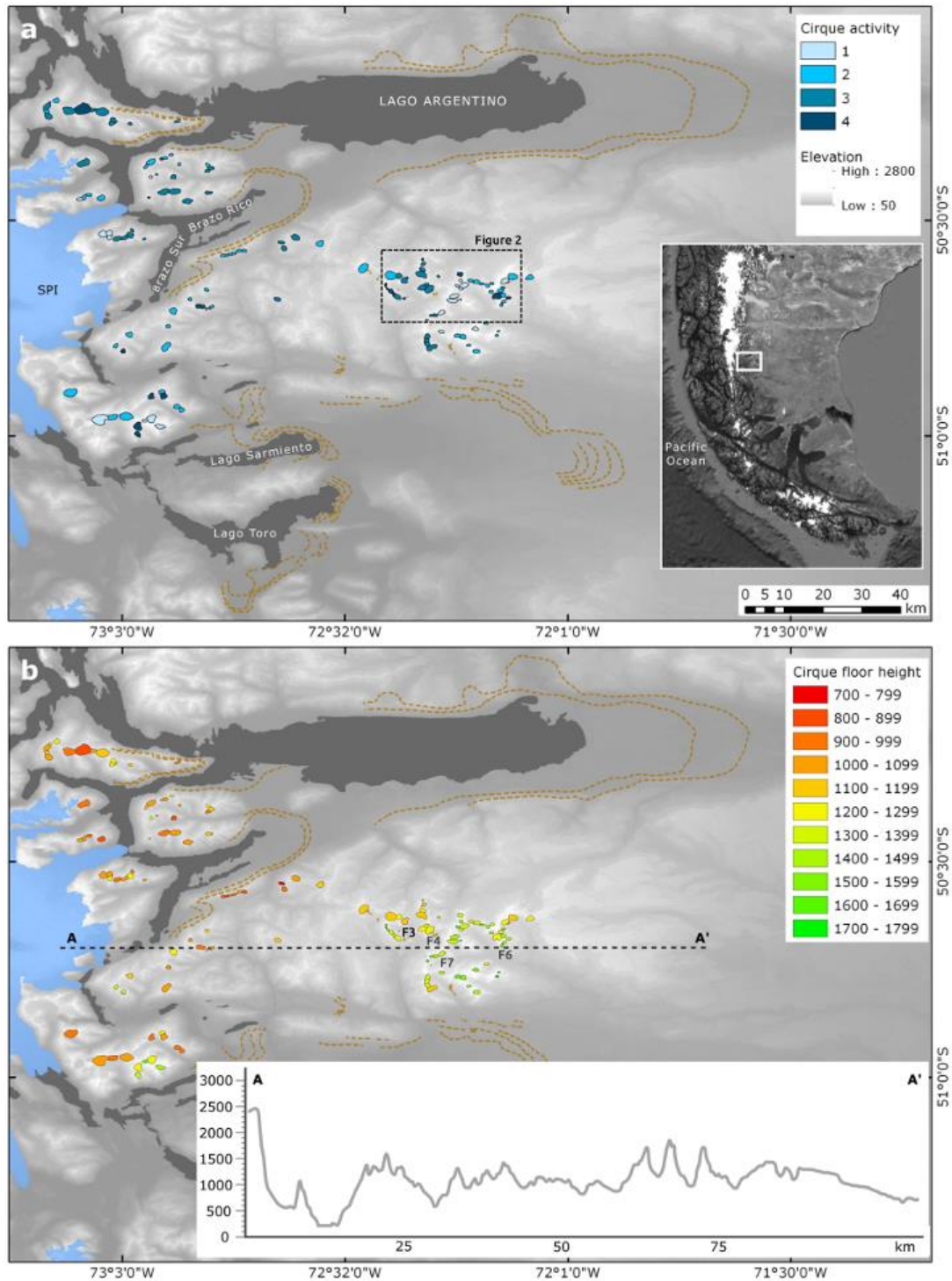


Figure 2.1 a. Right box shows the location of the study area. Elevations were obtained from the SRTM model. The brown dotted line shows the major moraine systems east of Lago Argentino, Brazo Rico and Brazo Sur (Mercer, 1976; Strelin and Malagnino, 2000; and references therein), and south and east of Lago Toro and Lago Sarmiento respectively (Sagredo *et al.*, 2011; Garcia *et al.*, 2013). Cirque activity corresponds to 1). current glacier activity, 2). perennial snow activity, 3). no glacier or snow activity, 4). not categorized. Figure 2.1 b. Mapped cirque floor elevations, which



show the increase in elevation towards the east. A – A' shows a topographic profile from the SPIF to the easternmost SBMR

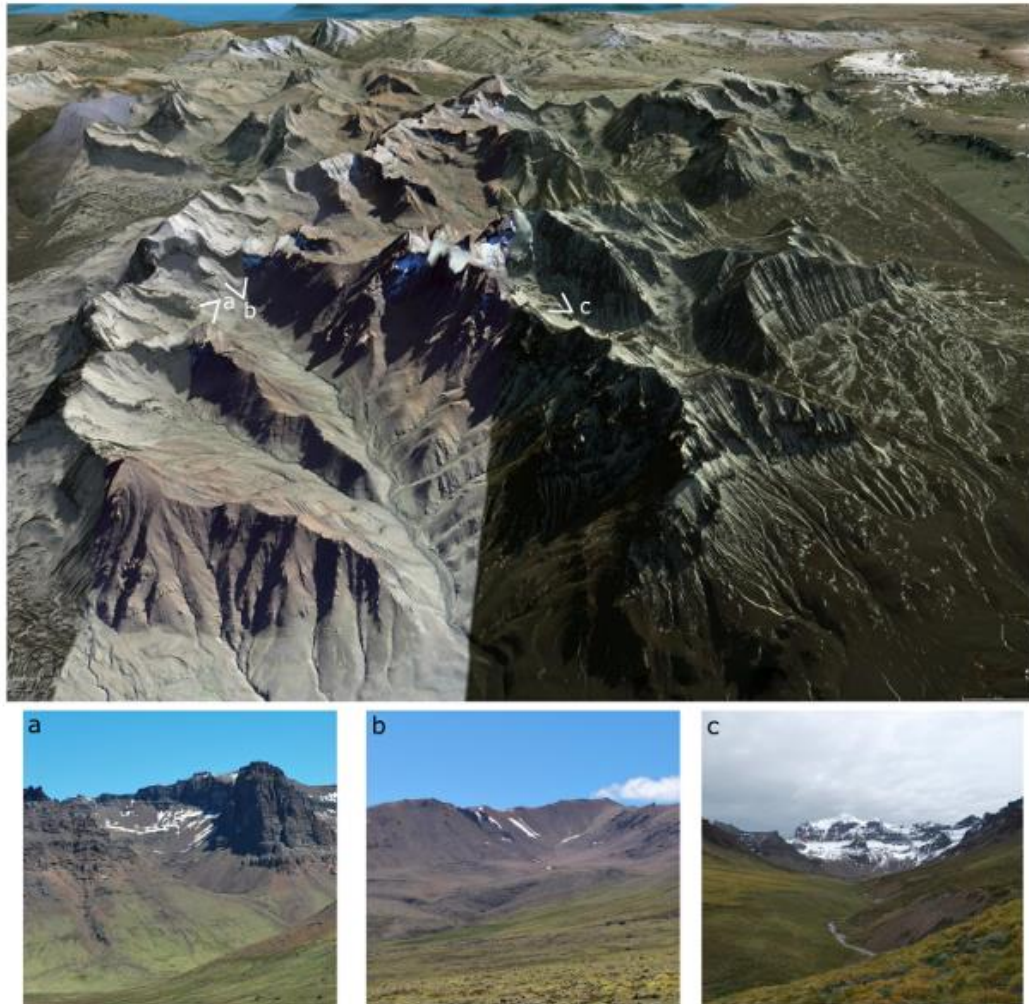


Figure 2.2. Google Earth © image showing the study area from the SW. Photographs a) and b) (see location on Google image) show a hanging valley and glacial cirque, and photo c) shows a glacial valley. Current snow and glacier processes are particularly active along the high elevations on the eastern side of the SBMR (i.e., see Figure. 2.1).



Figure 2.3. Lateral moraine (dark lines) below the cirques shown in figure 2a (F3 in Fig. 2.1b).



**Figure 2.4. Striated erratic (F4 in Fig. 2.1b).**

Data type	Total	Resolution (m)	Vertical accuracy (m)	Date
Aerial photos	12	4	< 10	1998
Landsat 7	3	30		1999 - 2001
Landsat 8	2	15		2013
ASTER GLOBAL DEM	1	10	10-25	2011
GMTED2010	1	26-30	< 10	2010

**Table 1.1. Data source for cirque mapping.**

The identified cirques were digitized on satellite images and aerial photos. These were superimposed on ASTERGDEM and a slope map to provide a suitable topographic context, which is useful in identifying morphologies in areas with complex terrains (Horta *et al.*, 2013). The boundaries of the cirques were defined considering the criteria used by Evans and Cox (1995), Cossart *et al.* (2012), Křížek *et al.* (2012) and Barr and Spagnolo (2013). The crest-lines were considered as the upper limits of the cirques. Lower limits were marked, in some cases, by the crests of frontal moraines. However, for most of the cirques, the lower limit was considered as the transition between the

gentle slope of the cirque floor and an abruptly sloping valley below. Visible topographic features on the photographs, images, and contour levels, were also considered in the definition of the cirque limits, including lateral moraines (Fig. 2.5).

Each cirque was digitized as a closed polygon with a unique ID number, upon which a table containing associated morphometric information was generated. Calculations of planimetric and hypsometric indices (Křížek *et al.*, 2012) were conducted using the open source software QuantumGIS 2.2 and GRASS 6.0. The calculation of variables such as length and width of the cirques was performed in ArcView 3.2.

Following Delmas *et al.* (2013), morphometric variables were defined in such a way as to make them directly comparable with previous work on glacial cirques located in middle and high latitudes around the globe (Evans and Cox, 1974; Aniya and Welch, 1981; Garcia-Ruiz *et al.*, 2000; Federici and Spagnolo, 2004; Evans, 2006; Ruiz-Fernandez *et al.*, 2009; Mindrescu *et al.*, 2010; Křížek and Milda, 2013; Delmás *et al.*, 2013; Gómez-Villar *et al.*, 2015). The variables considered are: surface (S), perimeter (P), length (L), width (W), cirque depth (H), maximum elevation ( $E_{max}$ ), mean elevation ( $E_{med}$ ), minimum elevation ( $E_{min}$ ), aspect (A), ratio of length to elevation range (L/H), ratio of width to elevation range (W/H), ratio of length to width (L/W), mean slope ( $S_{mean}$ ), and circularity (C).

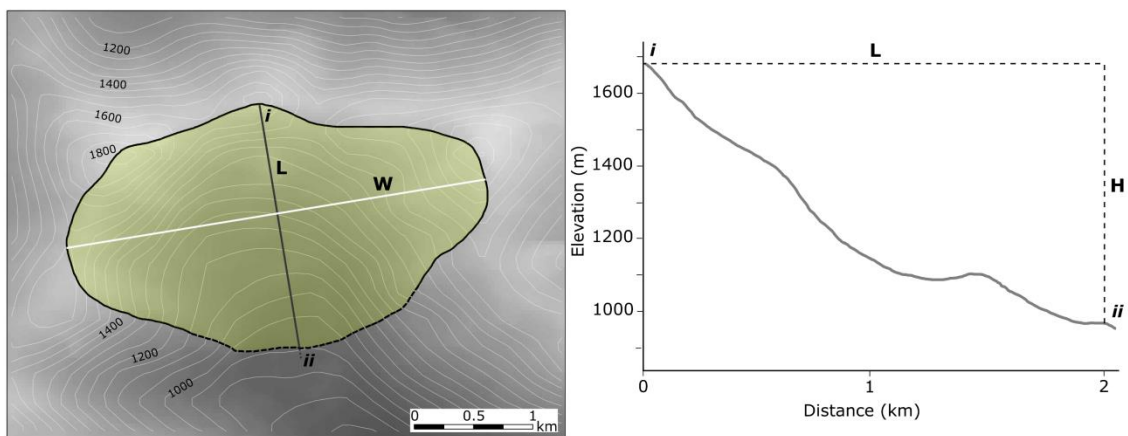


**Figure 2.5. Definition of key morphometric attributes. Left box shows the length (L) and azimuth (for aspect) in a grey line and width (W) in a white dashed line. i - ii correspond to a topographic profile on ASTERGDEM. The right box shows the characteristics of range (H) and the topographic profile.**

Surface (S) corresponds to cirque area estimated in GIS, cirque length (L) was calculated as that of the mean axis line which passes through the midpoint of the cirque's lowest boundary (usually a moraine or a bedrock rim), and divides the surface of the cirque into two equal halves. The width (W) is the longest perpendicular line to the L axis (Federici and Spagnolo, 2004). The cirque depth (H) corresponds to the difference between the maximum elevation ( $E_{max}$ ), defined by the divide located immediately above the glacial cirque, and minimum elevation ( $E_{min}$ ) measured in the lowest part of the cirque, coinciding most of the time with a narrowing between the lateral walls or with a glacial threshold (Aniya and Welch, 1981; Garcia-Ruiz *et al.*, 2000) (Fig. 2.5). Five altitudinal cirque classes were distinguished using the "Jenks" natural breaks classification method, based on a histogram of minimum cirque floor elevation ( $E_{min}$ ): A (113 – 981 m a.s.l.), B (982 – 1,125 m a.s.l.), C (1,126 – 1,292 m a.s.l.), D (1,293 – 1,471 m a.s.l.), and E (1,472 – 1,741 m a.s.l.). Table 1.2 presents a summary of the morphometric characteristics of the cirques in the study area. The estimated elevation of morphometric parameters such as  $E_{max}$ ,  $E_{med}$  and  $E_{min}$  may present an error of  $\pm 50$  m, due to the horizontal and vertical resolution of DEMs (Table 1.1) and possible photo-interpretation errors.

	S	P	L	W	$E_{max}$	$E_{med}$	$E_{min}$	H	A	L/H	W/H	L/W	$S_{mean}$	C
	( $km^2$ )	(m)	(m)	(m)	(m asl)	(m asl)	(m asl)	(m)	(rad)				( $^\circ$ )	
Min	0.093	1.240	210	350	1089	905	721	94	0.15	1.163	1.270	0.447	5.85	1.013
Mean	0.729	3.236	870	1010	1520	1316	1215	320	2.22	2.816	2.987	0.907	2.025	1.065
Average	0.983	3.481	960	1095	1554	1332	1216	339	2.44	3.086	3.473	0.920	21.10	1.075
Max	5.489	8.958	2520	3000	2025	1795	1741	737	5.99	9.292	10.088	1.821	54.28	1.252
Sdev	0.893	1.518	422	514	214	198	208	145	1.20	1.383	1.503	0.248	7.27	0.039

**Table 1.2. Summary of cirque morphometric characteristics.**

The L/H ratio provides insight into the cross-sectional shape of the cirque, W/H describes the extent of the incision, and L/W indicates the planimetric shape of the cirque (Graf, 1976; Garcia-Ruiz *et al.*, 2000; Gómez-Villar *et al.*, 2015). The values of maximum, medium and minimum elevation and slope ( $S_{mean}$ ) were extracted from the ASTERGDEM using GIS tools (Křížek *et al.*, 2012). The aspect (A) was measured using the length axis orientation and expressed in radians (Křížek and Milda, 2013). The circularity (C) was obtained by dividing the perimeter of the cirque by the perimeter of a circumference of a circle that has the same area as the cirque (Aniya and Welch, 1981).

The L/W ratio was used to estimate former activity on cirques, as this parameter is considered to provide insight into the processes that affected their development. For example, cirques that are subject to erosion at their threshold by periglacial and fluvial processes after glaciations typically show L/W ratios  $< 0.5$ ; cirques that are or were extensively/solely occupied by a cirque glacier prior to deglaciation show  $0.5 < L/W$  ratios  $< 1$ ; and cirques that are or were extensively occupied by a valley glacier with a long ablation tongue show an L/W ratio  $> 1$  (Damiani and Panuzzi, 1987; Federici and Spagnolo, 2004; Steffanova and Mentlík, 2007). Also, erosion dominated by cirque-type glaciers should be greatest when ELAs are at or near the cirque floor height, which may occur during the initial stages of glaciation and during glacier retreat. On the other hand, cirque erosion may be minimal if the ELA lies below the cirque floor elevation and consequently glaciers grow into cirque-valley systems.

Each parameter was analyzed in terms of its minimum, maximum and average values. Correlations between dependent (surface, perimeter, length, width, cirque depth, minimum elevation, mean slope and circularity) and independent (maximum elevation, aspect) morphometric variables were detected using Pearson correlation coefficients. The statistical significance was obtained using a t - test with a significance level of  $p = 0.05$ . Morphologically similar cirque groups were identified by tree cluster analysis based on the Ward method and Euclidean distances.

For the first time in a cirque morphometric analysis, a composite map methodology (Le Roux and Rust, 1989; Merriam and Jewett, 1989; Le Roux, 1997; Sepúlveda *et al.*, 2013) was used to assist in the cirque characterization. This technique was originally designed for paleogeographic reconstructions and uranium exploration and is based on the combination of different parameters (characteristics of cirques in this case) into single, combined values, which are eventually plotted on a composite map. The methodology has the advantage that for a specific data point, any number of different parameters pertaining to that location can be combined into a single, non-dimensional value, as long as the inherent meaning of the different parameters are understood. For example, if cirques are classified into two morphological types (1 and 2), type 1 may be characterized by a steep floor slope, small surface area, and small width/length ratio, whereas type 2 could have gentle slopes, large surface areas and high width/length ratios.

For the composite map, because the original parameters are expressed in different dimensions (degrees, km<sup>2</sup>, and a dimensionless ratio), they cannot be combined unless they are first normalized into non-dimensional values with the same range. This is carried out as follows: As a first step, each parameter is allotted a standard percentage value (*S*) given by  $100/n$ , where *n* is the number of morphometric attributes analyzed. In the case above,  $n = 3$ , so that each parameter would have an *S*-value of 33.33. The range of numerical data of each parameter for all the different data points (individual cirques) in the study area is then standardized by using a conversion factor (*C*), given by  $S/(G_h - G_l)$ , where  $G_h$  and  $G_l$  are the highest and lowest values of each parameter for all the cirques. If the slopes of the different cirques range between 2 and 15°, *C* would be  $33.33/(15 - 2) = 2.5638$ . The numerical value  $G_i$  of a specific parameter at each cirque is then converted by first calculating its transition value *T*, given by  $(G_i - G_l)$ , and then by multiplying *T* with the conversion factor *C* of the parameter.

The cirque with the lowest floor slope of 2° would thus have a *T*-value of  $(2 - 2) = 0$ , whereas the cirque with the highest slope would have  $T = (15 - 2) = 13$ . Therefore, the first case would have a new dimensionless slope value of  $0 \times 2.5638 = 0$ , and in the second case,  $13 \times 2.5638 = 33.33$ . A cirque with a 7° slope would have a normalized value of 12.82. The other two parameters will also have a range of normalized, dimensionless values between 0 and 33.33, so that they can easily be combined. However, bearing in mind that type 1 cirques have high slopes but small surface areas and width/length ratios, the converted slope values (*V*) have to be inverted by subtracting them from *S* so that type 1 cirques are reflected by the lowest values of all three parameters. Therefore, for the cirque with the highest floor slope, the inverted slope value (*I*) would be  $33.33 - 33.33 = 0$ , which would coincide with lower surface area and width/length ratio values of type 1 cirques.

Adding the three normalized values for each cirque thus produces a dimensionless combined value (*D<sub>c</sub>*) which reflects the type of cirque or transitions into other cirque types in an unbiased, objective manner. Specific cirques that fall in-between the two morphological classes defined above might have steep slopes and low surface areas but intermediate or high width/length ratios. However, they should still have a lower combined value than type 2 cirques, thus classifying as type 1 cirques, if the

combined value is less than 50. Transitional cirque types, with values between 33.33 and 66.66, can also be considered.

The composite values of all the cirque stations are finally plotted on a map and interpolated, in this case using the Inverse Weighted Distance (IWD) technique in ArcMap. This shows the spatial distribution of the cirque types (Fig. 2.7 in the Results section).

## **Results**

### **Cirque classification according to their activity**

The interpretation of aerial photos, satellite imagery and field work allowed the identification of three cirque categories according to the presence/absence of snow or ice. These categories are distributed from the eastern margin of the SPIF, towards the interior of the continent to the easternmost section of the SBMR (Figs. 2.1, 2. 2):

i) Cirques with current glacier activity (14.7%) (Fig. 2.6), which are mainly located in two areas: surrounding the SPIF (9 cirques) and around the eastern sector of the SBMR (12 cirques) at an average elevation of 1,395 m and 1,544 m, respectively, with a SE aspect bias.

ii) Cirques with perennial snow activity (42%) (Fig. 2.7), distributed as follows: surrounding the SPIF (35 cirques), an intermediate zone, a topographic depression between the Icefield and the adjacent mountain ranges, (6 cirques) and in the eastern sector of the SBMR(20 cirques) with an average elevation of 1,224 m, 1,081 m and 1,537 m, respectively. Aspects ranges are wide, from E to S.

iii) Cirques with no glacier or perennial snow activity (28.7%) (Fig. 2.1 a, b), located in the vicinity of the SPIF (20 cirques), intermediate zone (4 cirques) and the eastern sector of the SBMR (17 cirques) at average elevations of 1,198 m, 1,061 m and 1,367 m respectively. These have a similar aspect as group ii) but with more of an E bias.

Finally, 14.6% (20 cirques) of the entire population was not classified due to a lack of adequate information because of image quality or coverage.



Figure 2.6. Cirque showing evidence of glacier activity, at the easternmost section of the SBMR (F6 in Fig. 2.1b).



Figure 2.7. Cirque showing perennial snow activity (F7 in Fig. 2.1 b).

### Cirque shape

Table 1.2 presents a summary of the morphometric characteristics of the cirques. Surface area values vary between 0.093 km<sup>2</sup> and 5.489 km<sup>2</sup>, with an average value of



0.98±0.1 km<sup>2</sup>. Their length ranges between 210 and 2,520 m, with an average value of 960±35 m. The width varies between 130 and 3,000 m, with an average of 1,095±43 m. Fig. 2.8 shows the frequency distribution of L, W and H. Extreme values for S, L and W are distributed geographically in two particular areas (Fig. 2.1): i) Easternmost section of the SBMR, where the smallest (also the shortest) cirques are located, at an average elevation of 1,700 m; ii) Eastern margin of the SPIF, where the largest and widest cirques are located at an average elevation of 1,000 m. The spatial distribution of the cirque surface areas and shape parameters appear to be a function of the type of cirque activity, which is related to the elevation range, climate and glacial history.

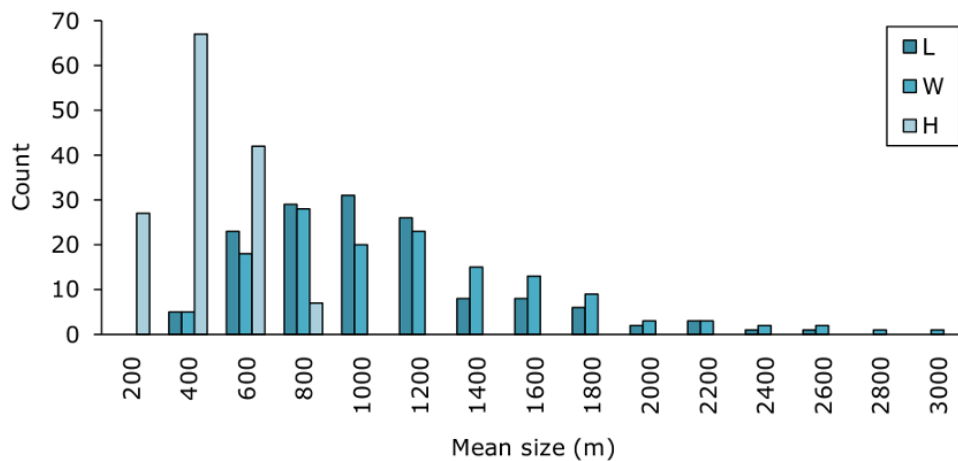


**Figure 2.8. Frequency distribution of L, W and H. Cirque mean surface (km<sup>2</sup>) decreases with an increasing in depth (H). Otherwise, when the average slope becomes gentle (i.e. decrease of H), cirques are most likely to grow longitudinally and laterally. As shown in figure 2.1, large cirques are concentrated along the eastern margin of the SPIF and gradually get smaller towards the interior of the continent around the SBMR.**

The positive and statistically significant correlations between the shape parameters L and S (0.905), and W and S (0.935), shown in Table 1.3, allow us to infer that cirques tend to grow equally in both dimensions. This inference is further reflected by the average value of circularity (Table 1.2), 1.075 illustrating that those cirques tend to maintain a naturally circular shape (Aniya and Welch, 1981).

## Elevation, slope and aspect

Average elevations for  $E_{\min}$ ,  $E_{\text{med}}$  and  $E_{\max}$  correspond to  $1,216\pm 17$  m,  $1,322\pm 17$  m and  $1,554\pm 18$  m, respectively. As shown in Table 1.3,  $E_{\max}$  has a positive correlation with the elevation range, mean slope and parameters that define the shape of cirques (S, L, W). The correlation between  $E_{\min}$  and cirque shape parameters is negative, which is particularly noticeable in the higher sections of the SBMR.

	S	P	L	W	$E_{\max}$	$E_{\text{med}}$	$E_{\min}$	H	A	L/H	W/H	L/W	$S_{\text{mean}}$	C
S	1													
P	0.964	1												
L	0.905	0.919	1											
W	0.935	0.967	0.834	1										
$E_{\max}$	-0.009	0.011	0.003	0.031	1									
$E_{\text{med}}$	-0.279	-0.302	-0.278	-0.287	0.849	1								
$E_{\min}$	-0.372	-0.403	-0.383	-0.375	0.764	0.960	1							
H	0.520	0.593	0.554	0.582	0.379	-0.126	-0.307	1						
A	0.102	0.096	0.191	0.036	-0.157	-0.223	-0.268	0.153	1					
L/H	0.320	0.302	0.423	0.222	-0.358	-0.148	-0.066	-0.433	0.013	1				
W/H	0.414	0.412	0.320	0.450	-0.325	-0.154	-0.068	-0.381	-0.159	0.805	1			
L/W	-0.154	-0.192	0.137	-0.372	-0.115	-0.034	-0.026	-0.133	0.278	0.281	-0.293	1		
$S_{\text{mean}}$	-0.301	-0.293	-0.380	-0.227	0.361	0.167	0.086	0.410	-0.007	-0.789	-0.683	-0.262	1	
C	0.129	0.230	0.052	0.238	0.001	-0.108	-0.090	0.131	-0.116	-0.090	0.107	-0.277	-0.005	1

**Table 1.3. Correlation between analyzed morphometric characteristics. S, P, L, and W parameters have a high positive correlation followed by the altitude range (H). These variables are dependent and determine mainly the shape and cirque development. On the other hand, the  $E_{\text{med}}$ ,  $E_{\min}$  and  $S_{\text{mean}}$  parameters have a weak negative correlation with the shape parameters. Particularly M has a strong negative correlation with the planimetric development and cirque incision. See Table 1.2 for definition of attributes.**

Slope values vary between  $5.9^\circ$  and  $54.3^\circ$  with an average value of  $21.1\pm 0.6^\circ$ . Cirques with steeper slopes show a negative correlation with L/H and W/H ratios (Table 1.3), i.e. the steeper the cirque, the smaller its size. Particularly at greater H, the cross-section and incision of cirques are reduced as the glacier occupied a smaller area thereof, which limited erosion; therefore, these cirques have lower surface areas. Otherwise, gentle slope cirques (i.e. lower H) show larger surface areas and eroded floors.

Aspect values in radians vary in a range between 0.15 and 5.99, averaging  $2.44\pm 0.4$ , showing an E to SE bias (Fig. 2.9). Seventeen cirques ( $11.89\%\pm 1.4\%$ ) have aspect values between 0.2 and 5.3, showing WNW to NE aspects, while 37 cirques ( $25.87\%\pm 3.1\%$ ) are between 2.95 and 4.91, showing S to W aspects. Eighty-nine

cirques, which represent 62.64% of the total, are between 0.98 and 2.95, showing a preponderant aspect of ENE to SSE. The aspect has a positive correlation with L and L/H attributes and a negative correlation with elevation parameters.

Table 1.4 shows a summary of cirque attributes by aspect. Larger cirques show aspects that range from SE to W, and are located in a wide elevation range, from B to E altitudinal classes. Smaller cirques show aspects that range from SSE to N, and are located in higher sectors, mainly in altitudinal classes D and E. Larger cirques show a gradual size increase moving from W to S aspects, and smaller cirques from N to SW aspects. In both cases circularity decreases moving towards S-facing aspects, as here cirques tend to be longer than wider.

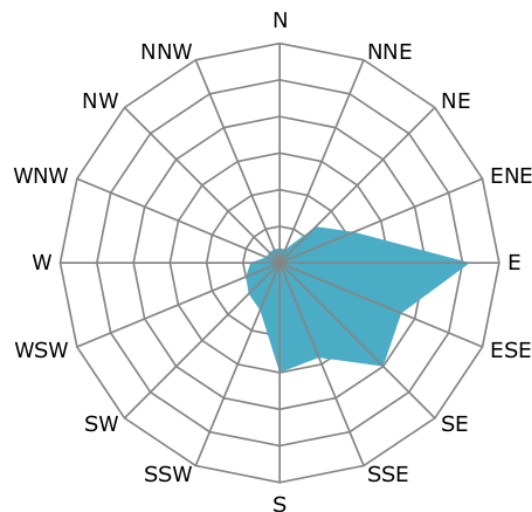


**Figure 2.9.** Rose diagram showing frequency distribution of aspect. Cirques with a SW aspect tend to be located in the intermediate zone and altitudinal range E (1,472 – 1,741 m a.s.l), while cirques with S aspects are preferably located at the SPIF. Otherwise cirques with a S to SE aspect show a homogeneous distribution within the study area and an altitudinal range between C to D (1,126 –1,292 and 1,293 – 1,471 m a.s.l.). Moreover, cirques with W to SW aspects tend to show larger surface areas.

### **L/H W/H and L/W ratios**

The highest L/H values are given by those cirques with NNW, NNE, NE, and S aspects. W/H values are higher in the NNE, ENE NE and S aspects. Considering this,

cirques whose predominant aspect is NE, NNE and S, show broader cross section and deep incision (Table 1.4).

	N	NNE	NE	ENE	E	ESE	SE	SSE	S	SSW	SW	WSW	W	WNW	NW	NNW
Count	2	2	7	11	26	18	20	14	15	7	6	5	4	2	2	2
S	0.568	0.954	0.809	0.742	0.791	1.052	1.341	0.710	1.293	0.780	0.683	1.527	1.600	1.081	0.716	0.452
P	2.727	3.599	3.344	3.048	3.179	3.689	3.944	2.994	3.952	3.281	2.768	4.450	4.462	3.926	3.210	2.565
L	735	840	926	813	824	952	1076	862	1149	1019	848	1330	1233	995	820	920
W	845	1205	1050	1019	1009	1221	1253	918	1159	987	850	1408	1378	1250	1045	600
E <sub>max</sub>	1824	1415	1574	1634	1619	1567	1577	1539	1361	1373	1663	1469	1595	1806	1598	1451
E <sub>med</sub>	1610	1246	1411	1458	1410	1305	1312	1315	1172	1144	1465	1225	1314	1459	1413	1273
E <sub>min</sub>	1506	1123	1308	1351	1302	1209	1194	1198	1054	1005	1312	1073	1155	1283	1296	1216
H	318	292	266	283	317	358	383	341	306	369	351	396	440	523	302	235
L/H	2.336	3.806	3.774	3.047	2.966	2.794	2.846	3.112	3.983	2.888	2.555	3.334	2.885	1.918	2.862	4.007
W/H	2.670	5.088	4.403	3.785	3.588	3.545	3.243	3.178	3.890	2.913	2.569	3.640	3.236	2.395	3.520	2.572
L/W	0.874	0.718	0.869	0.824	0.863	0.830	0.917	0.974	1.058	1.013	1.007	0.941	0.949	0.801	0.803	1.544
S <sub>mean</sub>	22.550	17.535	16.986	21.282	23.312	20.864	20.528	23.807	16.283	20.057	25.527	20.372	23.473	26.525	20.910	14.865
C	1.038	1.062	1.094	1.063	1.086	1.090	1.076	1.062	1.072	1.066	1.049	1.061	1.074	1.077	1.074	1.077

**Table 1.4. Distribution of cirque attributes with aspect. See Table 2 for definition of attributes.**

The descriptive L/W ratio can also be used for classifying cirques according to their former activity (Damiani and Panuzzi, 1987; Federici and Spagnolo, 2004; Steffanova and Mentlík, 2007). In the case of the SBMR, 64% of cirques were occupied for the most part by cirque-type glaciers, while 34% of the cirques flowed into valley glaciers. About 1% of the cirque topography was deeply affected by post-glacial processes such as rock weathering, landslides and deposition. This is consistent with landform preservation, including cirques and alpine-glaciated topography, in the arid rain shadow of the Andes (Rabassa *et al.*, 2011).

### Morphological cirque types

Based on cluster analysis, two morphological cirque types can be distinguished (Fig. 2.10, Table 1.5). They differ mainly in their surface and shape parameters (S, L, W). Type 1, located at the eastern margin of the SPIF and mainly in the higher areas of the SBMR, has a mean surface area of 0.361 km<sup>2</sup> (644 m length and 668 m width), while Type 2, broadly distributed over the study area, has a mean area of 1.487 km<sup>2</sup> (1,215 m length and 1,440 m width). Both types show a similar overall aspect distribution with a S to E bias and a similar mean slope.

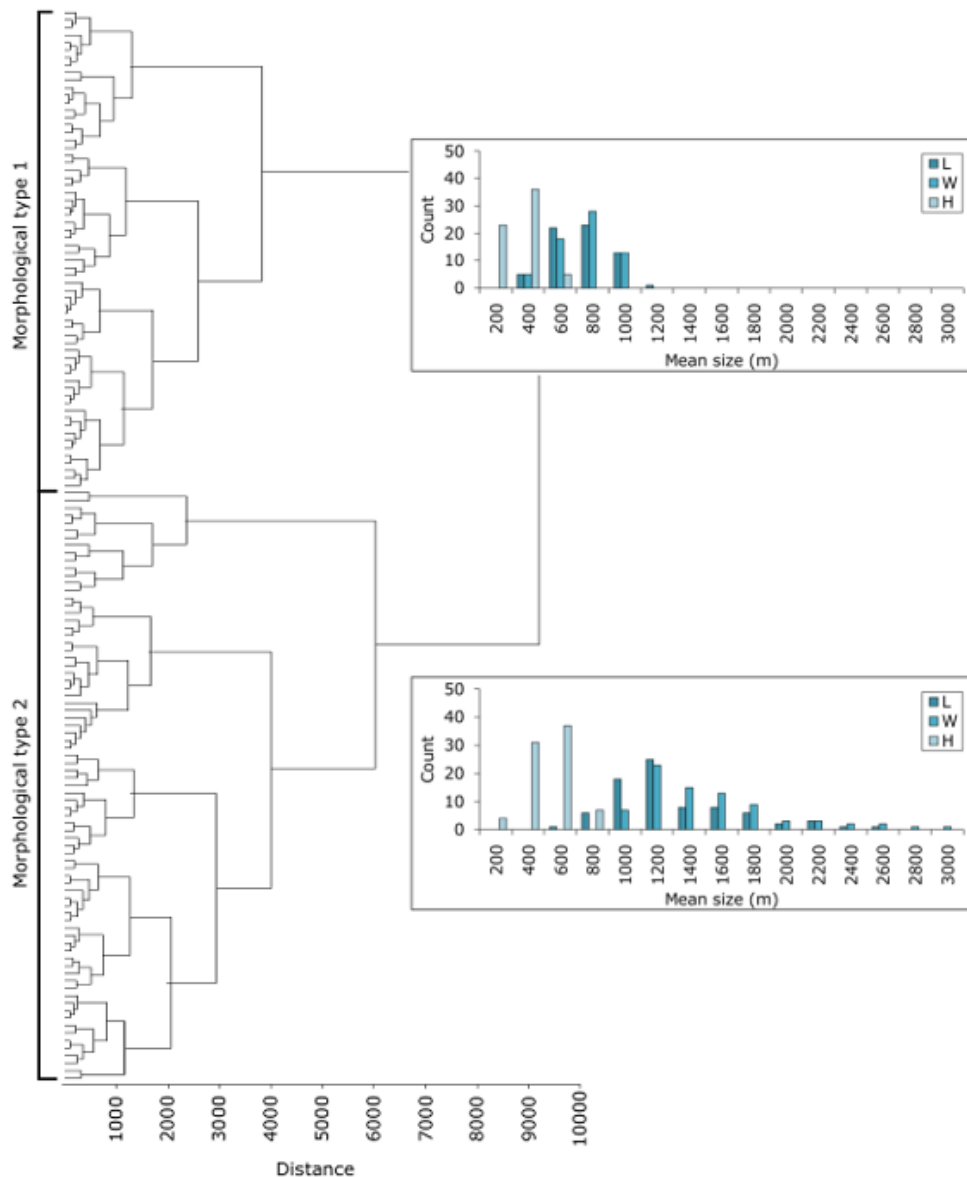


**Figure 2.10. Tree cluster of cirques (Euclidean distance measurements and amalgamation conducted by Ward's method). The analysis shows two major morphological types where the differences are based on the cirque activity (i.e. glacial, perennial snow, or absence of both), surface, shape and spatial distribution. Morphological type 2 tends to show largest cirques compared with the morphological type 1.**

Morphological type 1 shows a cirque floor average elevation of 1,273 m, and these usually show current glacial activity. On the other hand, morphological type 2 shows a cirque floor average elevation of 1,169 m, and usually contains either perennial snow or a lack of snow/ice activity (possibly due to their lower elevation).

This morphological type distribution indicates that the proximity to the SPIF has played a key role in the development of the studied cirques. This could be related to a specific climatic gradient across the region. In particular, it is plausible that the larger cirques near the SPIF were more dynamic due to high ice flux facilitated by higher winter precipitation and summer temperatures (*sensu* Barr and Spagnolo, 2015) than the smaller cirques to the east. The latter hypothesis concurs with the present-day precipitation gradient across the study area.

	Type 1 (64 cirques)			Type 2 (79 cirques)		
	Mean	Median	Standard Deviation	Mean	Median	Standard Deviation
S	0.361	0.347	0.153	1.487	1.206	0.927
P	2.209	2.203	0.496	4.511	4.307	1.264
L	644	650	179	1215	1110	389
W	668	680	161	1440	1320	436
E <sub>max</sub>	1521	1504	228	1581	1563	199
E <sub>med</sub>	1364	1350	224	1305	1281	172
E <sub>min</sub>	1273	1288	237	1169	1175	169
H	248	235	99	413	410	134
A	2.51	2.31	1.25	2.38	2.17	1.16
L/H	2.836	2.596	0.949	3.288	2.906	1.632
W/H	2.993	2.731	1.102	3.863	3.172	1.670
L/W	0.990	0.952	0.272	0.863	0.830	0.212
S <sub>mean</sub>	22.668	21.460	7.531	19.824	19.090	6.835
C	1.064	1.057	0.032	1.083	1.075	0.042

**Table 1.5. Summary statistics of morphometric characteristics for cirque types obtained from cluster analysis. See Table 2 for definition of attributes.**

### Composite map

Composite values of the ten parameters considered, vary between 39.80 and 82.47 (Fig. 2.11). The higher values are related to cirques that show current glacier or perennial snow activity (Figs. 2.6, 2.7), where the predominant aspects range from E to S. These cirques are spatially concentrated in the highest sections (altitudinal cirque classes D and E) of the eastern SPIF and along the high elevations of the eastern side of the SBMR. The high composite values agree spatially with those cirques that were occupied by cirque-type glaciers that show current snow and ice activity, which

increases in elevation to the east of the SBMR. This would be linked to topographical effects (rain shadow) and local weather conditions (temperature descent), which favor snowfall.

Lower values are associated with cirques that show no evidence of present-day glacier or perennial snow activity (e.g., Fig. 2.2 a, b). These cirques have aspects that range from NW to NE and show a broad spatial distribution at lower elevations (altitudinal cirque classes B and C). Lower composite values coincide spatially with cirques extensively occupied by valley glaciers with a long ablation tongues that may have been influenced by activity associated with outlet glaciers from the Pleistocene ice sheet when it existed. The outlet glaciers may have overrun and occupied these cirques, or they may have co-existed with the development of contemporary glaciers in these cirques, which may also have flowed into the valleys and merged with the larger ice mass.

The current cirque activity is mainly controlled by elevation and aspect. On the one hand, the higher elevation enables the development of snow and/or ice activity, particularly in cirques with a gentle slope ( $S_{\text{mean}}$ ) determined by a narrow elevation range (H), which favors snow accumulation. On the other hand, the cirque aspect can favor the persistence of ice or snow coverage, especially if oriented E to SE, due to the effect of lower solar radiation during the warmest part of the day and lower direct sunlight in the afternoon; this effect has already been described in Evans (1977), Evans and Cox (1995), Garcia-Ruiz *et al.* (2000), and Mindrescu *et al.* (2010).

## **Discussion**

The glacial cirques in the SBMR result from the combination of several climatic and non-climatic variables (Delmas *et al.*, 2013; Křížek and Milda, 2013; Ruiz-Fernandez *et al.*, 2009; Evans, 2006; Federici and Spagnolo, 2004). The relative importance of these variables is difficult to rank. Also, it is difficult to estimate the duration of glacial activity based exclusively on morphometric proxy variables. Previous studies have concluded that, based on glacial morphometry, it is difficult to establish clear relationships between independent (environmental factors) and dependent (size and shape of the cirques) variables due to the structural and lithologic complexity of mountain environments. For example, Aniya and Welch (1981) indicate that the

morphological differences between cirques may reflect stages in the cirque development rather than differences in environmental factors. In our opinion the difficulty in separating long and complex histories of cirques from the isolated influences of factors such as altitude, lithology and exposure can be overcome – at least in part – by using statistical analysis to estimate overall relations (*sensu* Ruiz-Fernandez *et al.*, 2009).

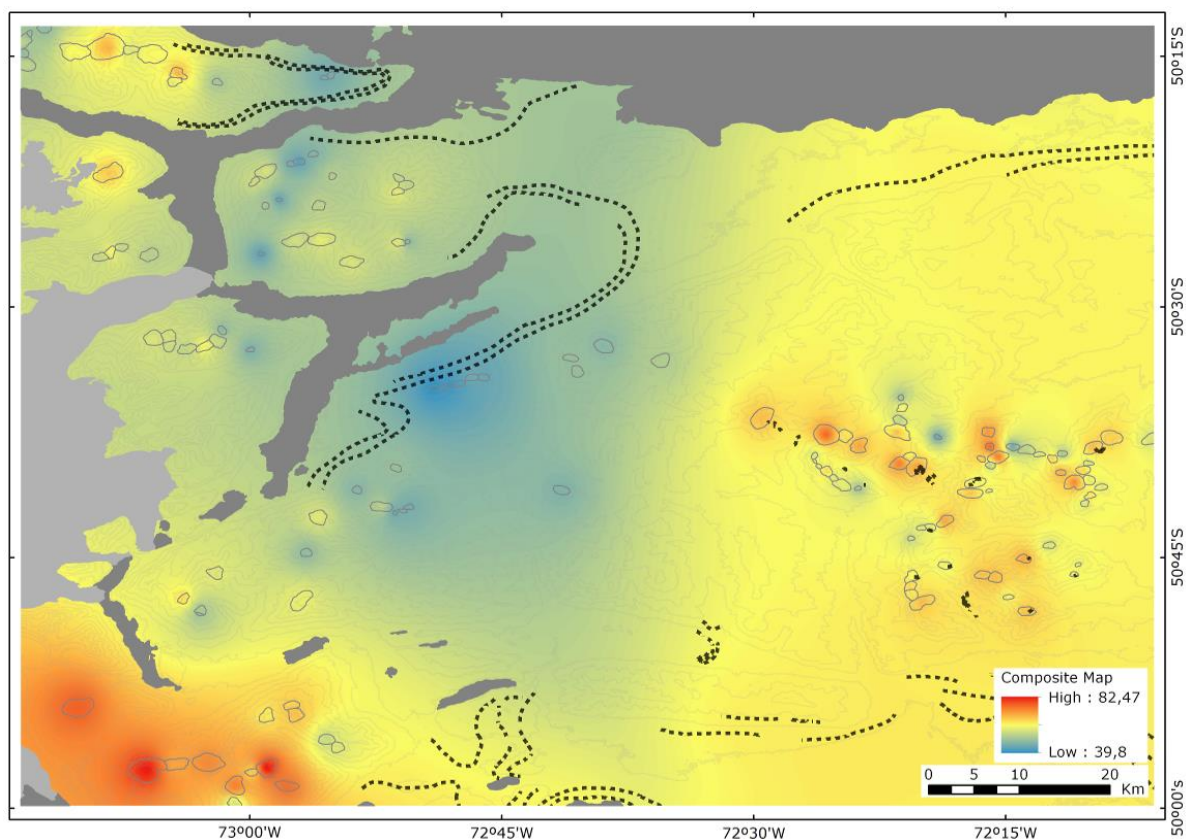


**Figure 2.11. Composite map of study area. Cirques were categorized using 10 parameters extracted from the morphometric analysis (Table 1.2). Black dotted lines show outlines of LGM lobes. Cirque areas closest to the SPIF, such as in the far SW, were partly covered or adjacent to the large ice sheet during the LGM (Garcia *et al.*, 2012; Strelin *et al.*, 2011). This contributed to their higher areal development in relation to those located in the eastern SBMR, which were isolated from the ice sheet outlet lobes. Note that high values show the spatial distribution of currently active snow/ice processes, which particularly for the eastern SBMR, are conditioned by cirque floor elevations (Fig. 2.1) and the rainshadow effect. The lowest values spatially match with evidence of areas covered or adjacent to former outlet glaciers of the SPIF, and cirques with no evidence of current glacier or snow activity.**



Considering the above, we consider that some uncertainties will always remain with regard to the influence of factors such as pre-glacial topography, tectonic structures, as well as the bedrock geology of the SBMR, on the location of the cirques and changes in their surface and shape over time, as well as their overall spatial development.

### **Cirque distribution, elevation and dimensions**

For the SBMR it is possible to differentiate two glaciation limits, where the divide between these is defined by the boundary of the glacial cirque morphological types. The first (Type 1) includes cirques which mainly show evidence of perennial snowy activity, and in some cases evidence of glacial activity. Some of these cirques contain latero-terminal moraines, and are distributed in an elevation range from 1,395 to 1,554 m. On average, these elevations appear to be about 180 m above the altitude limit reached by the former LGM expansion of the SPIF.

The second (Type 2) groups together cirques showing no evidence of current glacial or snow activity and is found at relatively low elevations ranging from 1,198 to 1,367 m, as we move from the SPIF region to the east.

### **Paleoglacial significance**

Topographic and climatic conditions, besides the west to east climate contrast across Patagonia (Glasser *et al.*, 2008) were reflected in the extent and dynamics of Icefields and glaciers during the LGM and subsequent deglaciation. Western Patagonian Ice Sheet glaciers showed a highly dynamic behavior, in part due to high precipitation and a positive mass balance (Hulton *et al.*, 2002), which favored the development of ice sheet glaciations associated with outlet glaciers. These occupied the valleys located west of the SBMR, and east of the present-day SPIF. As soon as the large ice sheet outlet glaciers retreated to the west of the study area, due to an uninterrupted climatic change (i.e., prior to the Late Glacial; Marden, 1997; McCulloch *et al.*, 2000; Sagredo *et al.*, 2011; Strelin *et al.*, 2011; Garcia *et al.*, 2012), the higher sections of the SBMR region could have become dominated by only cirque-type glaciers that prevailed because of sufficiently high elevations and cold enough pre-Holocene temperature conditions (Garreaud, 2007; Villa-Martinez and Moreno, 2007; Moreno *et al.*, 2009).

However, our results indicate that the evolution of cirques in the study area was not uniform. Most likely because of a climatic gradient, cirque glaciers that developed to the west, near the SPIF, were more dynamic, and therefore their cirques experienced more erosion and enlarged more, than those to the east.

Differences in area and shape parameters of morphological types would be linked to the geographical evolution and climate of the study area, as well as aspect, exposure to the Westerly Winds, and elevation. Morphological type 1 cirques, mainly located at altitudinal classes D and E, represent cirques that experienced glacial processes that persisted during the Holocene, isolated from the SPIF and under cold and dry weather conditions towards the interior of continent, this favored the presence of current snow and ice coverage controlled mainly by aspect and local topographic conditions (Figs. 2.1, 2.11). On the other hand, morphological type 2 cirques, mainly located at altitudinal classes B and C, most likely experienced higher precipitation and temperature, meaning that their glaciers were more erosive (Barr and Spagnolo, 2015). Given their lower elevations, these cirques may have also been abandoned by active ice more quickly than the cirques to the east (Figs. 2.1, 2.11).

## **Conclusions**

Uplift of the SBMR was influenced by the tectonic setting that allowed paleogeographic changes to take place east of the Main Andean Range. Given the Westerly Winds, tectonic uplift allowed intensification of the orographic effect, which favored the development of independent alpine glaciers even at relatively low elevations (1,293 to 1,741 m.). This defined a new glacial morphoclimatic setting, which can be considered as a satellite of the SPIF (Mercer, 1967, 1976). Glacier variations associated with this domain have hardly been studied, and represent an opportunity to assess and interpret those factors that enabled the development of individual, small and independent glaciations, which provide a sensitive proxy of past environmental changes in the eastern foothills of the Southern Andes.

The analysis of 14 morphometric parameters and morphological classification of the SBMR glacial cirques, as well as the development of a composite map, in which the morphometric parameters were combined and standardized, suggest that the study area

is characterized by the presence of two glaciations limits related to the climatic and glacial history.

The lower limit, located mainly in an intermediate zone between the eastern margin of the SPIF and lower sections of the SBMR (982 to 1,292 m, at altitudinal classes B to C), has cirques that do not show current evidence of perennial snow activity or glacial processes. The surface and shape of those cirques suggest that they were highly dynamic, i.e. experienced comparatively higher erosion than other cirques in the region.

The upper limit, particularly around the eastern side of the SPIF and in the most elevated sectors (1,293 to 1,741 m, altitudinal classes D to E) of the SBMR has cirques that show mainly perennial snow activity followed by glacial processes and in some cases, remnants of latero-terminal moraines. The surface and shape of these cirques could be influenced by the action of alpine glaciers that persisted throughout the Holocene, due to low temperature and humidity conditions prevailing here.

Along with the climatic gradient, other control factors that favored the development of cirque-type glaciations, mainly around the upper level of the SBMR, include cirque floor elevation, mean slope, aspect and orientation (aspect) relative to the Westerly Winds. Cirques located in the highest sections of the SBMR had favorable conditions for the development of snow and/or ice activity, due to the thermal gradient. Finally, if the cirque floor had a gentle slope this favored accumulation processes, and cirques with an easterly aspect favored the persistence of ice and/or snow cover due to low solar radiation during the warmest part of the day and less direct sunlight in the afternoon.

## **Acknowledgements**

We are grateful for grants from the “Becas de Doctorado en Chile” Scholarships Program and “Gastos Operacionales para Proyecto de Tesis Doctoral” of CONICYT. Juan MacLean and his family kindly allowed access to the farms Las Cumbres and Baguales and Juan Pablo Riquez allowed access to the farm Verdadera Argentina. Juan Carlos Aravena and Rodrigo Villa-Martinez of the Universidad de Magallanes, José Luis Oyarzun, and Juan José San Martín provided much-appreciated logistical support. Ricardo Arce, Mauricio Gonzales, and Carly Peltier lent invaluable assistance in field

activities. Kaplan is supported by NSF BCS 1263474, and Le Roux by Project CONICYT/FONDAP/15090013. This is LDEO contribution XXXX.

## **Bibliography**

Aniya, M., Sato, H., Naruse, R., Skvarca, P. and Casassa, G. 1996. The use of satellite and airborne imagery to inventory outlet glaciers of the Southern Patagonia Icefield, South America. *Photogrammetric Engineering & Remote Sensing*, 62 (12), 1361–1369.

Aniya, M. and Welch, R. 1981. Morphometric analyses of Antarctic cirques from photogrammetric measurements. *Geografiska Annaler, Series A: Physical Geography*, 63 (1/2), 41–53.

Barr, I. and Spagnolo, M. 2015. Glacial cirques as palaeoenvironmental indicators: their potential and limitations. *Earth-Science Reviews*, 151, 48-78.

Barr, I. and Spagnolo, M. 2013. Palaeoglacial and palaeoclimatic conditions in the NW Pacific, as revealed by a morphometric analysis of cirques upon the Kamchatka Peninsula. *Geomorphology*, 192, 15–29.

Bostelmann, J., Le Roux, J.P., Vásquez, A., Gutierrez, N., Oyarzun, J., Carreño, C., Torres, T., Otero, R., Llanos, A., Fanning, M. and Herve, F. 2013. Burdigalian deposits of the Santa Cruz Formation in the Sierra Baguales, Austral (Magallanes) Basin: Age, depositional environment and vertebrate fossils. *Andean Geology*, 40 (3), 458–489.

Carlson, A., Murray, D., Anslow, F., He, F., Singer, B., Liu, Z. and Otto-Bliesner, B. 2010. Assessing the Paleo-forcings of Southeastern Patagonia deglaciation using general circulation model simulations. American Geophysical Union, Fall Meeting 2010, Abstract #GC23H-04.

Carrasco, J., Osorio, R. and Casassa, G. 2008. Secular trend of the equilibrium-line altitude on the western side of the southern Andes, derived from radiosonde and surface observations. *Journal of Glaciology*, 54, 538–550.

Casassa, G., Rodriguez, J. and Loriaux, T. 2014. A new glacier inventory for the Southern Patagonia Icefield and areal changes 1986–2000. In *Global Land Ice Measurements from Space*. Springer, Berlin, pp. 639–660.

Cossart, E., Fort, M., Boulès, D., Braucher, R., Perrier, R. and Siame, L. 2012. Deglaciation pattern during the Late Glacial/Holocene transition in the southern French Alps. Chronological data and geographical reconstruction from the Clarée Valley (upper Durance catchment, southeastern France). *Palaeogeography, Palaeoclimatology, Palaeoecology*, 315–316, 109–123.

Charrier, R., Pinto, L. and Rodriguez, M., 2007. Tectonostratigraphic evolution of the Andean orogen in Chile. In *The Geology of Chile*. The Geological Society Publishing House, Bath, UK. 21–115.

Damiani, A. and Panuzzi, I. 1987. Carta di geomorfologia dinamica in funzione de la pianificazione territoriale. *Boll. Serv. Geol, XCIC*, 77–84.

Delmas, M., Gunnell, Y. and Calvet, M. 2013. Environmental controls on alpine cirque size. *Geomorphology*, 206, 318–329.

Diraison, M., Cobbold, P., Gapais, D., Rossello, E. and Le Corre, C. 2000. Cenozoic crustal thickening, wrenching and rifting in the foothills of the southernmost Andes. *Tectonophysics*, 316, 91–119.

Evans, I. 2006. Allometric development of glacial cirque form: Geological, relief and regional effects on the cirques of Wales. *Geomorphology*, 80 (3–4), 245–266.

Evans, B. and Cox, N. 1995. The form of glacial cirques in the English Lake District, Cumbria, *Zeitschrift für Geomorphologie*, 39 (2), 175–202.

Evans, B. 1977. World wide variations in the direction and concentration of cirque and glacier aspects. *Geografiska Annaler, Series A: Physical Geography*, 59 (3), 151–175.

Evans, I. and Cox, N. 1974. Geomorphometry and the operational definition of cirques. *Area*, 6 (2), 150–153.

Federici, P. and Spagnolo, M. 2004. Morphometric analysis on the size, shape and areal distribution of glacial cirques in the Maritime Alps (Western French – Italian Alps). *Geografiska Annaler, Series A: Physical Geography*, 86 (3), 235–248.

Fogwill, C. and Kubik, P. 2005. A glacial stage spanning the Antarctic Cold Reversal in Torres del Paine (51 ° S), Chile, based on preliminary cosmogenic exposure ages. *Geografiska Annaler, Series A: Physical Geography*, 87 (2), 403–408.

García, J., Kaplan, M., Hall, B., Schaefer, J., Vega, R., Schwartz, R. and Finkel, R. 2012. Glacier expansion in southern Patagonia throughout the Antarctic Cold Reversal. *Geology*, 40 (9), 859–862.

Garcia-Ruiz, J., Gomez-Villar, M., Ortigosa, L. and Marti-Bono, C. 2000. Morphometry of glacial cirques in the central Spanish Pyrenees. *Geografiska Annaler, Series A: Physical Geography*, 82 (4), 433–442.

Garreaud, R. 2007. Precipitation and circulation covariability in the extratropics. *Journal of Climate*, 20, 4789-4797.

Glasser, N., Jansson, K., Harrison, S. and Kleman, J. 2008. The glacial geomorphology and Pleistocene history of South America between 38°S and 56°S. *Quaternary Science Reviews*, 27 (3–4), 365–390.

Gómez-Villar, A., Santos-González, J., González-Gutiérrez, R. and Redondo-Vega, J. 2015. Glacial cirques in the southern side of the Cantabrian Mountains of southwestern Europe. *Geografiska Annaler Series A Physical Geography*, DOI: 10.1111/geoa.12104.

Graf, W. 1976. Cirques as glacier locations. *Arctic and Alpine Research*, 8 (1), 79–90.

Gutierrez, N., Le Roux, J.P., Bostelmann, E., Oyarzun, J., Ugalde, R., Vásquez, A., Otero, R., Araos, J., Carreño, C., Fanning, M., Torres, T. and Herve, F. 2013. Geology and stratigraphy of Sierra Baguales, Ultima Esperanza province, Magallanes, Chile. *Bolletino di Geofisica Teorica ed Applicata*, 54, 327–330.

Horta, L., Busnelli, J., Georgieff, C. and Aschero, C. 2013. Landform analysis of the Pueyrredón Lake area in northwestern Santa Cruz, Argentina. *Quaternary International*, 317, 19–33.

Hughes, P., Gibbard, P. and Woodward, J. 2007. Geological controls on Pleistocene glaciation and cirque form in Greece. *Geomorphology*, 88 (3–4), 242–253.

Hulton, N., Purves, R., McCulloch, R., Sugden, M. and Bentley, M. 2002. The Last Glacial Maximum and deglaciation in southern South America. *Quaternary Science Reviews*, 21, 233–241.

Hulton, N., Sugden, D., Payne, A. and Clapperton, C. 1994. Glacier modeling and the climate of Patagonia during the Last Glacial Maximum. *Quaternary Research*, 42 (1), 1–19.

Kaplan, M., Hein, A., Hubbard, A. and Lax, S. 2009. Can glacial erosion limit the extent of glaciation? *Geomorphology*, 103, 172–179.

Křížek, M. and Milda, P. 2013. The influence of aspect and altitude on the size, shape and spatial distribution of glacial cirques in the High Tatras (Slovakia, Poland). *Geomorphology*, 198, 57–68.

Křížek, M., Vočadlova, K. and Engel, Z. 2012. Cirque overdeepening and their relationship to morphometry. *Geomorphology*, 139–140, 495–505.

Le Roux, J.P., Puratich, J., Mourgues, A., Oyarzun, J., Otero, R., Torres, T. and Herve, F. 2010. Estuary deposits in the Río Baguales Formation (Chattian-Aquitanean), Magallanes Province, Chile. *Andean Geology*, 37 (2), 329–344.

Le Roux, J.P. 1997. Palaeogeographic reconstructions using composite maps, with the case studies from three continents. *Palaeogeography, Palaeoclimatology, Palaeoecology*, 131, 51–63.

Le Roux, J.P. and Rust, I. 1989. Composite facies map: a new aid to palaeo-environmental reconstruction. *South Africa Journal of Geology*, 92, 436–443.

- Marden, C. 1997. Late-glacial fluctuations of South Patagonian Icefield, Torres del Paine National Park, southern Chile. *Quaternary International*, 38–39, 61–68.
- McCulloch, R., Bentley, M., Purves, R., Hulton, N., Sugden, D. and Clapperton, C. 2000. Climatic inferences from glacial and palaeoecological evidence at the last glacial termination, southern South America. *Journal of Quaternary Science*, 15 (4), 409–417.
- Merriam, D. and Jewett, D. 1989. Methods of thematic map comparison. In *Current Trends in Geomatics*, Plenum press, New York, pp. 9–18.
- Mindrescu, M., Evans, I. and Cox, N. 2010. Climatic implications of cirque distribution in the Romanian Carpathians: palaeowind directions during glacial periods. *Journal of Quaternary Science*, 25 (6), 875–888.
- Montgomery, D., Balco, G. and Willett, S. 2001. Climate, tectonics, and the morphology of the Andes. *Geology*, 29 (7), 579–582.
- Moreno, P., Francois, J., Villa-Martinez, R. and Moy, C. 2009. Millennial-scale variability in Southern Hemisphere Westerly Wind activity over the last 5000 years in SW Patagonia. *Quaternary Science Reviews*, 28, 25–38
- Moreno, P., Francois, J., Moy, C. and Villa-Martinez, R. 2010. Covariability of the Southern Westerlies and atmospheric CO<sub>2</sub> during the Holocene. *Geology*, 38 (8), 727–730.
- Olyphant, G. 1981. Allometry and cirque evolution. *Geological Society of America Bulletin*, 92 (9), 679–685.
- Peña, H. and Gutierrez, R. 1992. Statistical analysis of precipitation and air temperature in the Southern Patagonian Icefield. In *Glaciological Researches in Patagonia*, Nagoya, Japanese Society of Snow and Ice, Data Center for Glacier Research, pp. 95–108.
- Rabassa, J., Coronato, A. and Martínez, O. 2011. Late Cenozoic glaciations in Patagonia and Tierra del Fuego: an updated review. *Biological Journal of the Linnean Society*, 103 (25), 316–335.



Rabassa, J. and Coronato, A. 2009. Glaciations in Patagonia and Tierra del Fuego during the Ensenadan Stage/Age (Early Pleistocene–earliest Middle Pleistocene). *Quaternary International*, 210 (1–2), 18–36.

Rabassa, J., Coronato, A. and Salemme, M. 2005. Chronology of the Late Cenozoic Patagonian glaciations and their correlation with biostratigraphic units of the Pampean region (Argentina). *Journal of South American Earth Sciences*, 20 (1–2), 81–103.

Ramos, V. and Ghiglione, M. 2008. Tectonic evolution of the Patagonian Andes. In *The Late Cenozoic of Patagonia and Tierra del Fuego*. Elsevier, Amsterdam, pp. 57–71.

Ramos, V. 1989. Andean foothills structures in northern Magallanes Basin, Argentina. *AAPG Bulletin*, 73, 887–903.

Rodbell, D., Smith, J. and Mark, B. 2009. Glaciation in the Andes during the Late Glacial and Holocene. *Quaternary Science Reviews*, 28 (21–22), 2165–2212.

Rojas, M., Moreno, P., Kageyama, M., Crucifix, M., Hewitt, C., Abe-Ouchi, A., Ohgaito, R., Brady, E. and Hope, P. 2009. The Southern Westerlies during the Last Glacial Maximum in PMIP2 simulation. *Climate Dynamics*, 32, 525–548.

Ruiz-Fernández, J., Poblete-Piedrabuena, M., Serrano-Muela, M., Martí-Bono, C. and García-Ruiz, J. 2009. Morphometry of glacial cirques in the Cantabrian Range (Northwest Spain). *Zeitschrift für Geomorphologie*, 53 (1), 47–68.

Sagredo, E., Rupper, S. and Lowell, T. 2014. Sensitivities of the equilibrium line altitude to temperature and precipitation changes along the Andes. *Quaternary Research*, 81 (2), 355–366.

Sagredo, E., Moreno, P., Villa-Martínez, R., Kaplan, M., Kubik, P. and Stern, C. 2011. Fluctuations of the Última Esperanza ice lobe (52°S), Chilean Patagonia, during the last glacial maximum and termination 1. *Geomorphology*, 125, 92–108.

Sepulveda, S., Le Roux, J.P. and Palma, G. 2013. Application of the composite maps method for landslide susceptibility assessment and its potential use for other natural risk analyses. *Investigaciones Geograficas*, 46, 47–56.

Solari, M.A., Calderon, M., Airo, A., Le Roux, J.P. and Hervé, F. 2012. Evolution of the Great Tehuelche Paleolake in the Torres del Paine National Park of Chilean Patagonia during the Last Glacial Maximum and Holocene. *Andean Geology*, 39, 1-21.

Steffanova, P. and Mentlík, P. 2007. Comparison of morphometric characteristics of cirques in the Bohemian Forest. *Silva Gabreta*, 13 (3), 191–204.

Strelin, J., Kaplan, M., Vandergoes, M., Denton, G., & Schaefer, J. 2014. Holocene glacier history of the Lago Argentino basin, Southern Patagonian Icefield. *Quaternary Science Reviews*, 101, 124–145.

Strelin, J., Denton, G., Vandergoes, M., Ninnemman, U. and Putman, A. 2011. Radiocarbon chronology of the late-glacial Puerto Bandera moraines, Southern Patagonian Icefield, Argentina. *Quaternary Science Reviews*, 30, 2551–2569.

Sudgen, D., Bentley, M., Fogwill, C., Hulton, N., McCulloch, R. and Purves, R. 2005. Late-glacial glacier events in southernmost south America: A blend of “northern” and “southern” hemispheric climatic signals? *Geografiska Annaler, Series A: Physical Geography*, 87 (2), 273–288.

Vieira, G. 2008. Combined numerical and geomorphological reconstruction of the Serra da Estrela plateau icefield, Portugal. *Geomorphology*, 97 (1-2), 190–207.

Villa-Martinez, R. and Moreno, P. 2007. Pollen evidence for variations in the southern margin of the Westerly Winds in SW Patagonia over the last 12,600 years. *Quaternary Research*, 68, 400–409.

## CHAPTER II:

### RELICT GLACIAL LANDSCAPE IN THE SIERRA BAGUALES MOUNTAIN RANGE (50°-51° S): EVIDENCE OF GLACIATION DYNAMICS AND STYLES IN THE EASTERN FOOTHILLS OF THE SOUTHERN PATAGONIAN ANDES.

*Manuscript submitted in the Journal Mountain Science*

Araos, J M<sup>1,2</sup>; Le Roux, J P<sup>1,3</sup>; Gutiérrez, N M<sup>1</sup>.

<sup>1</sup> Programa de Doctorado en Ciencias, mención Geología. Departamento de Geología, Facultad de Ciencias Físicas y Matemáticas, Universidad de Chile, Plaza Ercilla # 803, Santiago, Chile.

<sup>2</sup> Departamento de Geografía. Facultad de Ciencias Sociales. Universidad Alberto Hurtado, Cienfuegos # 41, Santiago, Chile.

<sup>3</sup> Departamento de Geología, Universidad de Chile/AndeanGeothermal Centre of Excellence, Plaza Ercilla # 803, Santiago, Chile.

#### **Abstract**

The glacial morphology of southern South American presents invaluable evidence to reconstruct former glacier behavior and its relation to climate and environmental changes. However, there are still spatial and temporal gaps in the reconstruction of the Holocene Patagonian glacial landscape. Here we present the first geomorphological record for the Sierra Baguales Mountain Range (SBMR), forming the eastern foothills of the Southern Patagonian Andes 200 km from the Pacific coast. This area is topographically isolated from the Southern Patagonian Icefield (SPIF), and is affected by the Westerly Winds.

The study area shows evidence of continental and alpine glaciations related to Andean uplift, which caused a marked climatic contrast between its western and eastern flanks since the Last Glacial Maximum (LGM). The regional rock mass strength and

precipitation gradient acted as a controlling factor in the glacial cirque distribution and sizes, as well as in the development of glaciation styles.

We report new radiocarbon dates related to warm/dry to cold/wet climatic changes during the middle Holocene, when former small alpine glaciers were located in the uppermost section of the SBMR basins, and eventually converged to form a small Icefield at lower elevations. This can be explained by an estimated regional atmospheric temperature drop of  $3.8 \pm 0.8^\circ \text{C}$ , based on a  $585 \pm 26 \text{ m}$  Equilibrium Line Altitude (ELA) descent, inferred by geomorphological evidence and the Accumulation Area Ratio (AAR), in addition to a free-air adiabatic lapse rate. Subsequently, the glaciers receded due to climatic factors including a rise in temperature, as well as non-climatic factors, mainly the glacier bedrock topography.

## **Keywords**

Glacial morphology, Sierra Baguales, continental glaciation, alpine glaciation, middle Holocene.

## **Introduction**

Patagonia has the most complete record of Quaternary glaciations in the world (Mercer, 1983; Clapperton, 1993; Coronato *et al.*, 2004; Rabassa *et al.*, 2005). Its landscape, influenced by a succession of alpine and continental glaciations of different ages and extensions, was first described by Darwin (Clapperton *et al.*, 1993; Rabassa *et al.*, 2005; 2011; Rabassa and Coronato, 2009; Strelin and Malagnino, 2000), and according to Montgomery *et al.* (2001); Ramos and Ghiglione (2008), and Kaplan *et al.* (2009) these glaciations were the result of the interaction between tectonic uplift and large-scale climatic patterns.

Continental glaciations were initially studied in the pioneering work of Nordenskjöld (1899) and Caldenius (1932) on the moraine belts located in the eastern section of Patagonia and Tierra del Fuego, while work was carried out in the Magallanes region by McCulloch *et al.* (2000), Heusser (2003), Coronato *et al.* (2004), and Sugden *et al.* (2005). Further north, research continued in the Los Lagos district (Lowell *et al.*, 1995; Bentley, 1997; Denton *et al.*, 1999) and around Lake Buenos Aires (Kaplan *et al.*,

2004; Douglass and Bockheim, 2006), where features such as terminal and lateral moraines are the clearest record of the Pleistocene glacial expansion in southern South America (Fogwill and Kubik, 2005).

However, in mountainous areas, morphologic and stratigraphic evidence of the spatial distribution and dynamics of alpine glaciers are difficult to observe, since glacial processes may have been eroded or obliterated by extensive ice advance associated with colder conditions, or the effect of fluvial erosion and gravitational processes (Ehlers and Gibbard, 2007; Hughes *et al.*, 2007).

According to Mercer (1983), some older (~7 Ma) glacial deposits can be observed in various locations in Patagonia, where they are located in valleys that currently do not have active glaciers, and could be considered as relict surfaces resulting from the relationship between the orogen development and glacial dynamics (Lagabriele *et al.*, 2010).

The Sierra Baguales Mountain Range (SBMR), a large glaciated area beyond the spine of the Main Andean Cordillera, shows features that can be considered as examples of recent relict surfaces. Located 50 km northeast of the Torres del Paine National Park, it represents the easternmost foothills of the Andes, within the area of influence of the Westerly Winds, and topographically isolated from the Southern Patagonian Icefield (SPIF). Here, in the lower parts of the main valleys, there is evidence of former continental glaciation, while in the upper sections of the major river basins, the morphological evidence indicates the action of alpine glaciation.

Considering that continental ice bodies tend to react slowly to climate change, compared to mountain glaciers that generally react quickly even under small climatic oscillations (Sugden and John, 1976; Vieira, 2008), the SBMR presents a site of interest to study the morphologies produced by different glaciation styles, which presumably showed individual responses to climate changes that occurred since the LGM.

## **Study area**

The SBMR is located in the eastern sector of the fold-and-thrust belt of the Southern Patagonian Andes between 50° and 51° S (Fig.3.1). Here, uplift of the mountain range occurred during the second and third stages of the Andean tectonic cycle (late Early Jurassic-Present), being a product of a series of extensional and

contractional episodes related to a strong increase in the convergence rate and a decrease in the obliquity between the Nazca and South America Plates (Charrier *et al.*, 2007; Ramos and Gigliohne, 2008).

The regional geology is characterized by the presence of a metasedimentary Paleozoic basement (Devonian - Carboniferous) formed by accretion, whereas the overlying lithology consists of Cretaceous sedimentary rocks. The latter include thin sections of marine clastic deposits and limestone, evidencing transgressions of the Pacific and Atlantic Oceans during the Tithonian and Cretaceous, respectively (Ramos and Gigliohne, 2008). Within the SBMR are the Man Aike Formation, a sequence of shales, sandstones and conglomerates with numerous mollusk fossils, overlying the Cretaceous Dorotea Formation and in turn being covered by shales and sandstones rich in continental plant fossils belonging to the Río Leona Formation. The latter is succeeded by the Estancia 25 de Mayo and Santa Cruz Formations (Le Roux *et al.*, 2010; Bostelmann *et al.*, 2013).

The study area is presently characterized by a cold temperate climate, with a significant west-east rainfall and temperature gradient associated with the presence of the Andes. The Westerly Winds generate high amounts of rainfall and low temperatures that directly affect the local climate (Garreaud, 2007). West of the study area, the annual precipitation reaches up to 10,000 mm in the SPIF accumulation zone (Cassasa *et al.*, 2014), but further east, including the sector focused on here, the climate becomes drier and the annual precipitation only reaches 200 mm at Lago Argentino (Strelin *et al.*, 2011). To the south of the SBMR, a weather station at < 100 m altitude in the Torres del Paine National Park records an annual precipitation of about 700 mm (Peña and Gutiérrez, 1992).

Previous studies indicate that the well-preserved till deposits in the vicinity of the Torres de Paine National Park are evidence of a Tardiglacial advance of SPIF outlet glaciers (Marden, 1997; Fogwill and Kubik, 2005). Garcia *et al.* (2012) also indicate that during the Quaternary, the SPIF was the main source of ice in the region, and together with the alpine ridge system fed Paine glaciers flowing eastward (Glasser *et al.*, 2008) and deposited terminal moraines in the sector of Lago Argentino and the Ultima Esperanza Basin (Coronato *et al.*, 2004; Rabassa *et al.*, 2005; Kaplan *et al.*, 2009).

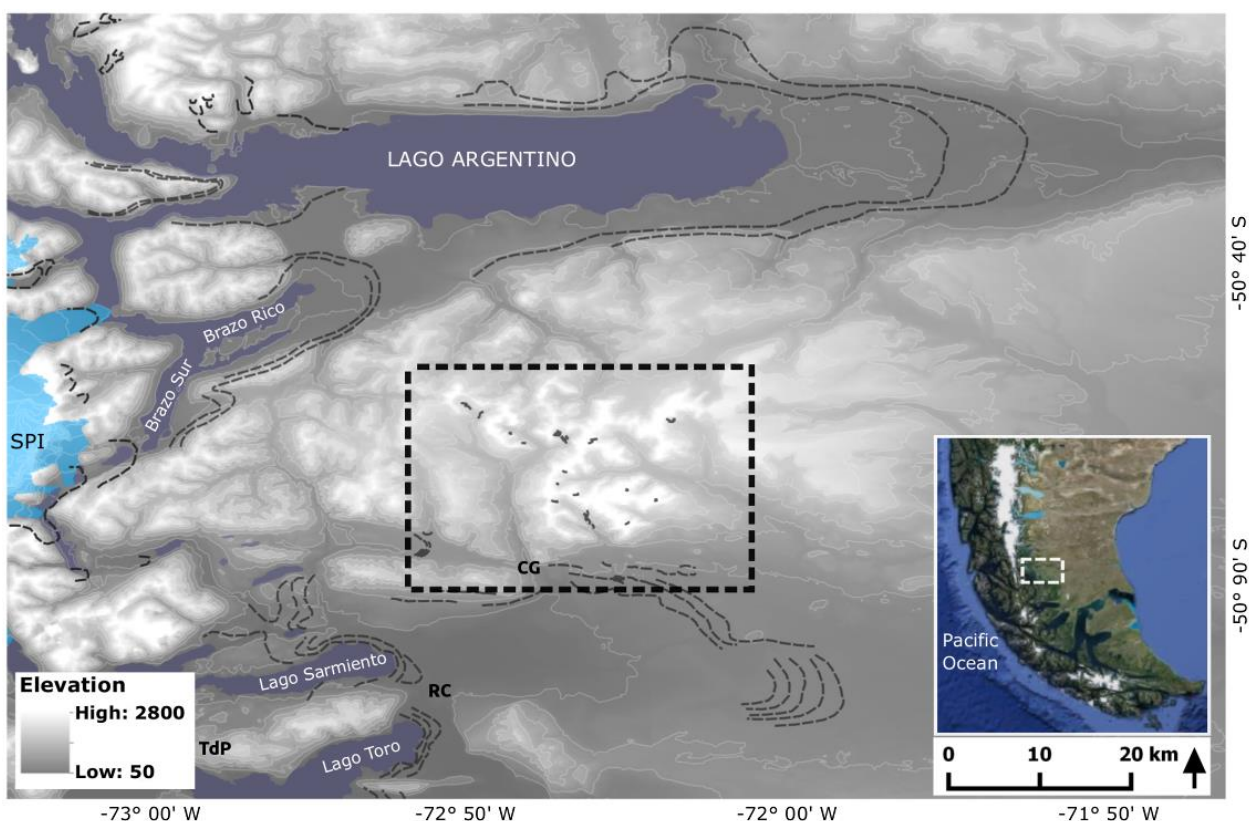


**Figure 3.1.** The right box shows the general location of the study area, and the blackstippled box shows the SBMR. Major lakes appear in dark blue, SPIF is shown in light blue. The black stippled line shows an outline of the mapped moraine systems around Lago Argentino (Strelin and Malagnino, 2009, and references therein, Kaplan *et al.*, 2005; 2008; 2011; Strelin *et al.*, 2014), and Lagos Toro and Sarmiento (Marden, 1997, Sagredo *et al.*, 2011; Garcia *et al.*, 2012). CG: Cerro Guido; RC: Rio Las Chinas; TdP: Torres del Paine, which correspond to meteorological stations of the Direccion General de Aguas (DGA). Elevations were obtained from an SRTM model.

Moreover, the highest sectors of the SBMR are characterized by the presence of several glacial cirques, some of which are still occupied by active glaciers and hanging valleys, which have been subject to various processes of erosion. This may be interpreted as evidence of alpine glaciation that occurred in the highest areas of the mountain ranges.

Considering the particular geographical location of the SBMR, as well as the climatic setting and glacial history of the region, the study area represents a suitable site for the description and analysis of factors involved in the development of different glaciation styles that operated in shaping the relief of southern Patagonia. It can also

cast light on palaeoenvironmental variables that influenced the behaviour of former ice bodies deployed in this sector.

## **Methods**

### **Geomorphological mapping**

In order to identify the characteristics of glacial and periglacial geomorphology of the SBMR, aerial photographs obtained from the Servicio Aerofotogramétrico de la Fuerza Aérea de Chile (SAF), at a scale of 1:70,000, were photo-interpreted using a Sokkia MS27 mirror stereoscope. Interpretation of the geomorphology was supported by the use of topographic maps obtained from the Instituto Geográfico Militar Chileno (IGM) at a scale of 1:50,000 (Portezuelo Baguales, Cerro La Mesa, Sierra Contreras). Satellite images (Landsat 7 ETM + at 30 m resolution) and digital elevation models (ASTERGDEM at 1 arc-second resolution with a vertical uncertainty 10-25 m, and GMTED2010 at 7.5 arc-second resolution with a vertical uncertainty 26-30 m) obtained from the website of the USGS Earth Explorer (<http://earthexplorer.usgs.gov/>), were employed together with images available on Google Earth©.

Previous studies by Mercer (1967, 1976) related to the main moraine systems associated with outlet glaciers of the SPIF, those carried out around Lake Argentino by Strelin and Malagnino (2000) Kaplan *et al.* (2005; 2011), and Strelin *et al.* (2014), and in the surroundings of Lake Sarmiento and Lake Toro by Marden (1997), Sagredo *et al.* (2011), and Garcia *et al.* (2012), were also considered in order to provide a suitable geomorphological and chronological context on a regional scale (Fig. 3.1).

Geomorphological mapping was undertaken using the open source software QuantumGIS, where digitized aerial photographs and satellite images were superimposed on the DEMs to provide a proper topographical context and assist in the identification of relief in areas of complex terrain (Glasser *et al.*, 2008).

During 2013 and 2014, three field surveys reaching a total of eight weeks were carried out in order to validate the preliminary mapping, take samples for dating, and measure stratigraphic sections to identify different sedimentary facies, depositional environments and morphogenetic processes.

The SBMR geology was considered in terms of the rock mass strength, which is a controlling factor in cirque development. References on the geology of the study area



(Le Roux *et al.*, 2010; Bostelmann *et al.*, 2013; Gutierrez *et al.*, 2013), field observations of the Geological Strength Index (GSI) (Marinos *et al.*, 2005), and theoretical parameters to estimate the value of the rock deformation modulus, according to the generalized criterion of Hoek-Brown, using the RocLab© free software (Hoek and Diederichs, 2006), were used to define eight resistance classes (1: 0.854 kg/cm<sup>2</sup>; 2: 1.257 kg/cm<sup>2</sup>; 3: 1.708 kg/cm<sup>2</sup>; 4: 3,576 kg/cm<sup>2</sup>; 5: 4.013 kg/cm<sup>2</sup>; 6: 4.103 kg/cm<sup>2</sup>; 7: 4.684 kg/cm<sup>2</sup>; 8: 5.334 kg/cm<sup>2</sup>) and were compared with the glacial cirque surfaces.

### **Radiocarbon dates**

Three morphostratigraphic sections were selected to collect samples for <sup>14</sup>C dating. Samples were obtained from a peat deposit in a cirque floor located in the western section of the study area and a flat area located downstream of cirques in the upper section of the Baguales River basin, where two former glaciers possibly converged. We were unable to obtain samples from the eastern part of SBMR where active glaciation predominates.

Bulk samples including peat layers, as well as horizons of soil and plant debris (Strelin *et al.*, 2014) were dated by AMS at BETA Analytics Laboratories, where radiocarbon ages were converted to calendar years using the INTCAL13 calibration curve (Talma and Vogel, 1993).

### **ELA estimation and reconstruction of surface profile of former glaciers**

Palaeo-ELA estimation is useful to infer those environmental factors that could influence the development of different glaciation styles (Dahl and Nesje, 1996; Nesje and Dahl, 2000; Benn and Ballantyne, 2005). Foster *et al.* (2008) also stated that ELA behavior can be used as proxy data that can be extrapolated to a regional scale, because the ELA pattern is largely a function of climate (Hostetler and Clark, 1997; Meyer and Wagner, 2008).

The present ELA elevation was obtained from DEM. Cirques were defined as closed polygons in GIS, and their centroids were considered to represent their average elevation (Mitchell and Montgomery, 2006). An AAR ratio of 55% was applied (Nesje, 1992; Nesje and Dahl, 2000), in order to obtain a rough approximation of the ELA elevation for cirques with evidence of current glacial activity (Benn and Lehmkuhl, 2000).

These ELA's represent the active area of glaciation for just a sector of the study area. In order to estimate the ELA elevation during the maximum ice extent, the Porter methodology (1989) was followed. For this purpose, the average SBMR cirque floor elevation was considered as the maximum elevation ( $E_{\max}$ ), whereas the maximum ice extent as estimated by the geomorphological maps of Kaplan *et al.* (2011), Strelin *et al.* (2011), and Garcia *et al.* (2012) was considered as the minimum elevation ( $E_{\min}$ ). Considering both these elevations and the criteria of Mitchell and Montgomery (2006), the former regional ELA elevation can be estimated as the elevation located halfway between  $E_{\max}$  and  $E_{\min}$ .

To characterize the former alpine glaciers and complement the analysis of local and regional behavior of their ELA's, the topographic profiles of some glaciers were reconstructed using the methodology of Been and Hulton (2010). The latter is based on a model of perfect plasticity, which uses the topography of the bed and a yield rate to develop profiles on an Excel<sup>TM</sup> spreadsheet.

### **SBMR temperature variation based on former ELA position**

Glacial records in mountain settings provide valuable clues to the frequency and magnitude of climate change. The areal extent and volume of glacier ice in a drainage basin depends on the history of its mass balance, and the ELA position reflects the mass added to the glacier, which is mainly dependent on winter precipitation and the mass lost during higher summer temperatures (Meierding, 1982).

The ELA can be deduced from climatic variables such as temperature and precipitation (Ohmura *et al.*, 1992). In principle the ELA rises with a temperature increase and/or a precipitation decrease and falls with a temperature decrease and/or precipitation increase. Thus reconstruction of past variations in the ELA is often considered to be a proxy for palaeoclimate (Condom *et al.*, 2007; Putnam *et al.*, 2012; Lorrey *et al.*, 2013).

In order to estimate a first approximation of the SBMR temperature variation during the Tardiglacial maximum ice extent (Kaplan *et al.*, 2011; Strelin *et al.*, 2011; Garcia *et al.*, 2012), the ELA altitudinal variation, determined by the criteria of Mitchell and Montgomery (2006), was considered, in addition to Instrumental records of

atmospheric temperatures at 3 meteorological stations (Table 2.1) at a location close to the study area (Fig. 3.1).

	Latitude (degrees)	Longitude	Elevation (masl)	Available data (years)
Torres del Paine (TdP)	51° 11' 03"	72° 58' 01"	25	2006 - 2016
Rio Las Chinas (RC)	51° 03' 03"	72° 31' 01"	75	2010 - 2014
Cerro Guido (CG)	50° 53' 55"	72° 19' 53"	230	2006 - 2014

**Table 2.1. Meteorological stations and data obtained from the DGA of the Chilean Ministerio de Obras Publicas website (<http://snia.dga.cl/BNAConsultas/reportes>).**

Considering that ELA elevations are sensitive to variations in atmospheric temperature, following Oerlemans (1992), Condom *et al.* (2007), Puttnam *et al.* (2012), and Lorrey *et al.* (2013), an adiabatic lapse rate of  $-6.5^{\circ}\text{C}/\text{km}$  was used to convert the former ELA elevation to temperature, and thus estimate the local temperature descent.

## Results

### Glacial geomorphology

The SBMR is characterized by the presence of several glacial cirques, located at about 1,100 m a.s.l. A smaller number of cirques, concentrated along the eastern edge of the mountain range, and mainly of southern and eastern aspect, have active glaciers and/or snow patches. However, most cirques do not show active glaciers, and have suffered varying degrees of erosion. Generally, the slopes and cirque floors show gravitational deposits and boulders. Those cirques located in the highest section of the basin also show hanging valleys. The geomorphological evidence indicates that the former glaciers located in cirques and on slopes, possibly converged towards the valley where they fed a larger glacier located in the lower section of the Río Baguales basin (Fig. 3.2). On the Pacific side of the Baguales River basin, glacial deposits were largely eroded due to slope processes and fluvial action. On the Atlantic side in the Vizcachas and Pelque River basins, located in a distal section of the SBMR, lateral moraines and some evidence of frontal moraines are better preserved.

The study area shows U-shaped valleys (Fig. 3.3), as well as remnants of lateral moraines in the upper (Fig. 3.4) and lower (Fig. 3.5) sections of the Baguales River

basin, and particularly in the upper sections of the Pelque and Vizcachas River basins. In the middle section of the Baguales River basin there is field evidence of hummocky terrains (Fig. 3.6) and kame terraces (Fig. 3.7), as can also be observed on a topographic profile of the Baguales River (Fig. 3.8). Such evidence is useful to support the hypothesis of the existence of a former Icefield in the middle section of the Baguales River basin.

The decrease in height of the lateral moraines in the upper basins can be considered as an indicator of flow and possible periods of stagnant ice. The absence of push moraine could indicate that the deglaciation process was continuous, with no evidence of ice re-advances. However, it should be borne in mind that this kind of moraine could have been eroded by fluvial processes, thus limiting the interpretation of the behavior of these ancient glaciers.

South of the SBMR are well preserved moraine deposits, previously studied and mapped by Garcia *et al.* (2012). They represent evidence of continental glaciations related to outlet glaciers of the SPIF (Fig. 3.1; Major moraine systems in Fig. 3.2). However, the larger glacier located in the lower section of the Baguales River basin apparently ended in an outwash plain at the foot of the SBMR, for which there is ample evidence in deposits along the eastern side of the Baguales River.

Figure 3.9 compares the surface areas of cirques with the bedrock cohesive strength. The cirque surface areas reach a maximum in the middle sector of the Baguales River basin, where the existence of a small Icefield or at least a larger valley glacier resulting from coalescing alpine glaciers is indicated by geomorphological evidence. To the west of this central area, cirque sizes are slightly larger than to the east thereof, which could be attributed to the lesser rock strength as well as the marked west–east rainfall gradient. To the east, smaller cirques can be related to the higher rock strength, lower precipitation, and consequently thinner alpine glaciers.

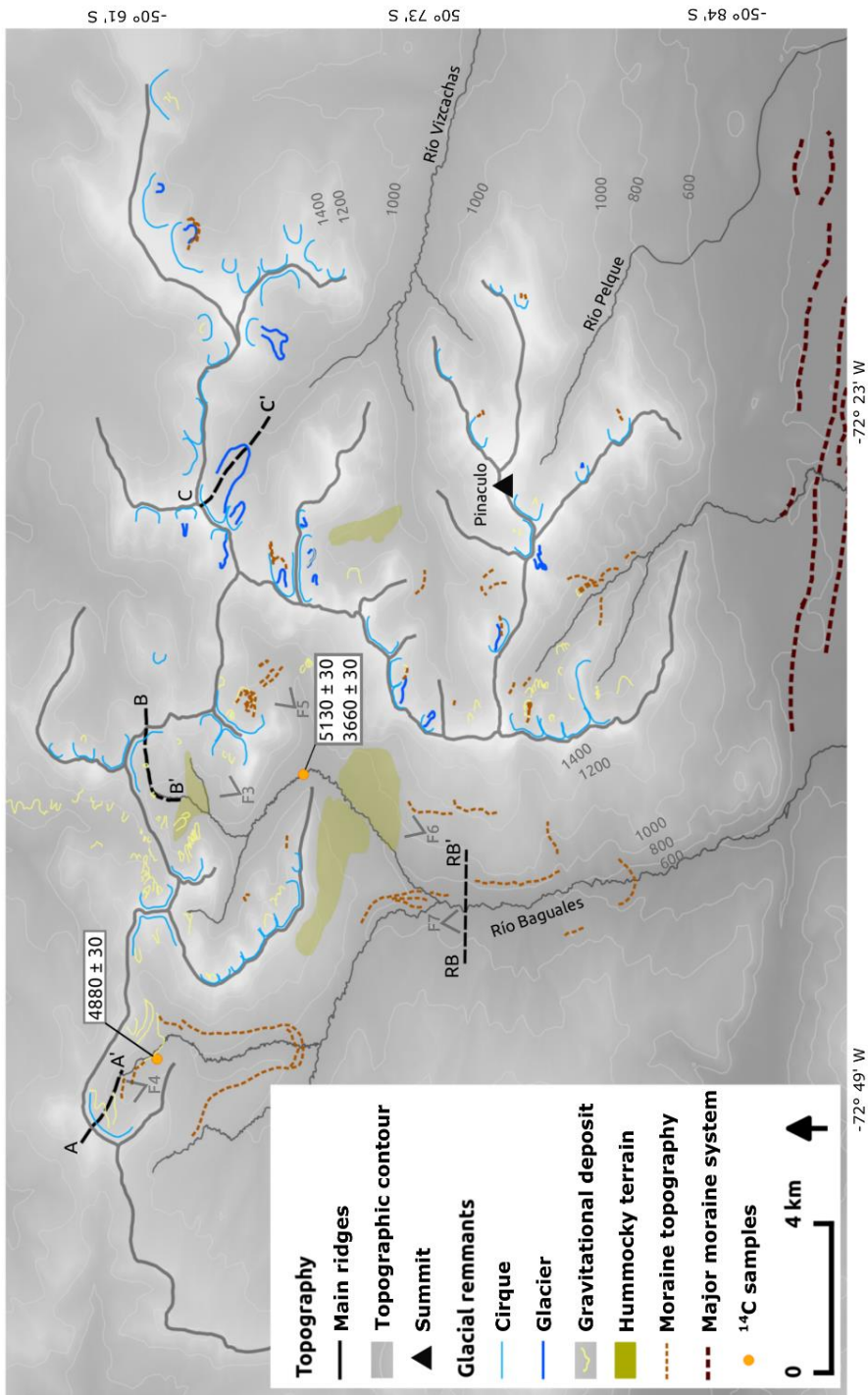


Figure 3.2. SBMR glacial geomorphology. White boxes show the location of samples for radiocarbon dating. RB-RB` shows the location of the topographic profile (Figure 3.8). AA`, BB`, CC` show the former surface topography of alpine glaciers (Figure 3.10).



Figure 3.3. U-shaped valley in the area where the former Alpine glaciers coalesced to form a small Icefield (F3 in Fig. 3.2).



Figure 3.4. Remnant of lateral moraine and boulders deposited and aligned with the moraine (F4 in Fig. 3.2).



**Figure 3.5. Lateral moraine and boulders below the U-shaped valley shown in Figure 3 (F5 in Fig. 3.2).**



**Figure 3.6. Hummocky terrain and remnants of lateral moraine. These deposits, located in the middle section of the Baguales River basin, constitute evidence of a former Icefield (F6 in Fig. 3.2).**



Figure 3.7. Eroded kame terraces along the Baguales River (see also Figure 3.8) (F7 in Fig. 3.2).

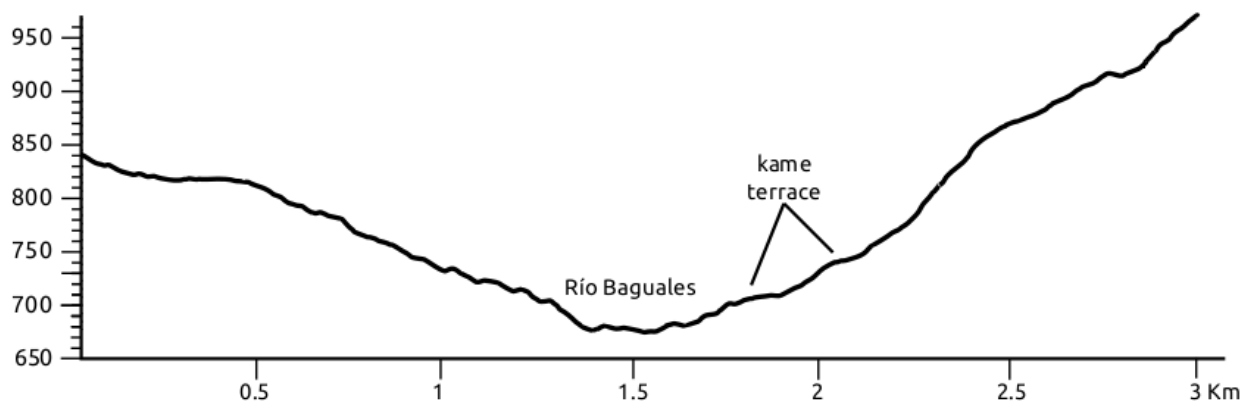
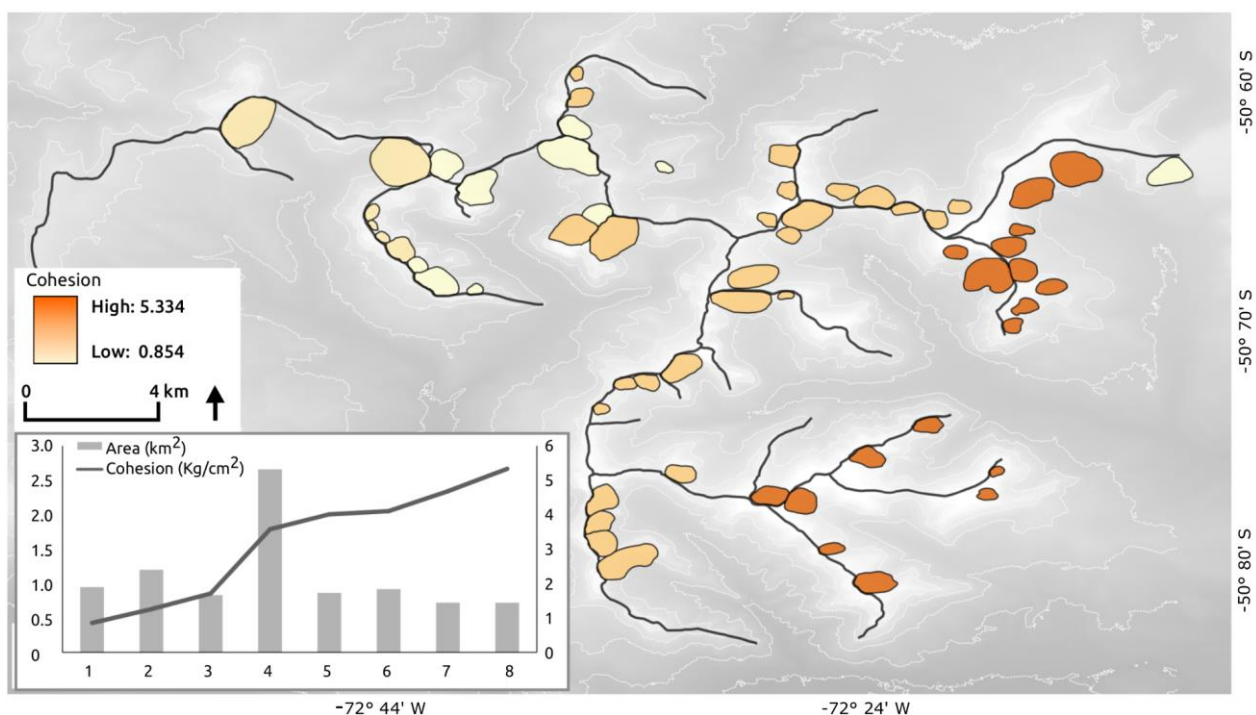


Figure 3.8. RB-RB' topographic profile.





**Figure 3.9. Spatial distribution of rock mass strength in SBMR, the box on the left shows that at greater rock resistance cirque areas tend to decrease.**

### Radiocarbon dates

Three <sup>14</sup>C dates ages were obtained from peat deposits, viz. 4,880±30 Kyr for a cirque floor located west of the study area, and 5,130±30 - 3,660±30 Kyr for samples from the middle-upper section of the Baguales River basin, where two glaciers possibly converged (Fig. 3.2). The glaciers located in this area flowed southward to join a former valley glacier located in the lower section of the basin.

These minimum ages are related to the onset of organic sedimentation in the bogs after a warm/dry to cold/wet climatic change around 6 Kyr (Neoglacial). However, it is also possible that these ages are related to glacial advances that occurred in the Frias Lobe, located west of the SBMR, during the mid-Holocene (Strelin *et al.*, 2014). Nevertheless, taking into account the potential <sup>14</sup>C reservoir effect, these ages must be considered with caution, and as only a first approximation to the environmental changes that operated in the study area.

## **ELA behavior and temperature variation**

The current ELA for active glaciers in the SBMR, whose aspects vary from southern to eastern, is about  $1,146\pm 45$  m, approximately 400 m above the estimated ELA for outlet glaciers of the SPIF located at a similar latitude.

For the Tardiglacial interval a theoretical ELA of  $561\pm 71$  m was estimated, which is located halfway between the average cirque floor elevation (1,382 m) and the estimated average elevation for the boundaries of the maximum ice extent (290 m) in the vicinity of the SBMR. Therefore, a descent in the ELA of  $585\pm 26$  m below present-day values, allows us to estimate that local temperatures in this area were at least  $3.8\pm 0.8^{\circ}\text{C}$  cooler than today, being also cooler compared to the regional post Tardiglacial context. This leads us to speculate that the SBMR was already a topographically elevated area around 6– 5 Kyr, which favored the development of alpine glaciations, and probably a small icefield.

## **Surface profiles of former glaciers**

Given the presence of moraine topography and lateral moraines, three glacial cirques were selected to generate surface profiles of the former glaciers (Fig.3.2). The decreasing downstream elevation of lateral moraines was considered as an indicator of ice extent and used as a target reference elevation for the surface profile.

Figure 3.10 shows Profile A-A` (Fig.3.10 A), located in the western part of the study area, with an average bedrock slope of 24% and a southeast aspect. The surface profile of the ancient glacier was flat and gently sloping. Profile B-B` (Fig. 3.10 B) is located in the main tributary of the Baguales River, where the average bedrock slope is 25.5% and the aspect is southwest, with the former glacier surface profile being very similar to profile A-A`. Finally, Profile C-C` (Fig. 3.10 C) located on the eastern side of the SBMR, is the longest profile, with an average bedrock slope of 2.1% and a southeast aspect. Unlike the previous profiles, the surface topography and ice thickness show variations depending on the bedrock slope changes (Fig. 3.10 D). For these cases, variables such as the elevation range and aspect did not affect the

characteristics of the former glacier surface profile. However, the topography and ice thickness (44 m average) can vary depending on the topography of the bedrock.

## Discussion

The radiocarbon dates (Fig. 3.2), which can be considered as minimum ages associated with the onset of organic sedimentation, would indicate that past climatic variations in the SBMR were under the regional context of a warm/dry to cold/wet climatic change around 6 Kyr. These ages could be associated with middle Holocene glacial advances, as reported for the Frias Lobe (Strelin *et al.*, 2014), on the eastern margin of the SPIF and at the same latitude as the SBMR.

However, it is important to consider the reservoir effect on these ages, which may appear up to several hundreds of years too old or too young. Particularly at the SBMR sample sites, younger carbon because of root penetration, infiltration of dissolved modern organic carbon (humics), or the hard-water effect could have contributed to the reservoir effect (Turetsky *et al.*, 2012; Blaauw *et al.*, 2004).

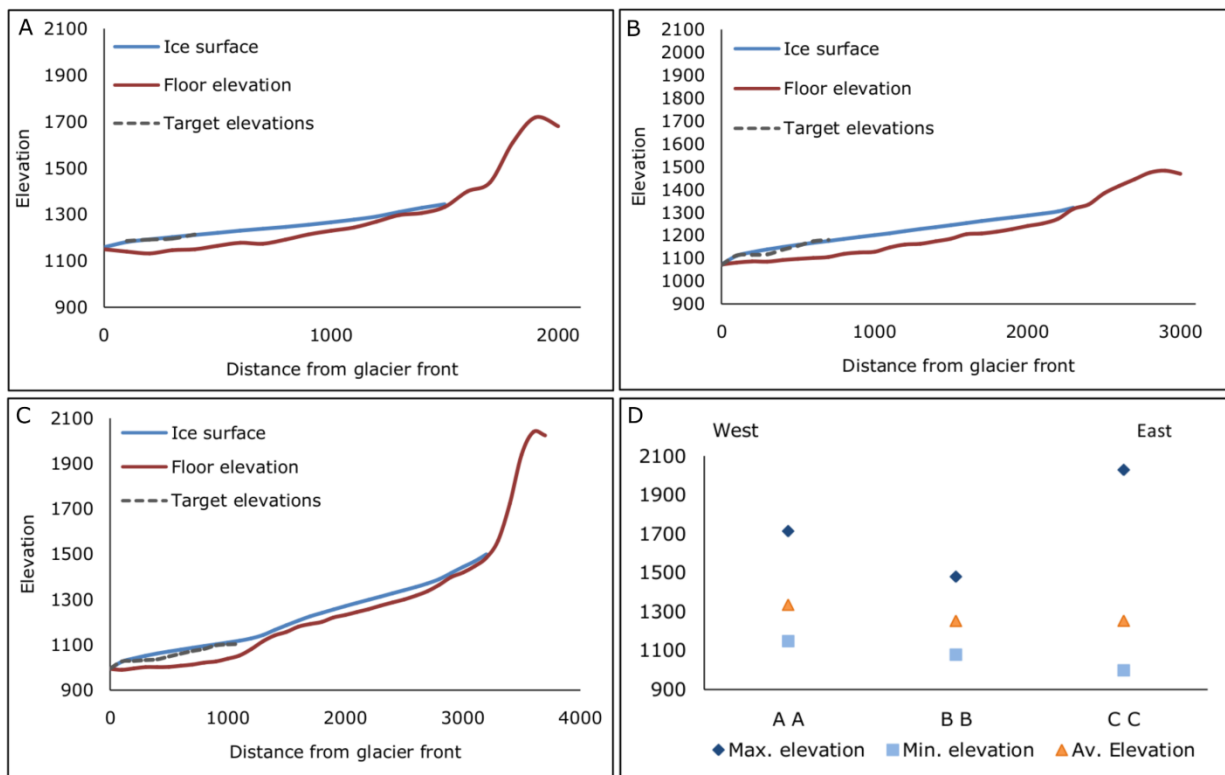


**Figure 3.10. Former surface topography profiles of alpine glaciers. Topography and ice thickness vary depending on changes in the bedrock slope.**

On the other hand, the ELA variation was converted to temperature change by multiplying an average atmospheric lapse rate by the ELA descent (e.g. Porter, 2001). This method is useful as an estimate of palaeo-temperatures in regions where modern meteorological data are not available or scarce. However, this technique has limitations because thermodynamic processes on glacial surfaces are complex and the ELA responds to more than just changes in atmospheric temperature (Putnam *et al.*, 2012). Therefore, it must be considered as a first approach.

In spite of these potential problems, however, the temperature change estimation ( $3,8 \pm 0,8^{\circ}$  C for a decrease in ELA of  $585 \pm 26$  m) lies within the context proposed by Douglas *et al.* (2005) of a  $2.4^{\circ}$  C variation for a ELA descent of 300 m at Lago General Carrera, and Putnam *et al.* (2012), who proposed a temperature variation of  $1.6^{\circ}$  C for a ELA descent of 300 m at the Cameron Glacier ( $43^{\circ}$  S) in the Southern Alps of New Zealand. Since the SBMR is a higher region towards the interior of the South American continent, this temperature estimation is consistent with the regional temperature decrease and precipitation increase that peaked at ca. 5000 cal yr. BP, after an extremely warm and dry phase. Such climatic variations would be linked to a latitudinal shift that controlled the strength of the southern Westerlies (Moreno, 2004; Villa-Martinez and Moreno, 2007).

Although there is still no clear chronology for the study area and the temperature variation estimation can have a certain degree of uncertainty, the geomorphologic evidence allows us to assume that alpine glaciers of the SBMR advanced down valley and converged to form a small Icefield, possibly prior to the regional middle Holocene climate change. This could be partially explained by the persistence of cold temperatures after the Late Glacial and Antarctic Cold Reversal (ACR), mainly due to the cold and dry climate prevailing towards the interior of the continent and the high elevation of the Baguales River and associated basin, where the presence of moraine deposits close to glacial cirque floors indicates former glacial activity. It can also be speculated that these glaciers began to recede at a later stage partially due to middle Holocene, non-climatic factors such as the abrupt topography casting shadows and preventing sunlight from reaching the glacier valleys. However it is still necessary to undertake more detailed studies in order to identify in detail when higher sections of the SBMR were occupied by ice, and its implications for the regional climatic context.

## Conclusions

The SBMR comprises part of the eastern foothills of the Southern Patagonian Andes, located 200 km from the Pacific coast and topographically isolated from the SPIF. Here, evidence exists of continental and alpine glaciations controlled by climatic (Westerly Winds) and tectonic (Andean uplift) factors, in addition to the regional geological setting (rock strength) and the Patagonian west–east climate contrast, which prevailed since the LGM. Therefore, a transition in glaciation styles exists between continental glaciation near the Pacific coast, that resulted in outlet glaciers forming during the Pleistocene ice cap advance in the SBMR, and alpine glaciations developing in the higher sectors of the SBMR towards the interior of continent.

The former continental glacier development was linked to maritime and temperate conditions together with high precipitation, which favored a positive mass balance, and glacier advances which eroded and deposited material in the lowest areas of the major valleys. Here the presence of larger glacial cirques can also be explained by the lower strength of the rock mass in comparison to the highest sectors of SBMR.

The predominance of an alpine glaciation style towards the east, in the higher sectors of the SBMR, can be explained by the prevalence of lower temperature conditions. Limited glacial erosion was here controlled by the strength of the rock mass and a decrease in precipitation, which may also explain the better preservation of glacial deposits located towards the interior of the continent.

Based mainly on the geomorphological evidence, in addition to an estimation of the temperature variation and radiocarbon dates, it is possible to infer that former alpine glaciers of the SBMR were not outside the context of regional, repeated ice fluctuations during the Holocene, Alpine glaciers eventually formed an Icefield at an early stage of the middle Holocene climate change. The development of glacial activity would have been controlled primarily by the prevalence of a cold and dry climate in the easternmost, higher sections of the SBMR. A detailed chronology is required in order to know when the glaciers occupied these sites, and to ascertain whether the formation of this Icefield is associated with the regional ice regrowth during the Late Glacial and ACR, which ranged from ~ 14 to 13 Kyr.

## **Acknowledgements**

We are grateful for grants from the “Becas de Doctorado en Chile” Scholarships Program and “Gastos Operacionales para Proyecto de Tesis Doctoral” of CONICYT. Juan MacLean and his family kindly allowed access to the farms Las Cumbres and Baguales and Juan Pablo Riquez allowed access to the farm Verdadera Argentina. Juan Carlos Aravena and Rodrigo Villa-Martinez of the Universidad de Magallanes, José Luis Oyarzun, and Juan José San Martín provided much-appreciated logistical support. Ricardo Arce, Mauricio Gonzales, Mike Kaplan and Carly Peltier lent invaluable assistance in field activities. Le Roux is supported by Project CONICYT/FONDAP/15090013.

## **Bibliography**

Benn, D. and Hulton, N. 2010. An Excel™ spreadsheet program for reconstructing the surface profile of former mountain glaciers and ice caps. *Computers & Geosciences*, 36 (5), 605-610.

Benn, D. and Lehmkuh, I. 2000. Mass balance and equilibrium-line altitudes of glaciers in high-mountain environments. *Quaternary International*, 65, 15-29.

Benn, D. and Ballantyne, C. 2005. Palaeoclimatic reconstruction from Loch Lomond readvance glaciers in the West Drumochter Hills, Scotland. *Journal of Quaternary Science*, 20 (6), 577-592.

Bentley, M. 1997. Relative and radiocarbon chronology of adjacent former outlet glaciers in the Chilean Lake District. *Journal of Quaternary Science*, 12, 25-33.

Blaauw, M., van der Plicht, J. and van Geel, B. 2004. Radiocarbon dating of bulk peat samples from raised bogs: non-existence of a previously reported ‘reservoir effect’?. *Quaternary Science Reviews*, 23, 1537–1542

Bostelmann, J., Le Roux, J., Vásquez, A., Gutierrez, N., Oyarzun, J., Carreño, C., Torres, T., Otero, R., Llanos, A., Fanning, M. and Herve, F. 2013. Burdigalian deposits of the Santa Cruz Formation in the Sierra Baguales, Austral (Magallanes) Basin: Age, depositional environment and vertebrate fossils. *Andean Geology*, 40 (3), 458–489.

Caldenius, C. 1932. Las glaciaciones Cuaternarias en la Patagonia and Tierra del Fuego. *Geografiska Annaler*, 14, 1 – 164.

Carlson, A., Murray, D., Anslow, F., He, F., Singer, B., Liu, Z. and Otto-Bliesner, B. 2010. Assessing the paleo-forcings of southeastern Patagonia deglaciation using General Circulation Model Simulations (invited). American Geophysical Union, Fall Meeting 2010, Abstract #GC23H-04.

Casassa, G., Rodriguez, J. and Loriaux, T. 2014. A new glacier inventory for the Southern Patagonia Icefield and areal changes 1986–2000. In: *Global Land Ice Measurements from Space*. Springer, Berlin, pp 639–660.

Clapperton, C. 1993. Nature of environmental changes in South America at the Last Glacial Maximum. *Palaeogeography, Palaeoclimatology, Palaeoecology*, 101 (3-4), 189–208.

Condom, T., Coudrain, A., Sicart, J. and Théry, S. 2007. Computation of the space and time evolution of equilibrium-line altitudes on Andean glaciers (10 degrees N-55 degrees S). *Global and Planetary Change*, 59 (1-4), 189-202.

Coronato, A., Meglioli, M. and Rabassa, J. 2004. Glaciations in the Magellan Straits and Tierra del Fuego, Southernmost South America. In: Ehlers, J. and Gibbard, P (Eds.) *Quaternary Glaciations: Extent and Chronology. Part III: South America, Asia, Africa, Australia and Antarctica*. Quaternary Book Series, Elsevier, Amsterdam, pp. 45–48.

Charrier, R., Pinto, L. and Rodriguez, M. 2007. Tectonostratigraphic evolution of the Andean orogen in Chile. In: *The Geology of Chile*. The Geological Society Publishing House. Bath, UK, pp 21–115.

Dahl, S. and Nesje, A. 1996. A new approach to calculating Holocene winter precipitation by combining glacier equilibrium-line altitudes and pine-tree limits: a case study from Hardangerjøkulen, central southern Norway. *The Holocene*, 6, 381–398.

Denton, G., Lowell, T., Heusser, C., Schlüchter, C., Andersen, B., Heusser, L., Moreno, P. and Marchant, D. 1999. Geomorphology, stratigraphy, and radiocarbon chronology of Llanquihue Drift in the area of the Southern Lake District, Seno Reloncaví and Isla

Grande de Chiloé, Chile. *Geografiska Annaler. Series A Physical Geography*, 81, 167–229.

Douglass, D. and Bockheim, J. 2006. Soil-forming rates and processes on Quaternary moraines near Lago Buenos Aires, Argentina. *Quaternary Research*, 65, 293–307.

Douglas, D., Singer, B., Kaplan, M., Ackert, R., Mickelson, D. and Caffee, M. 2005. Evidence of early Holocene glacial advances in southern South America from cosmogenic surface-exposure dating. *Geology*, 33 (3), 237-240.

Ehlers, J. and Gibbard, P. 2007. The extent and chronology of Cenozoic global glaciations. *Quaternary International*, 164, 6-20.

Fogwill, C. and Kubik, P. 2005. A glacial stage spanning the Antarctic Cold Reversal in Torres del Paine (51° S), Chile, based on preliminary cosmogenic exposure ages. *Geografiska Annaler, Series A: Physical Geography*, 87 (2), 403–408.

Foster, D., Brocklehurst, S. and Gawthorpe, R. 2008. Small valley glaciers and the effectiveness of the glacial buzzsaw in the northern Basin and Range, USA. *Geomorphology*, 102 (3), 624-639.

García, J., Kaplan, M., Hall, B., Schaefer, J., Vega, R., Schwartz, R. and Finkel, R. 2012. Glacier expansion in southern Patagonia throughout the Antarctic Cold Reversal. *Geology*, 40 (9), 859–862.

Garreaud, R. 2007. Precipitation and Circulation Covariability in the Extratropics. *Journal of Climate*, 20, 4789-4797.

Glasser, N., Jansson, K., Harrison, S. and Kleman, J. 2008. The glacial geomorphology and Pleistocene history of South America between 38°S and 56°S. *Quaternary Science Reviews*, 27 (3–4), 365–390.

Gutierrez, N., Le Roux, J., Bostelmann, E., Oyarzun, J., Ugalde, R., Vasquez, A., Otero, R., Araos, J., Carreño, C., Fanning, M., Torres, T. and Herve, F. 2013. Geology and stratigraphy of Sierra Baguales, Ultima Esperanza Province, Magallanes, Chile. *Bolletino di Geofisica Teorica ed Applicata*, 54, 327–330.



Heusser, C. 2003. Ice age southern Andes: a chronicle of palaeoecological events. New York University 260 pages.

Hoek, E. and Diederichs, M. 2006. Empirical estimation of rock mass modulus. *International Journal of Rock Mechanics and Mining Sciences*, 43, 203–215.

Hostetler, S. and Clark, P. 1997. Climatic controls of western US glaciers at the Last Glacial Maximum. *Quaternary Science Reviews*, 16 (6), 505-511.

Hughes, P., Gibbard, P. and Woodward, J. 2007. Geological controls on Pleistocene glaciation and cirque form in Greece. *Geomorphology*, 88 (3–4), 242–253.

Hulton, N., Purves, R., McCulloch, R., Sudgen, D. and Bentley, M. 2002. The Last Glacial Maximum and deglaciation in southern South America. *Quaternary Science Reviews*, 21, 233–241.

Kaplan, M., Strelin, J., Schaefer, J., Denton, G., Finhele, R., Schwartz, R., Putman, A., Vandergoes, M., Goehring, B. and Travis, S. 2011. In-situ cosmogenic  $^{10}\text{Be}$  production rate at Lago Argentino, Patagonia: Implications for late-glacial climate chronology. *Earth and Planetary Science Letters*, 309 (1), 21-32.

Kaplan, M., Hein, R., Hubbard, A. and Lax, S. 2009. Can glacial erosion limit the extent of glaciation? *Geomorphology*, 103 (2), 172-179.

Kaplan, M., Douglas, D., Singer, B., Ackert, R. and Caffee, M. 2005, Cosmogenic nuclide chronology of pre-last glacial maximum moraines at Lago Buenos Aires, 46°S, Argentina. *Quaternary Research*, 63, 301–315.

Kaplan, M., Ackert, R., Singer, B., Douglas, D. and Kurz, M. 2004. Cosmogenic nuclide chronology of millennial-scale glacial advances during O-isotope stage 2 in Patagonia. *Geological Society of America Bulletin*, 116 (3-4), 308-321.

Lagabrielle, Y., Labaume, P. and Blanquat, M. 2010. Mantle exhumation, crustal denudation, and gravity tectonics during Cretaceous rifting in the Pyrenean realm (SW Europe): insights from the geological setting of the Iherzolite bodies. *Tectonics*, 29, 4.

Le Roux, J., Puratich, J., Mourgues, F., Oyarzun, J., Otero, R., Torres, T. and Herve, F. 2010. Estuary deposits in the Río Baguales Formation (Chattian-Aquitanean), Magallanes Province, Chile. *Andean Geology*, 37 (2), 329–344.

Lorrey, A., Fauchereau, N., Stanton, C., Chappell, P., Phipps, S., Mackintosh, A., Renwick, J., Goodwin, I. and Fowler, A. 2013. The Little Ice Age climate of New Zealand reconstructed from Southern Alps cirque glaciers: a synoptic type approach. *Climate Dynamics*, 42 (11), 3039-3060.

Lowell, T., Heusser, J., Andersen, G., Moreno, P., Hauser, A., Heusser, L., Schlüchter, C., Marchant, D. and Denton, G. 1995. Interhemispheric correlation of late Pleistocene events. *Science*, 269, 1541-1549.

Marinos, V., Marinos, P. and Hoek, E. 2005. The geological Strength index: applications and limitations. *Bull. Eng. Geol. Environ*, 64, 55-65.

Marden, C. 1997. Late-glacial fluctuations of South Patagonian Icefield, Torres del Paine National Park, southern Chile. *Quaternary International*, 38–39, 61–68.

Meierding, T. 1982. Late Pleistocene glacial equilibrium-line altitudes in the Colorado front range: a comparison of methods. *Quaternary Research*, 18, 289–310

McCulloch, R., Bentley, M., Purves, R., Hulton, N., Sudgen, D. and Clapperton, C. 2000. Climatic inferences from glacial and palaeoecological evidence at the last glacial termination, southern South America. *Journal of Quaternary Science*, 15 (4), 409–417.

Mercer, J. 1983. Cenozoic glaciation in the Southern Hemisphere. *Annual Review of Earth and Planetary Sciences*, 11, 99–132.

Mercer, J. 1976. Glacial history of southernmost South America. *Quaternary Research*, 6 (2), 125–166.

Mercer, J. 1967. Southern hemisphere glacier atlas. Office Chief on Research and Development. 650 Department of the Army. Technical report 67-76-ES. 325 pp.

Meyer, I. and Wagner, S. 2008. The Little Ice Age in southern Patagonia: comparison between paleoecological reconstructions and downscaled model output of a GCM simulation. *Pages News*, 16, 12–13.

Mitchell, S. and Montgomery, D. 2006. Influence of a glacial buzzsaw on the height and morphology of the Cascade Range in central Washington State, USA. *Quaternary Research*, 65 (1), 96–107.

Montgomery, D., Balco, G. and Willett, S. 2001. Climate, tectonics, and the morphology of the Andes. *Geology*, 29 (7), 579–582.

Moreno, P. 2004. Millennial-scale climate variability in northwest Patagonia over the last 15 000 yr. *Journal of Quaternary Science*, 19 (1), 35–47.

Moreno, P., Francois, J., Moy, C. and Villa-Martinez, R. 2010. Covariability of the Southern Westerlies and atmospheric CO<sub>2</sub> during the Holocene. *Geology*, 38 (8), 727–730.

Nesje, A. and Dahl, S. 2003. The ‘Little Ice Age’—only temperature? *The Holocene*, 13 (1), 139-145.

Nesje, A and Dahl, S. 2000. Is the North Atlantic Oscillation reflected in Scandinavian glacier mass balance records? *Journal of Quaternary Science*, 15 (6), 587-601.

Nordenskjöld, O. 1899. Geological map of the Magellan territories with explanatory notes. Kungl. Boktryckeriet. PA Norstedt & Söner, 1 (3), 81-85.

Oerlemans, J. (1992). Climate sensitivity of glaciers in southern Norway: application of an energy-balance model to Nigardsbreen, Hellstugubreen and Alfotbreen. *Journal of Glaciology*, 38 (129), 223-232.

Ohmura, A., Kasser, P. and Funk, M. 1992. Climate at the equilibriumline of glaciers. *Journal of Glaciology*, 38, 397–411.

Peña, H. and Gutierrez, R. 1992. Statistical analysis of precipitation and air temperature in the Southern Patagonian Icefield. In: *Glaciological Researches in Patagonia*. Nagoya, Japanese Society of Snow and Ice, Data Center for Glacier Research, pp 95–108.

Porter, S. 1989. Some geological implications of average Quaternary glacial conditions. *Quaternary Research*, 32 (3), 245–261.

Putnam, A., Schaefer, J., Denton, G., Barrell, D., Finkel, R., Andersen, B., Schwartz, R., Chinn, T. and Doughty, A. 2012. Regional climate control of glaciers in New Zealand and Europe during the pre-industrial Holocene. *Nature Geosciences Letters*, 5, 627-630.

Rabassa, J., Coronato, A. and Martínez, O. 2011. Late Cenozoic glaciations in Patagonia and Tierra del Fuego: an updated review. *Biological Journal of the Linnean Society*, 103 (25), 316–335.

Rabassa, J. and Coronato, A. 2009. Glaciations in Patagonia and Tierra del Fuego during the Ensenadan Stage/Age (Early Pleistocene–earliest Middle Pleistocene). *Quaternary International*, 210 (1–2), 18–36.

Rabassa, J., Coronato, A. and Salemme, M. 2005. Chronology of the Late Cenozoic Patagonian glaciations and their correlation with biostratigraphic units of the Pampean region (Argentina). *Journal of South American Earth Sciences*, 20 (1–2), 81–103.

Ramos, V. and Ghiglione, M. 2008. Tectonic evolution of the Patagonian Andes. In: *The Late Cenozoic of Patagonia and Tierra del Fuego*. Elsevier, Amsterdam. pp 57–71.

Sagredo, E., Moreno, P., Villa-Martínez, R., Kaplan, M., Kubik, P. and Stern, C. 2011. Fluctuations of the Última Esperanza ice lobe (52°S), Chilean Patagonia, during the last glacial maximum and termination 1. *Geomorphology*, 125, 92–108.

Strelin, J., Kaplan, M., Vandergoes, M., Denton, G. and Schaefer, J. 2014. Holocene glacier history of the Lago Argentino basin, Southern Patagonian Icefield. *Quaternary Science Reviews*, 124, 715–145.

Strelin, J., Denton, G., Vandergoes, M., Ninnemann, U. and Putnam, A. 2011. Radiocarbon chronology of the late-glacial Puerto Bandera moraines, Southern Patagonian Icefield, Argentina. *Quaternary Science Reviews*, 30, 2551–2569.

Strelin, J. and Malagnino, E., 2000. Late-Glacial History of Lago Argentino, Argentina, and Age of the Puerto Bandera Moraines. *Quaternary Research*, 54 (3), 339–347.

Sudgen, D., Bentley, M., Fogwill, C., Hulton, N., McCulloch, R. and Purves, R., 2005. Late-glacial glacier events in southernmost south America: A blend of “northern” and “southern” hemispheric climatic signals? *Geografiska Annaler, Series A Physical Geography*, 87 (2), 273–288.

Sugden, D. and John, B. 1976. *Glaciers and Landscape*. E. Arnold. London. 376 pages.

Talma, A. and Vogel, J. 1993. Mathematics use for calibration scenario – A simplified approach to calibrating C14 dates. *Radiocarbon*, 35 (2), 317-322.

Turetsky, M., Manning, S. and Wieder. 2012. Dating recent peats deposits. *Wetlands*, 24 (2), 324-356.

Vieira, G., 2008. Combined numerical and geomorphological reconstruction of the Serra da Estrela Plateau Icefield, Portugal. *Geomorphology*, 97 (1-2), 190–207.

Villa-Martinez, R. and Moreno, P. 2007. Pollen evidence for variations in the southern margin of the 789 westerly winds in SW Patagonia over the last 12,600 years. *Quaternary Research*, 68, 400–409.

## FINAL REMARKS

The geographical distribution of continental and alpine glaciations between 50° and 51° S were partially controlled by the Andean uplift, related to a strong increase in the convergence rate and a decrease in the obliquity between the Nazca and South America Plates (Charrier *et al.*, 2007). This affected the regional climate pattern, linked to the intensification of the rain shadow due to the Andean orographic effects (Fig. 1.2) on the Westerly Winds in southern Patagonia (Ramos and Ghiglione, 2008).

The SBMR located approximately 200 km from the Pacific coast, in an area topographically isolated from the SPIF and under the influence of the Westerly Winds, shows geomorphologic evidence of both types of glaciations, besides the presently active easternmost alpine glaciers (Figs. 2.1, 3.2). Thus the SBMR can be considered as a natural laboratory useful to recognize the controlling factors involved in the glacial history in these eastern foothills of the Patagonian Andes, and to estimate the local environmental changes that occurred since the LGM.

In these eastern foothills of the Main Andean Range, geomorphological evidence of the spatial and altitudinal extent of continental and alpine glaciations highlights the influence of the SPIF to the west, the regional geological setting, and the Southern Patagonian climate contrast that involves the west-east precipitation gradient, ranging from more than 10,000 mm in the accumulation zone of the SPIF (Casassa *et al.*, 2014) to 200 mm towards the interior of the continent, at Lago Argentino (Strelin *et al.*, 2011).

From the eastern margin of the SPIF to the easternmost SBMR, two glaciation levels that rise inland can be recognized. The lower level includes glacial cirques that show no clear evidence of glacial or snow activity. They correspond to cirques that were probably covered (in part) by outlet valley glaciers during the LGM (and prior glaciations). On the other hand, the upper level includes glacial cirques that show lateral and terminal moraines, which can be considered as evidence of alpine glaciers that prevailed throughout the Holocene.

Outlet valley glaciers from the former Patagonian Ice Cap, influenced by the west Patagonian maritime and temperate climate, experienced periods of positive mass balance, favored by a temperature decrease and rainfall increase controlled by latitudinal and strength variations of the Westerly Winds (Hulton *et al.*, 2002; Moreno, 2004; Villa-Martinez and Moreno, 2007). It is plausible that the larger cirques near the

SPIF were more dynamic due to a high ice flux facilitated by higher winter precipitation and summer temperatures (Barr and Spagnolo, 2015) and advanced into the main surrounding valleys during the Holocene to occupy large glacial cirques, which can also be explained by the lower rock strength in this sector.

After the mid-Holocene, once the outlet glaciers from the former Patagonian Ice Cap retreated towards the west (Marden, 1997; McCulloch *et al.*, 2000; Sagredo *et al.*, 2011; Strelin *et al.*, 2011; Garcia *et al.*, 2012), the cold and dry eastern Patagonian climate favored the persistence of alpine glaciations, due to the effect of lower temperatures, particularly in the easternmost, highest areas of the SBMR. This was especially noted in those cirques that show an E to S aspect and where the cirque floor slopes were gentle. Such cirques were subject to reduced sunlight exposure during the warmest part of the day and also received less direct sunlight in the afternoon. However, these alpine glaciers eroded smaller cirques compared to continental glaciers, due to the higher rock strength and the precipitation gradient across the study area.

Although there is still no detailed chronology of the glacial variations, carried out particularly in the highest section of the SBMR, estimation of the temperature variation range indicates that the temperature since the Tardiglacial was  $3.8 \pm 0.8^\circ \text{C}$  colder than at present. In addition to  $^{14}\text{C}$  ages, which can be linked to organic sedimentation in the bogs after a warm/dry to cold/wet climatic change around 6 Kyr, and considering the morphological evidence of past glacial activity in the SBMR, it is possible to conjecture that in the past the higher section of the SBMR was occupied by a small Icefield.

This might be explained by the geographic and climatological setting of the SBMR that controlled the former glacial activity. The development of alpine glaciers in the easternmost highest sections of the SBMR, was favored by their location, aspect and cirque floor topography. These glaciers were active probably since the Tardiglacial interval or ACR, resulting from the effect of low temperatures that persisted due to the thermal gradient effect and the cold and dry weather prevailing towards the interior of the continent. These factors controlled glacier advances to the central valley, where they coalesced to form a small Icefield that may already have existed before the middle Holocene. The growth of this Icefield, due to a decrease in temperature and increase in precipitation, peaked at ca. 5000 years cal. BP, which was linked to a latitudinal shift that controlled the strength of the southern Westerlies (Moreno, 2004; Villa-Martinez and

Moreno, 2007). At a later stage in the middle Holocene, the Icefield began to shrink and alpine glaciers receded due to climatic factors including a temperature increase, as well as non-climatic factors such as the irregular topography of the glacier bedrock.

Considering the above, it can be concluded that:

1) The SBMR around 6–5 Kyr was already an elevated narrow topographic feature, resulting from deformation propagated since the Tertiary via a fold-and-thrust belt (Fig. 1.2), that according to Foskdik *et al.* (2011), contrasts with the broad, high-elevation Cordillera in the Central Andes.

2) The SBMR Icefield represents isolated glaciation, which presumably developed during the Lateglacial Interval or ACR (or prior glaciations), and eventually showed variations during the Holocene. However, so far, there is no conclusive evidence to infer that SBMR glaciers coalesced with outlet glaciers from the Pleistocene ice cap; this may be because glaciations of higher sections of the SBMR were indeed exclusively local, or that the glacial deposits, which could show major advances, were eroded by fluvial action.

3) After the retreat of SBMR glaciers, erosion continued within the ice-free glacial cirques. This could be linked to either fluvio-glacial or fluvial erosion associated with the loss of glacial mass. On the other hand, such erosion could also be linked to neotectonic activity, as suggested Rabassa *et al.* (2000) for the area of Tierra del Fuego, where faulting present in periglacial areas can be attributed to the deglaciation of the middle and late Holocene, when glacial isostasy was dominant. In agreement with the above, Stewart *et al.* (2000), Costa *et al.* (2006), and Fildani *et al.* (2008) suggested that in southern South America, deglaciation can generate regional or local seismic activity and mass movements, particularly in areas close to the Pleistocene ice cap.

In the case of fluvial erosion, field evidence indicates that this has reworked glacial cirques by mobilizing deposits, leaving only remnants of moraine topography (Figs 3.4, 3.5, 3.6 and 3.7). In the case of tectonic activity, there is no direct field evidence to estimate how effective seismic activity was in the mobilization or burial of glacial deposits. New studies are therefore required to characterize the role of neotectonics in the reworking of the SBMR glacial cirques.



4) Finally, radiocarbon dates are not conclusive in proving high frequency glacial variations. However, based on geomorphological evidence, it can be postulated that the former SBMR glaciers located in the nearby Andes experienced fluctuations throughout the middle Holocene (e.g., Strelin *et al.*, 2014). Such fluctuations appear to have been initially closer to the chronology proposed by Mercer (Fig. 1.1), particularly for the glacial advances of 4700–4200 <sup>14</sup>C years BP. This would be consistent with the Neoglacial, strong climatic cooling reported for this time (Glasser *et al.*, 2004). However, further dating is needed for a better characterization of the former glacial activity in the SBMR, in order to identify the timing of glaciations and its synchronization with the regional glacial context. This will provide new data useful to understand the high frequency climatic variations and the potential teleconnections between polar and temperate latitudes, which will assist in resolving current disputes about the behavior of the Westerly Winds during the Holocene.

## **Bibliography**

Casassa, G., Rodriguez, J. and Loriaux, T. 2014. A new glacier inventory for the Southern Patagonia Icefield and areal changes 1986–2000. In: Global Land Ice Measurements from Space. Springer, Berlin. pp 639–660.

Costa, C., Audemard, F., Bezerra, F., Lavenu, A., Machette, M. and Paris, G. 2006. An overview of the main Quaternary deformation of South America. *Revista de la Asociación Geológica Argentina*, 61 (4), 461-479.

Charrier, R., Pinto, L. and Rodriguez, M. 2007. Tectonostratigraphic evolution of the Andean orogen in Chile. In: *The Geology of Chile*. The Geological Society Publishing House. Bath, UK. 21–115.

Fildani, A., Romans, B., Fosdick, J., Crane, W. and Hubbard, S. 2008. Orogenesis of the Patagonian Andes as reflected by basin evolution in southernmost South America. *Arizona Geological Society Digest*, 22, 259-269.

Hulton, N., Purves, R., McCulloch, R., Sugden, M. and Bentley, M. 2002. The Last Glacial Maximum and deglaciation in southern South America. *Quaternary Science Reviews*, 21, 233–241.

McCulloch, R. and Davies, S. 2001. Late-glacial and Holocene palaeoenvironmental change in the central Strait of Magellan, southern Patagonia. *Palaeogeography, Palaeoclimatology, Palaeoecology*, 173, 143-173.

McCulloch, R., Bentley, M., Purves, R., Hulton, N., Sugden, D. and Clapperton, C. 2000. Climatic inferences from glacial and palaeoecological evidence at the last glacial termination, southern South America. *Journal of Quaternary Science*, 15 (4), 409–417.

Moreno, P. 2004. Millennial-scale climate variability in northwest Patagonia over the last 15 000 yr. *Journal of Quaternary Science*, 19 (1), 35–47.

Moreno, P., Francois, J., Villa-Martinez, R. and Moy, C. 2009. Millennial-scale variability in Southern Hemisphere Westerly Wind activity over the last 5000 years in SW Patagonia. *Quaternary Science Reviews*, 28, 25–38.

Rabassa, J., Coronato, A., Bujalesky, G., Salemne, M., Roig, C., Meglioni, A., Heusser, C., Gordillo, S., Roig, F., Borrromei, A. and Quattrocchio, M. 2000. Quaternary of Tierra del Fuego, Southernmost South America: an updated review. *Quaternary International*, 68 – 71, 217-240.

Ramos, V. and Ghiglione, M. 2008. Tectonic evolution of the Patagonian Andes. In: *The Late Cenozoic of Patagonia and Tierra del Fuego*. Elsevier, Amsterdam. pp 57–71.

Stewart, S., Sauber, J. and Rose, J. 2000. Glacio-seismotectonics: ice sheets, crustal deformation and seismicity. *Quaternary Science Reviews*, 19, 1367-1389.

Strelin, J., Denton, G., Vandergoes, M., Ninnemman, U. and Putman, A. 2011. Radiocarbon chronology of the late-glacial Puerto Bandera moraines, Southern Patagonian Icefield, Argentina. *Quaternary Science Reviews*, 30, 2551–2569.

Strelin, J., Kaplan, M., Vandergoes, M., Denton, G. and Schaefer, J. 2014. Holocene glacier history of the Lago Argentino basin, Southern Patagonian Icefield. *Quaternary Science Reviews*, 101, 124–145.

Vieira, G. 2008. Combined numerical and geomorphological reconstruction of the Serra da Estrela plateau icefield, Portugal. *Geomorphology*, 97 (1-2), 190–207.

Villa-Martinez, R. and Moreno, P. 2007. Pollen evidence for variations in the southern margin of the Westerly Winds in SW Patagonia over the last 12,600 years. *Quaternary Research*, 68, 400–409.

## APPEND1

Abstract accepted in XIV Congreso Geológico Chileno.

# Factors controlling alpine glaciations in the Sierra Baguales Mountain Range (50° - 51° S) as inferred from morphometric analysis of glacial cirques

José Araos\* \*\*, Jacobus Le Roux\* \*\*\* and Mike Kaplan\*\*\*\*

\*Departamento de Geología. Universidad de Chile. Plaza Ercilla 803, Santiago, Chile.

\*\* Departamento de Geografía. Universidad Alberto Hurtado. Cienfuegos 41, Santiago, Chile.

\*\*\* Andean Geothermal Centre of Excellence, Plaza Ercilla 803, Santiago, Chile.

\*\*\*\*LDEO of Columbia University, Palisades, NY 10964.

\*Contact email: [josearaos@ug.uchile.cl](mailto:josearaos@ug.uchile.cl)

**Abstract.** We mapped the spatial and elevation distribution of 143 cirques in southern Patagonia, between 50° and 51° S, and analyzed their morphometry using simple and multivariate statistical methods. The cirque basins are located east of the Southern Patagonian Icefield and around the Sierra Baguales Mountain Range, about 200 km from the Pacific coast. The geomorphologic evidence indicates that alpine glaciations have been the predominant style in the study area.

Two morphoclimatic configurations can be distinguished, which are located at different elevations: i) cirques with no evidence of present glacier or snow activity, which are distributed homogeneously throughout the lower sections of the study area, and whose development has been influenced by former outlet glaciers of the Patagonian Ice Sheet during glaciations periods. ii) cirques with current glacier and/or snow activity, located on average 180 m above the lower group, at the higher elevations near the eastern margin of the Southern Patagonian Icefield (SPI), but concentrated particularly in the Sierra Baguales Mountain Range, and presents evidence of alpine-style glaciation related to the close proximity of the former Pleistocene ice cap.

The distribution and activity on glacial cirques are influenced by both tectonic factors (Andean uplift) and climate (Westerly Winds). Morphometric characteristics indicates a persistent climate contrasts between the western (maritime, temperate) and eastern (dry and cold) sides of southern Patagonia since the Last Glacial Maximum (LGM).

Based on our analyses, we infer that glaciers located at the higher elevations were not affected by post LGM high-frequency climatic variations that would have led to only small glaciers of limited influence on cirque form evolution; on the other hand most glacial cirques analyzed shows an isometric developing trend, which could indicate that the deglaciation process in Sierra

Baguales occurred quickly and continuously, and equilibrium line altitudes (ELAs) experienced a relatively rapid rise of about 400 m after the last major occupation.

**Keywords:** Southern Patagonian Ice Sheet, alpine glaciations, ELA, Last Glacial Maximum.

## 1 Introduction

Patagonian past glacier variations have shaped the landscape, generating geomorphological, sedimentological and stratigraphic evidence, that according to Rabassa et al. (2011), represent the action of continental and alpine glaciations of varying ages and extensions. Glacial chronologies developed for the last glacial cycle in outlet glaciers located at the Torres del Paine massif and surroundings of the Patagonian Ice Cap, indicate that the ice retreat after the last glacial term T1 (~ 18-10 ka, 103 cal. Years) did not happen quickly, and in addition was interrupted by a glacial readvance or stabilization at about 11.8 Ka.

The Sierra Baguales Mountain Range in the eastern foothills of the Andes (Figure 1), located 50 km northeast of the Torres del Paine massif presents active alpine glaciers and geomorphological evidence that indicates the existence of an former system of glacial cirques located in the Westerly Winds area and topographically isolated from the SPI. The accumulation zone of these glacial cirques is located above 1000 m a.s.l. and more than 200 km from the Pacific coast. Therefore, it represents a suitable site for the description and estimation of the factors that controlled the variations of isolated alpine glaciers located toward the interior of the continent and that possibly responded independently to climatic changes

that operated since the LGM. The research will help to clarify the current knowledge gap identified by various authors (Rabassa et al., 2011), related to the duration and structure of the LGM in an area neighboring Torres del Paine (Marden, 1997; Garcia et al., 2012; Sagredo et al., 2011).

## 2 Method, Samples, Results

### 2.1 Cirques morphological types

Cirques mapping was carried out using topographic maps at a scale of 1:50,000, aerial photographs at a scale of 1:70,000, Landsat imagery and digital elevation models. Three field campaigns were carried out during 2013 and 2014 to map cirques and observe, describe and interpret the general geomorphology of the Sierra Baguales Mountain Range.

Each cirque was digitized as a closed polygon with a unique ID number, upon which a table containing morphometric information associated with each digitized polygon was generated. Calculations of planimetric and hypsometric indices (Křížek et al., 2012) were conducted using the open source software QuantumGIS 2.2 and GRASS 6.0.

Following Delmas et al. (2013), morphometric variables were defined in such a way as to make them directly comparable with previous work on glacial cirques located in middle and high latitudes. The variables considered are: Surface (S), perimeter (P), length (L), width (W), cirque depth (H), maximum elevation (E<sub>max</sub>), mean elevation (E<sub>med</sub>), minimum elevation (E<sub>min</sub>), aspect (A), ratio of length to elevation range (L/H), ratio of width to elevation range (W/H), ratio of length to width (L/W), slope (M), and circularity (C).

Two morphological types of cirques are distinguished, they differ mainly in their area and shape parameters. Group 1, is located in higher areas of the SPI margin and mainly in the Sierra Baguales Mountain Range, while Group 2, are homogeneously distributed in the study area. Cirques concentrated toward the interior of the continent, 200 km from Pacific coast, particularly in the higher and eastern sections of the Sierra Baguales, whose cirque floor is placed at an average elevation of 1,273 m, usually show current glacial activity, and may be associated with the Group 1. On the other hand, cirques located near the SPI, and in the transition zone, whose floors are at an average elevation of 1,169 m, usually contain either perennial snow or a lack of snow/ice activity, possibly due to their lower elevation, and can be related to Group 2. Thus location and mean elevation, and particularly the cirque floor height of cirques can be considered as controlling factors in the occurrence of glacial activity.

### 2.2 Composite map

A composite map methodology (Le Roux and Rust, 1989) was used to assist in the cirque characterization. This methodology was originally designed for paleogeographic reconstructions and uranium exploration and is based on the combination of different maps (characteristics of cirques in this case) in to a single composite map. The input data are standardized, so that all data types have the same range of values. The main advantage of this method is that the assignment of numerical results is completely objective (Sepulveda et al., 2013).

The higher composite values, spatially concentrated in the highest sections of the eastern SPI and particularly along the high elevations of the eastern side of Sierra Baguales, are related to cirques that show current glacier or perennial snow activity, where the predominant aspects range from east to south and the evidence indicates that alpine glaciation is the predominant glaciation style. On the other hand, lower values, located at lower elevations, in an intermediate zone between the eastern margin of the SPI and specific sectors of the Sierra Baguales, are associated with cirques occupied by alpine and valley glaciers with aspects ranging from NW to NE; these show no evidence of present day glacier or perennial snow activity and they have been subject to glaciofluvial erosion. Moreover, these cirques with low values were probably influenced or covered (in part) by valley glaciers during the LGM (and prior glaciations) and, because of their low elevation, became quickly deglaciated.

### 2.3 Past ELA estimation

The local ELA elevation trend for former alpine glaciers of the Sierra Baguales was estimated considering the cirque distribution. Since cirques develop cumulatively over many glacial cycles (Benn and Lehmkuhl, 2000), the elevations of cirque floors were used as a proxy to estimate the elevation of former glacier snowlines for Pleistocene glaciers (Nesje, 2007) reflecting average climatic conditions over longer timescales (Nesje, 2007). The criteria set by Porter (1989) and Mitchell and Montgomery (2006), who suggested that cirque floors occupy a level midway between the regional LGM and modern ELA were also considered.

The LGM ELA for outlet glaciers of the SPI was depressed around 750 to 890 m (Carlson et al., 2010) in relation to the actual ELA, which is located around 970 m, considering an ELA average elevation (based on Casassa et al., 2014, and references therein) for 7 outlet glaciers located between 50°22' and 51°16' S (Mayo,

Ameghino, Moreno, Frias, Grey, Pingo and Tyndall Glaciers) and an aspect ratio that varies from N to SE. On the other hand, based on the analysis of cirques and cirque floor distributions besides geomorphological evidence of cirques near outlet glaciers of the SPI, a rise in the ELA of around 400 m was estimated.

### 3 Discussion and Comments

The geomorphology and glacial cirque features of Sierra Baguales Mountain Range indicate that this region has been evolving relatively independent from the SPI, with dominant alpine style glaciation(s?). We infer that the overall morphology of the Sierra Baguales has been relatively more sensitive to the effects of the Westerlies Winds and other factors influencing geomorphic development, than the general region of the SPI to west. This sector may have also experienced much greater glacial erosion than what has been suggested for the area covered by the former South Patagonian Ice Sheet.

Geomorphological evidence and morphometric reconstructions allow us to estimate an ELA rise of about 400 meters since the last major occupation. Considering the smaller ELA change, it can be assumed that the deglaciation process of alpine glaciers in Sierra Baguales was probably quicker and more continuous (i.e., no evidence of regrowth), compared to the outlet glaciers of the SPI.

### Acknowledgements

We thank the Becas de Doctorado Chile Scholarships Program and “Gastos Operacionales para Proyecto de Tesis Doctoral” funds of CONICYT. Juan MacLean and his family allowed access to the farms “Las Cumbres” and “Baguales” and Juan Pablo Riquez allowed access to the farm “Verdadera Argentina”, for which we are grateful. Matteo Spagnolo of Aberdeen University help in data processing. Juan Carlos Aravena and Rodrigo Villa-Martinez of Universidad de Magallanes, Ricardo Arce, Mauricio Gonzales, Nestor Gutierrez and José Luis Oyarzun lent invaluable assistance in field activities. Mike Kaplan is supported by NSF BCS 1263474.

### References

Aniya, M.; Sato, H.; Naruse, R.; Skvarca, P.; Casassa, G. 1996. The Use of Satellite and Airborne Imagery to Inventory Outlet Glaciers of the Southern Patagonia Icefield, South America. *Photogrammetric Engineering & Remote Sensing*, 62 (12): 1361–1369.

Benn, D.; Lehmkuhl, F. 2000. Mass balance and equilibrium-line altitudes of glaciers in high-mountain environments. *Quaternary International* 65: 15–29.

Carlson, A.; Murray, D.; Anslow, F.; He, F.; Singer, B.; Liu, Z.; Otto-Bliesner, B. 2010. Assessing the Paleo-Forcings of Southeastern Patagonia Deglaciation using General Circulation Model Simulations. In *American Geophysical Union, Fall Meeting*, abstract #GC23H-04. San Francisco

Carrasco, J.; Osorio, R.; Casassa, G. 2008. Secular trend of the equilibrium-line altitude on the western side of the southern Andes, derived from radiosonde and surface observations. *Journal of Glaciology* 54: 538–550.

Casassa, G.; Rodriguez, J.; Loriaux, T. 2014. A new glacier inventory for the Southern Patagonia Icefield and areal changes 1986–2000. In *Global Land Ice Measurements from Space* (Kargel, J.; Leonard, G.; Bishop, M.; Kaab, A.; Raup, B.; Editors). Springer: 639 – 660. Berlin.

Delmas, M.; Gunnell, Y.; Calvet, M. 2013. Environmental controls on alpine cirque size. *Geomorphology* 206: 318–329.

García, J.; Kaplan, M.; Hall, B.; Schaefer, J.; Vega, R.; Schwartz, R.; Finkel, R. 2012. Glacier expansion in southern Patagonia throughout the Antarctic Cold Reversal. *Geology* 40 (9): 859–862.

Křížek, M.; Vočadlova, K.; Engel, Z. 2012. Cirque overdeepening and their relationship to morphometry. *Geomorphology* 139: 495–505.

Le Roux, J.; Rust, I. 1989. Composite facies map: a new aid to palaeo-environmental reconstruction. *South Africa Journal of Geology* 92: 436–443.

Marden, C. 1997. Late-glacial fluctuations of South Patagonian Icefield, Torres del Paine National Park, southern Chile. *Quaternary International* 38: 61–68.

Mitchell, S.; Montgomery, D. 2006. Influence of a glacial buzzsaw on the height and morphology of the Cascade Range in central Washington State, USA. *Quaternary Research* 65 (1): 96–107.

Nesje, A. 2007. Paleo ELAs. In *Encyclopedia of Quaternary Science* (Elias, S.; editor) Elsevier: 882–892. Amsterdam.

Porter, S. 1989. Some geological implications of average Quaternary glacial conditions. *Quaternary Research*, 32 (3): 245–261.

Rabassa, J.; Coronato, A.; Martínez, O. 2011. Late Cenozoic glaciations in Patagonia and Tierra del Fuego: an updated review. *Biological Journal of the Linnean Society* 103, (25): 316–335.

Sagredo, E.; Moreno, P.; Villa-Martínez, R.; Kaplan, M.; Kubik, P.; Stern, C. 2011. Fluctuations of the Última Esperanza ice lobe (52°S), Chilean Patagonia, during the last glacial maximum and termination 1. *Geomorphology* 125: 92–108.

Sepulveda, S.; Le Roux, J.; and Palma, G. 2013. Application of the composite maps method for landslide susceptibility assessment and its potential use for other natural risk analyses. *Investigaciones Geográficas*, 46: 47–56.

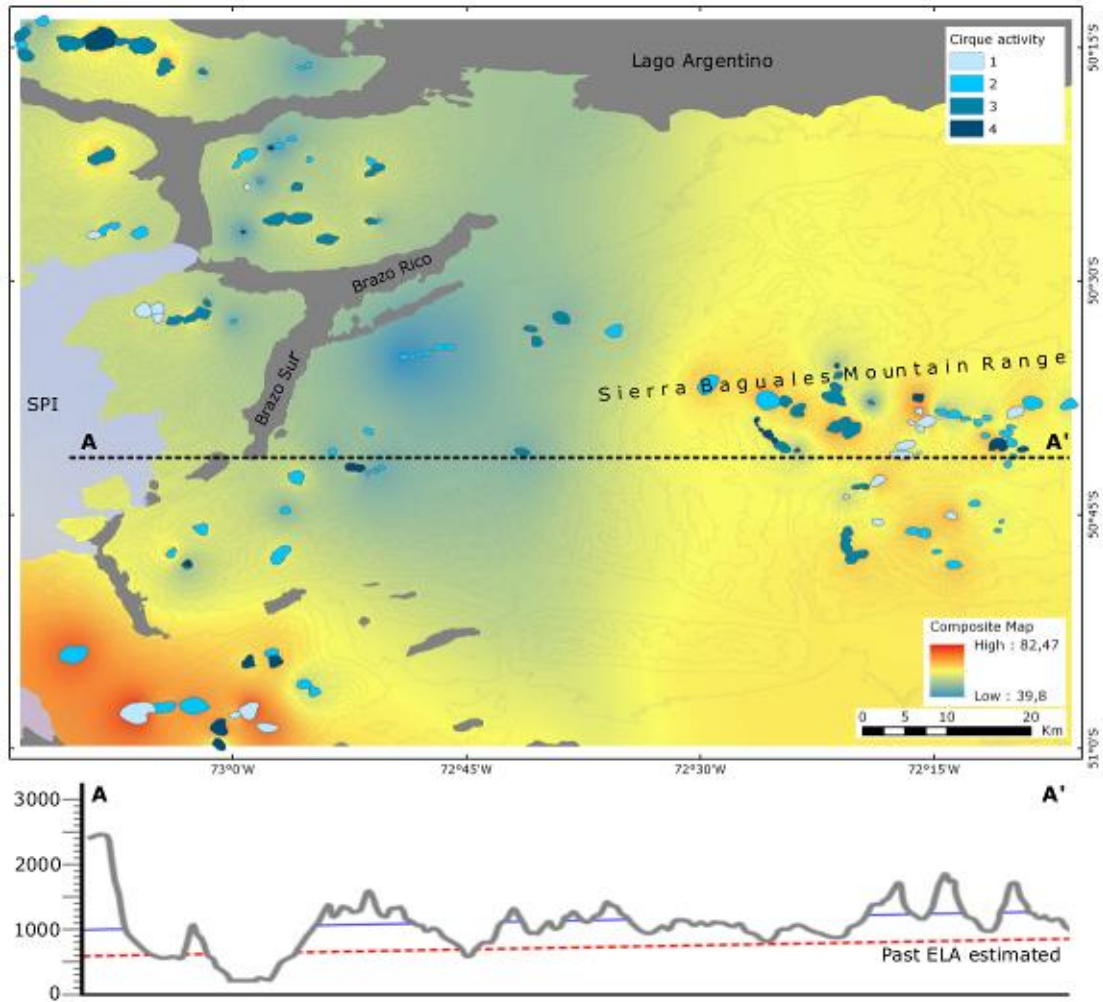


**Figure 1.** Composite map of study area. Cirques were categorized using 10 parameters extracted from the morphometric analysis. Cirque activity corresponds to 1. current glacier activity, 2. perennial snow activity, 3. no glacier or snow activity, 4. not categorized. The Current ELA position (blue line) is based on Aniya et al. (1996), Carrasco et al. (2008) and Casassa et al., (2014) and a paleo-ELA estimation (dotted red line), both represented in a topographic profile, is based on geomorphological and morphometric analysis as well as criteria set by Porter (1989) and Mitchell and Montgomery (2006).

## APPEND 2

Abstract accepted in XV Conferencia Iberoamérica de Sistemas de Información Geográfica (CONFIBSIG).

### FACTORES DE CONTROL DE LAS GLACIACIONES ALPINAS ACONTECIDAS ENTRE LOS 50° Y 51° S, INFERIDAS DE ANALISIS MORFOMETRICO DE CIRCOS GLACIARES.

Araos José <sup>a b</sup>, Le Roux Jacobus <sup>b c</sup>, Kaplan Michael <sup>d</sup>

<sup>a</sup>Departamento de Geología, Universidad de Chile, Chile.

<sup>b</sup>Departamento de Geografía Universidad Alberto Hurtado, Chile (jaraos@uahurtado.cl)

<sup>c</sup>Centro de Excelencia en Geotermia de Los Andes (CEGA), Chile.

<sup>d</sup>LDEO of Columbia University.USA.

#### RESUMEN

Se presenta el mapeo de la distribución geográfica y resultados del análisis morfométrico de 143 circos glaciales localizados entre los 50° y 51° S en el cordón montañoso de Sierra Baguales, estribación oriental de los Andes Patagónicos.

En el área de estudio se pueden distinguir dos configuraciones morfoclimáticas características, condicionadas por factores tectónicos (alzamiento andino), climáticos (Vientos del Oeste) y por la acción de la capa de hielo Pleistocena. El análisis espacial de la actividad en los circos glaciales indica la existencia de un patrón climático contrastante en la sección austral de Patagonia, y donde los circos ubicados en las secciones más elevadas de Sierra Baguales, posiblemente no fueron afectados por variaciones climáticas posteriores al Último Máximo Glacial (UMG), en estos circos el proceso de deglaciación pudo ser más bien rápido y continuo, en comparación a los glaciares efluentes del Campo de Hielo Sur (CHS).

#### INTRODUCCIÓN

La evolución morfoclimática de los Andes Patagónicos ha sido en gran medida influenciada por la relación entre el alzamiento tectónico, el clima y las glaciaciones (Montgomery *et al.*, 2001; Ramos y Ghiglione, 2008; Kaplan *et al.*, 2009). Tal relación ha sido ampliamente estudiada para las glaciaciones de tipo continental de diversas edades y extensiones (Rabassa y Coronato, 2009; Rabassa *et al.*, 2011), y particularmente para el caso de los glaciares efluentes del CHS (Hulton *et al.*, 1994; McCulloch *et al.*, 2000; Rabassa *et al.*, 2005; Sugden *et al.*, 2005; Rodbell *et al.*, 2009). Sin embargo, menor atención se ha prestado a las características y dinámica de las glaciaciones de tipo alpino, que se han desarrollado, evolucionado y en muchos casos desaparecido en las inmediaciones del CHS.

En el presente trabajo se analizan en detalle las características geomorfológicas y morfométricas de los circos glaciales alpinos localizados en el cordón montañoso de Sierra Baguales, estribación oriental de los Andes Patagónicos. Las características geomorfológicas de este sector representan un indicador útil para estimar los cambios climáticos acontecidos hacia el interior del continente, puesto que los glaciares más pequeños tienden a reaccionar más rápido que los glaciares



continentales frente a las oscilaciones climáticas (Vieira, 2008). Por otra parte las características morfométricas de los circos pueden considerarse evidencias necesarias para estimar los factores que controlaron el desarrollo de una topografía alpina en este sector de los Andes patagónicos (Hughes *et al.*, 2007; Křížek *et al.*, 2012; Delmas *et al.*, 2013).

## **MATERIALES Y MÉTODOS**

### **Área de estudio**

El cordón montañoso de Sierra Baguales corresponde a una estribación de los Andes patagónicos localizada entre los 50° y 51° S, que alberga glaciares activos y geoformas relictas de carácter alpino, ubicado en la zona de influencia de los Vientos del Oeste (Villa-Martínez y Moreno, 2007) y topográficamente aislado del CHS. La zona de acumulación de estos circos glaciales se encuentra sobre 1.000 m y a más de 200 Km de la costa pacífica, representando un sistema aislado, idóneo para el estudio de los factores que controlaron los procesos glaciales hacia el interior del continente, y que posiblemente respondieron de forma independiente a los cambios climáticos que operaron desde el UMG.

### **Fuente de datos**

Los circos fueron mapeados utilizando fotografías aéreas digitales escala 1:70.000 e imágenes satelitales Landsat. Para proveer de un adecuado contexto topográfico, en aquellos casos en que se presentaron dificultades en la interpretación de las geoformas, se utilizaron mapas topográficos 1:50.000 y modelos de elevación digital ASTERGDEM y GMTDE2010. Los rasgos geomorfológicos identificados y mapeados fueron validados en tres campañas de terreno realizadas los años 2013 y 2014.

### **Técnicas**

Cada circo fue digitalizado como un polígono cerrado, con un número único que se utilizó como identificador en una base de datos espacial que contiene información referente a los siguientes atributos: Superficie (S), perímetro (P), longitud (L), ancho (W), profundidad (H), elevación máxima ( $E_{max}$ ), elevación media ( $E_{med}$ ), elevación mínima ( $E_{min}$ ), exposición (A), relación longitud profundidad (L/H), relación ancho profundidad (W/H), relación longitud ancho (L/W), pendiente (M), y circularidad (C). (Křížek *et al.*, 2012, 2013; Delmas *et al.*, 2013) Los cálculos de los índices planímetros e hipsométricos se ejecutaron en los SIG de código abierto QuantumGIS 2.2 y GRASS 6.0.

Para cada parámetro se analizaron sus valores mínimos, medios y máximos. La correlación entre atributos dependientes (ej. largo o ancho del circo) e independientes (ej. elevación mínima) fue analizada utilizando el coeficiente de correlación de Pearson y su significancia fue evaluada mediante un test *t*, con un nivel de significancia  $p=0.05$ . Grupos morfológicos similares fueron identificados mediante análisis clúster basado en el método de Ward y distancias euclidianas. El análisis estadístico de la información se realizó mediante el software estadístico R 3.1.3.

Se empleó la metodología de los mapas compuestos (Le Roux y Rust, 1989; Merriam y Jewett, 1989) para representar gráficamente las características de los procesos glaciales acontecidos en el área de estudio. Los datos de entrada para este mapa son estandarizados por lo que todos los

atributos tienen el mismo rango de valores, por tanto la asignación de resultados numéricos es completamente objetiva (Sepulveda *et al.*, 2013). El procesamiento de los datos se realizó en una planilla Excel© y los valores resultantes para cada circo fueron interpolados en el SIG QuantumGIS 2.2 utilizando el algoritmo IDW para crear el mapa compuesto.

## RESULTADOS

Basándose en la clasificación morfológica de los circos es posible distinguir dos grupos, diferenciados por su área, parámetros de forma y elevación (Figura 1). El primer grupo incluye a aquellos circos cuyo piso presenta una elevación promedio de 1.169 m, distribuidos homogéneamente en los valles del área de estudio, y no presentan evidencia de procesos glaciales o nivales actuales. El segundo grupo comprende aquellos circos que presentan su piso a una elevación promedio de 1.273 m, concentrados en las zonas más elevadas del área de estudio, usualmente muestran actividad glacial o nival actual. Considerando lo anterior, la localización,  $E_{med}$  y  $E_{min}$  de los circos glaciales representan importantes factores de control en la presencia o ausencia de actividad glacial/ nival en los circos.

La distribución de la actividad de los circos se ve reflejada además en el mapa compuesto (Figura 2), donde los valores más bajos se asocian al primer grupo de circos descrito anteriormente, que además presentan un área promedio de 1.487 Km<sup>2</sup>, cuadruplicando el área promedio del segundo grupo anteriormente descrito (0.361 Km<sup>2</sup>). Esto se explicaría por la acción de los glaciares efluentes del CHP durante y después del UMG. La distribución de los glaciares del segundo grupo coincide con los valores más altos del mapa compuesto, representando la impronta espacial de la glaciación de tipo alpino.

## DISCUSIÓN

El sitio de estudio presenta evidencia de glaciación(es) de estilo continental asociadas a la Capa de hielo Pleistocena que ocuparon las secciones más bajas de los valles (Marden, 1997; García *et al.*, 2012). Tan pronto como estos glaciares retrocedieron hacia el oeste, Sierra Baguales fue dominada por glaciaciones de estilo alpino, condicionadas por el alzamiento tectónico al este de la Cordillera principal, intensificando el efecto orográfico asociado a los Vientos del Oeste, definiendo un nuevo dominio morfoclimático independiente de la principal capa de hielo Patagónica.

La existencia de un patrón climático contrastante en la sección austral de Patagonia (Glasser *et al.*, 2008) se ve reflejada en la dinámica de los Campos de Hielo durante el UMG y posterior deglaciación (Hulton *et al.*, 2002). Los glaciares occidentales mostraron un comportamiento muy dinámico, debido a la alta precipitación y consecuente balance de masa positivo, mientras que los glaciares orientales, incluyendo los glaciares alpinos localizados en Sierra Baguales, mostraron un comportamiento más estable principalmente debido a bajas temperaturas y escasas de humedad.

Las características geomorfológicas y morfométricas indican que Sierra Baguales ha evolucionado de forma independiente al CHS. Las glaciaciones de tipo alpino se relacionan fundamentalmente a la acción de los Vientos del Oeste, condicionando, para este sector en

particular, una erosión glaciaria mayor a lo que se ha sugerido para el área cubierta por la Capa de Hielo Pleistocena.

## **CONCLUSIONES**

Sierra Baguales representa un laboratorio natural único para el estudio de las evidencias que dan cuenta de las variaciones climáticas y glaciares acontecidas en la sección austral de Patagonia, así como de la evolución geomorfológica de una estribación oriental de los Andes Patagónicos caracterizada por el predominio de glaciaciones de tipo alpino. Tales glaciaciones se explicarían por la acción de factores tectónicos (alzamiento andino) y climáticos (Vientos del Oeste). Además, dada su particular ubicación, los glaciares alpinos de Sierra Baguales presentaron un comportamiento relativamente independiente a los cambios posteriores al UMG que sufrió la Capa de hielo Pleistocena.

## **AGRADECIMIENTOS**

Al programa de Becas para Doctorado Nacional de CONICYT. A los señores Juan McLean y su familia por permitirnos ingresar a las estancias “Las Cumbres” y Baguales”, Juan Pablo Riquez por permitirnos ingresar a la estancia “Verdadera Argentina”. Juan Carlos Aravena y Rodrigo Villa-Martinez de la Universidad de Magallanes, José Luis Oyarzun y Juan José San Martín por el importante soporte logístico. Ricardo Arce, Mauricio Gonzales y Néstor Gutiérrez quienes prestaron invaluable ayuda en las actividades de terreno.

## **REFERENCIAS BIBLIOGRÁFICAS**

- Delmas, M. Gunnell, Y. Calvet, M. 2013. Environmental controls on alpine cirque size. *Geomorphology*. 206, 318–329.
- García, J. Kaplan, M. Hall, B. Schaefer, J. Vega, R. Schwartz, R. Finkel, R. 2012. Glacier expansion in southern Patagonia throughout the Antarctic Cold Reversal. *Geology*. 40 (9), 859–862.
- Glasser, N. Jansson, K. Harrison, S. Kleman, J. 2008. The glacial geomorphology and Pleistocene history of South America between 38°S and 56°S. *Quaternary Science Reviews*. 27 (3–4), 365–390.
- Hughes, P., Gibbard, P. Woodward, J. 2007. Geological controls on Pleistocene glaciation and cirque form in Greece. *Geomorphology*. 88 (3–4), 242–253.
- Hulton, N. Sugden, D. Payne, A. Clapperton, C. 1994. Glacier modeling and the climate of Patagonia during the Last Glacial Maximum. *Quaternary Research*. 42 (1), 1–19.
- Kaplan, M. Hein, A. Hubbard, A. Lax, S. 2009. Can glacial erosion limit the extent of glaciation?. *Geomorphology*. 103, 172–179.
- Křížek, M. Milda, P. 2013. The influence of aspect and altitude on the size, shape and spatial distribution of glacial cirques in the High Tatras (Slovakia, Poland). *Geomorphology*. 198, 57–68.

- Křížek, M. Vočadlova, K. Engel, Z. 2012. Cirque overdeepening and their relationship to morphometry. *Geomorphology*. 139–140, 495–505.
- Le Roux, J. Rust, I. 1989. Composite facies map: a new aid to palaeo-environmental reconstruction. *South Africa Journal of Geology*. 92, 436–443.
- Marden, C. 1997. Late-glacial fluctuations of South Patagonian Icefield, Torres del Paine National Park, southern Chile. *Quaternary International*. 38–39, 61–68.
- McCulloch, R. Bentley, M. Purves, R. Hulton, N. Sugden, D. Clapperton, C. 2000. Climatic inferences from glacial and palaeoecological evidence at the last glacial termination, southern South America. *Journal of Quaternary Science*. 15 (4), 409–417.
- Merriam, D. Jewett, D. 1989. Methods of thematic map comparison. In: *Current Trends in Geomatics*. Plenum press, New York. 9–18.
- Montgomery, D. Balco, G. Willett, S. 2001. Climate, tectonics, and the morphology of the Andes. *Geology*. 29 (7), 579–582.
- Rabassa, J. Coronato, A. Salemme, M. 2005. Chronology of the Late Cenozoic Patagonian glaciations and their correlation with biostratigraphic units of the Pampean region (Argentina). *Journal of South American Earth Sciences*. 20 (1–2), 81–103.
- Rabassa, J. Coronato, A. 2009. Glaciations in Patagonia and Tierra del Fuego during the Ensenadan Stage/Age (Early Pleistocene–earliest Middle Pleistocene). *Quaternary International*. 210 (1–2), 18–36.
- Rabassa, J. Coronato, A. Martínez, O. 2011. Late Cenozoic glaciations in Patagonia and Tierra del Fuego: an updated review. *Biological Journal of the Linnean Society*. 103 (25), 316–335.
- Ramos, V. Ghiglione, M. 2008. Tectonic evolution of the Patagonian Andes. In: *The Late Cenozoic of Patagonia and Tierra del Fuego*. Elsevier, Amsterdam. 57–71.
- Rodbell, D. Smith, J. Mark, B. 2009. Glaciation in the Andes during the Lateglacial and Holocene. *Quaternary Science Reviews*. 28 (21–22), 2165–2212.
- Sepulveda, S. Le Roux, J. Palma, G. 2013. Application of the composite maps method for landslide susceptibility assessment and its potential use for other natural risk analyses. *Investigaciones Geograficas*. 46, 47–56.
- Sugden, D. Bentley, M. Fogwill, C. Hulton, N. McCulloch, R. Purves, R. 2005. Late-glacial glacier events in southernmost south America: A blend of “northern” and “southern” hemispheric climatic signals?. *Geografiska Annaler*. A 87 (2), 273–288.
- Vieira, G. 2008. Combined numerical and geomorphological reconstruction of the Serra da Estrela plateau icefield, Portugal. *Geomorphology*. 97 (1-2), 190–207.

Villa-Martinez, R. Moreno.P. 2007.Pollen evidence for variations in the southern margin of the westerly winds in SW Patagonia over the last 12600 years.QuaternaryResearch. 68, 400–409.

Figura 1. La clasificación morfológica de los circos muestra dos grandes grupos. El grupo morfológico 1 se correlaciona espacialmente con circos ubicados en zonas marginales al CHS y Sierra Baguales. El grupo morfológico 2 se correlaciona espacialmente con los circos que tienen una distribución espacial homogénea.

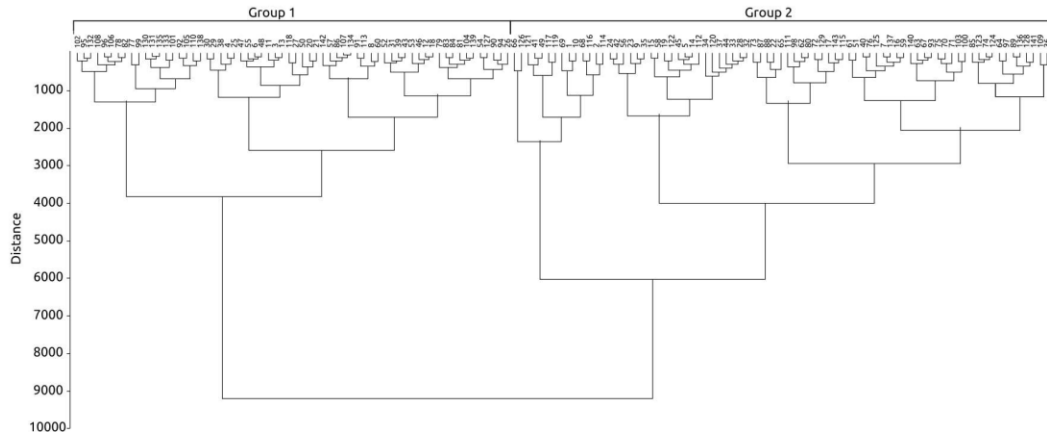


Figura 2. Mapa compuesto.

